

**The role of *Dictyostelium discoideum* annexin C1 in cellular
responses**

INAUGURAL-DISSERTATION
zur
Erlangung des Doktorgrades
der Mathematisch-Naturwissenschaftlichen Fakultät
der Universität zu Köln

vorgelegt von

Marko Marija
aus Belgrad, Serbien und Montenegro
2003

Referees/Berichterstatter

Prof. Dr. Angelika A. Noegel
Prof. Dr. M. Melkonian

Date of oral examination/
Tag der mündlichen Prüfung

13.02.2004.

The present research work was carried out under the supervision and the direction of Prof. Dr. Angelika A. Noegel in the Institute of Biochemistry I, Medical Faculty, University of Cologne, Cologne, Germany, from October 2000 to December 2003.

Diese Arbeit wurde von Oktober 2000 bis Dezember 2003 am Institut für Biochemie I der Medizinischen Fakultät der Universität zu Köln unter der Leitung und der Betreuung von Prof. Dr. Angelika A. Noegel durchgeführt.

Table of Contents

Chapter	Description	Page(s)
ABBREVIATIONS		1-2
I. INTRODUCTION		3-8
1.1	The protein family of annexins	3
1.2	The molecular structure of annexins	4
1.3	Biochemical properties and functions of annexins	6
1.4	<i>Dictyostelium discoideum</i> annexin	7
1.5	The aim of the work	7
II. MATERIAL AND METHODS		9-38
1.0 Material		9
1.1	Laboratory material	9
1.2	Instruments and equipments	9
1.3	Kits	11
1.4	Enzymes, antibodies, substrates, inhibitors and antibiotics	11
1.5	Chemicals and reagents	12
1.6	Media and buffers	12
1.6.1	Media and buffers for <i>Dictyostelium</i> culture	12
1.6.2	Media for <i>E. coli</i> culture	13
1.6.3	Buffers and other solutions	14
1.7	Biological materials	15
1.8	Plasmids	15
1.9	Oligonucleotide primers	15
2.0 Cell biological methods		16
2.1	Growth of <i>Dictyostelium</i>	16
2.1.1	Growth in liquid nutrient medium	16
2.1.2	Growth on SM agar plates	16
2.2	Development of <i>Dictyostelium</i>	17
2.3	Preservation of <i>Dictyostelium</i>	17
2.4	Transformation of <i>Dictyostelium</i> cells by electroporation	18
2.5	Endocytosis and exocytosis assays	19
3.0 Molecular biological methods		19
3.1	Purification of plasmid DNA	19

Chapter	Description	Page(s)
3.2	Digestion with restriction enzymes	20
3.3	Dephosphorylation of DNA fragments	21
3.4	Setting up of ligation reaction	21
3.5	PCR and generation of mutations by PCR-based site directed mutagenesis	21
3.6	DNA agarose gel electrophoresis	22
3.7	Recovery of DNA fragments from agarose gel	23
3.8	Transformation of <i>E. coli</i>	23
3.8.1	Standard protocol for the preparation and transformation of competent cells by SEM	23
3.8.2	Transformation of <i>E. coli</i> cells by electroporation	24
3.9	Glycerol stock of bacterial culture	25
3.10	Construction of vectors	25
3.10.1	Vectors for expression of annexin as GFP-fusion proteins	25
3.11	DNA sequencing	26
3.12	Computer analysis	26
4.0	Biochemical methods	26
4.1	Preparation of total protein from <i>Dictyostelium</i>	26
4.2	Subcellular fractionation	27
4.3	Triton X-100 extraction of <i>Dictyostelium</i> cells	27
4.4	Gelfiltration using the Smart System	29
4.5	Isolation of phagosomes	29
4.6	Immunoprecipitation experiments	29
4.7	2D gel electrophoresis	30
4.8	SDS-polyacrylamide gel electrophoresis	31
4.9	Western blotting using the semi-dry method	32
4.10	Immunodetection of membrane-bound proteins	33
5.0	Immunological methods	34
5.1	Indirect immunofluorescence of <i>Dictyostelium</i> cells	34
5.1.1	Preparation of <i>Dictyostelium</i> cells	34
5.1.2	Methanol fixation	34
5.1.3	Immunolabelling of fixed cells	34
5.1.4	Mounting of coverslips	35
5.2	Immunolabelling of GFP-annexin expressing <i>Dictyostelium</i> cells fixed during phagocytosis	35
6.0	Microscopy	36

Chapter	Description	Page(s)
6.1	Live cell imaging of <i>Dictyostelium</i> cells expressing GFP-annexin	37
6.1.2	Live cell imaging of GFP-annexin during pinocytosis	37
6.1.3	Manipulation of the cytoplasmatic pH of GFP-annexin expressing living cells	37
6.2	Microscopy of agar plates	38
III.	RESULTS	39-64
1	Biochemical studies	39
1.1	Expression of the full lenght annexin, a mutated annexin and the annexin core as GFP-fusion proteins in AX2 and SYN ⁻ cells	39
1.2	Subcellular localization of the constructs	41
1.3	Association of annexin with intracellular membranes	43
1.4	Gelfiltration experiments	45
1.5	Annexin associates with Triton X-100 insoluble fraction in the presence of calcium ions	46
1.6	pH-dependent shuttling of annexin between the cytoplasm and plasma membrane and effect of the pH value of the medium on growth of <i>Dictyostelium</i> cells	48
1.7	Detection of annexin binding partners	51
2	Localization of annexin during pinocytosis and phagocytosis	52
3	Phosphorylation of annexin	55
4	Development of SYN⁻ cells	57
4.1	Development on phosphate agar plates	57
4.2	Localization of annexin in slugs and fruiting bodies	62
IV.	DISCUSSION	65-74
4.1	Subcellular localization of <i>Dictyostelium</i> annexin C1	66
4.2	Annexin localizes on pinosomes and phagosomes	67
4.3	Ca ²⁺ -independent membrane binding of annexin C1	68
4.4	Nonlipid annexin ligands	70
4.5	The role of annexin during development	72

Chapter	Description	Page(s)
4.6	Phosphorylation of annexin C1	73
	V. SUMMARY/ZUSAMMENFASSUNG	75-78
	BIBLIOGRAPHY	79-89
	Erklärung	90
	Curriculum Vitae/Lebenslauf	91-92

Abbreviations

AP alkaline phosphatase
APS ammonium persulphate
ATP adenosine 5'-triphosphate
bp base pair(s)
BSA bovine serum albumine
Bsr blasticidin resistance cassette
cDNA complementary DNA
dNTP deoxyribonucleotide triphosphate
DABCO diazobicyclooctane
DMSO dimethylsulphoxide
DNA deoxyribonucleic acid
DTT 1,4-dithiothreitol
ECL enzymatic chemiluminescence
EDTA ethylenediaminetetraacetic acid
EGTA ethyleneglycol-bis (2-amino-ethylene) N,N,N,N-tetraacetic acid
G418 geneticin
GFP green fluorescent protein
HEPES N-[2-Hydroxyethyl] piperazine-N'-2-ethanesulphonic acid
HRP horse radish peroxidase
IgG immunoglobulin G
IPTG iso-propylthio-galactopyranoside
kb kilo base pairs
kDa kilodalton
MES morpholinoethansulphonic acid
 β -ME beta-mercaptoethanol
Mw molecular weight
OD optical density
PAGE polyacrylamide gel electrophoresis
PCR polymerase chain reaction
PIPES piperazine-N,N'-bis [2-ethanesulphonic acid]
PMSF phenylmethylsulphonylfluoride
RNA ribonucleic acid
RNase ribonuclease
rpm rotations per minute
SDS sodium dodecyl sulphate
TEMED N,N,N',N'-tetramethyl-ethylendiamine
TRITC tetramethylrhodamine isothiocyanate
UV ultra violet
vol. volume
v/v volume by volume
w/v weight by volume
X-gal 5-bromo-4-chloro-3-indolyl-D-galactopyranoside

Units of Measure and Prefixes

Unit Name

⁰C degree Celsius

D Dalton

g gram

h hour

L litre

m meter

min minute

s sec

V volt

Symbol Prefix (Factor)

k kilo (10^3)

c centi (10^{-2})

m milli (10^{-3})

μ micro (10^{-6})

n nano (10^{-9})

p pico (10^{-12})

1. Introduction

1.1 The protein family of annexins

Annexins are intracellular Ca^{2+} - and phospholipid-binding proteins composed of four (or eight in annexin A6) so called “annexin repeats” following an unique N-terminal domain. The members of this big protein family are described to be present in a great variety of organisms ranging from fungi and protists to plants and vertebrates including humans. So far, more than 160 annexins present in more than 65 different species are described. In 1999, a new annexin nomenclature was proposed and accepted at the 50th Harden Conference on Annexins held in the United Kingdom (Table 1.).

Name	Synonyms/Former name (s)	Human gene symbol	Non-human gene symbol	
annexin A1	lipocortin 1, annexin I	ANXA1	Anxa1	
annexin A2	calpactin 1, annexin II	ANXA2	Anxa2	
annexin A3	annexin III	ANXA3	Anxa3	
annexin A4	annexin IV	ANXA4	Anxa4	
annexin A5	annexin V	ANXA5	Anxa5	
annexin A6	annexin VI	ANXA6	Anxa6	
annexin A7	synexin, annexin VII	ANXA7	Anxa7	
annexin A8	annexin VIII	ANXA8	Anxa8	
annexin A9	annexin XXXI	ANXA9	Anxa9	
annexin A10		ANXA10	Anxa10	
annexin A11	annexin XI	ANXA11	Anxa11	
annexin A12	unassigned			
annexin A13	annexin XIII	ANXA13	Anxa13	

Name	Organism/Former name	Gene symbol	
annexin B9	3 species of insect, annexin IX	Anxb9	
annexin B10	4 species of insect, annexin X	Anxb10	
annexin B11	1 species of insect, annexin	Anxb11	
annexin B12	Cnidaria, annexin XII	Anxb12	
	3 species of flatworms, 5 annexins 10 species of roundworms, 5 annexins (including <i>C.elegans</i> annexins XV-XVII, XXX)		

Name	Organisms/Former name	Gene symbol	
annexin C1	<i>Dictyostelium</i> and <i>Neurospora</i> annexin XIV	Anxc1	
Annexin C2-C5	4 species of fungi/ molds/alveolates	Anxc2-c5	

Name	Organism/Former name (s)	Gene symbol	
annexin D1-D25	35 species including annexin XVIII and annexins XXII-XXIX	Anxd1-d25	

Name	Organism/Former name	Gene symbol	
annexin E1	Giardia annexin XXI	Anxe1	
Annexin E2	Giardia annexin XIX	Anxe2	
Annexin E3	Giardia annexin XX	Anxe3	

Table 1. (Previous page) **The new annexin nomenclature.** The five major annexin groups are shown (A-E). The nomenclature is proposed by Morgan R. and Fernandez P. The picture is taken from the review published by Gerke and Moss (2002). Although vertebrate annexins are unlikely to be widely represented in invertebrate species, the oldest of this group like, annexins A7, A11 and A13 are possible exceptions. The annexin A11 ortholog has been described in *Aplysia*.

1.2 The molecular structure of annexins

The property of annexins to bind phospholipids and Ca^{2+} is based on their structure. Annexins are composed of two typical domains, a divergent amino terminal domain and a conserved carboxy terminal core domain. This later domain is formed by a fourfold repeat (eightfold in annexin A6), with each repeat extending over approximately 70 amino acids and having a Ca^{2+} -binding site. The core domain forms a highly α -helical disc with its type II and type III Ca^{2+} -binding sites (Weng *et al.*, 1993) facing the membrane when the protein associates with phospholipids. The other (concave) side is facing the cell cytosol thus being open for interactions with possible binding partners. The unique amino terminal domains of different annexins vary in their length and amino acid composition. The C-terminal part of annexins is responsible for Ca^{2+} - and phospholipid-binding and the N-terminal part is thought to confer functional diversity (Raynal and Pollard, 1994).

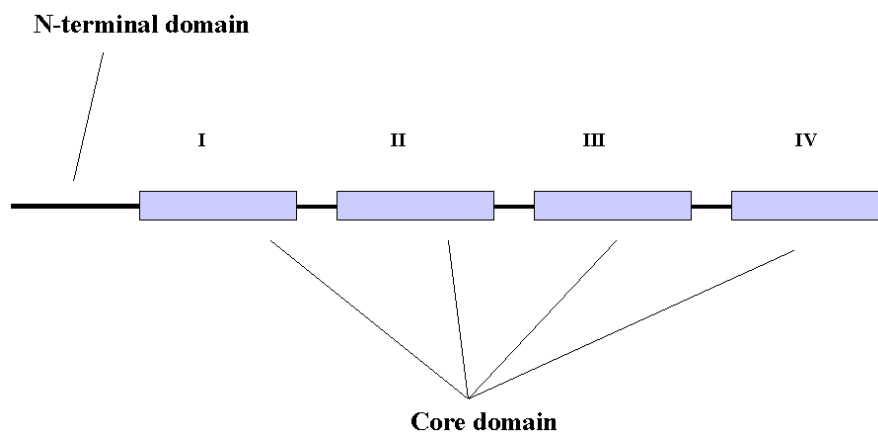


Fig.1. Primary structure of annexins. The core domain consists of four conserved repeats, eight in annexin A6. The core domain is responsible for Ca^{2+} - and phospholipid-binding. The core domains from different annexins show 45-55 % of homology while the N-terminal domains are variable.

Numerous crystal structures of annexin core domains which revealed the conservation of annexin's three-dimensional fold are described (Huber *et al.*, 1990; Lewit-Bentley *et al.*,

1992; Weng *et al.*, 1993; Kawasaki *et al.*, 1996). Furthermore, site directed mutagenesis gave valuable contribution to the characterization of certain amino acid residues and their importance in the maintenance of the overall fold of annexin cores. For example, conserved arginine residues present in each of the four annexin repeats were shown to be of crucial importance for stabilizing the tertiary structure of annexin A5. Substitution of different serine and threonine residues by alanine and substitution of the unique tryptophane in the same annexin, resulted in an altered membrane binding underlining the role of these amino acids in intermolecular contacts (Campos *et al.*, 1998; Campos *et al.*, 1999). There are two types of Ca^{2+} -binding sites present in annexin core domains. They differ not only in their architecture but also in their affinity for the bivalent cation. Three so-called type II sites are found in annexin repeats 2, 3 and 4, respectively. Two so-called type III sites are located in the first repeat (Jost *et al.*, 1994, Huber *et al.*, 1990, Weng *et al.*, 1993). Site directed mutational analysis revealed that type II sites show higher affinity for Ca^{2+} compared to type III sites. Annexin A2 mutants, for example, with defects in the type II and/or type III sites also show different subcellular distributions. The annexin A2 type III mutant protein acquires the typical location in the cortical cytoskeleton observed for the wild-type molecule. In contrast, mutation in the type II Ca^{2+} -binding site of annexin A2 changes localization of the protein which then remains essentially cytosolic, as does a mutant protein containing defects in both type II and type III Ca^{2+} -binding sites (Jost *et al.*, 1994). Furthermore, thermodynamic analysis revealed cooperativity in the binding of Ca^{2+} to annexin A1 (Rosengarth *et al.*, 2001).

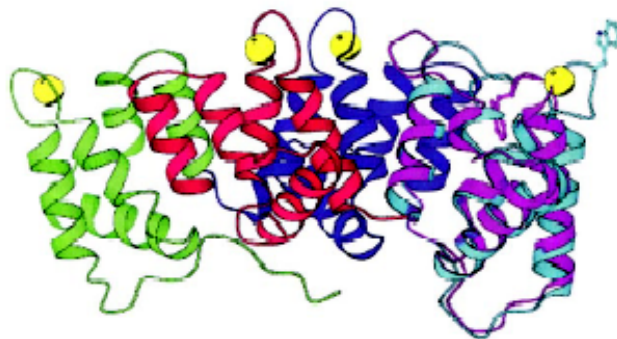


Fig.2. Crystal structure of human annexin A5. Highly α -helical folding of the protein core forms a slightly curved disk. The four annexin repeats are presented in different colors (repeat I: green; repeat II: blue; repeat III: red; repeat IV: violet/cyan). The N-terminal domain is unstructured, presented in green and it extends along the concave side of the molecule. Bound Ca^{2+} are depicted as yellow balls. The high and low Ca^{2+} forms are shown in violet and green

respectively, revealing the conformational change in repeat III, which leads to an exposure of Trp-187 (Gerke and Moss, 2002).

A similar approach in characterizing the N-terminal domain of annexin showed that replacement of Trp-5 by alanine in the unique N-terminal domain of annexin A3 led to a much stronger phospholipid binding (Hofmann *et al.*, 2000). In accordance with this finding it is possible that N-terminal domains of the smaller annexins affect the Ca^{2+} -dependent phospholipid binding through stabilizing or destabilizing slightly different conformations of the molecule. Also, unique N-terminal domains can carry the binding sites for protein ligands (Mailliard *et al.*, 1996; Seemann *et al.*, 1996) or possess sites for posttranslational modifications in these regions (Becker *et al.*, 1990).

1.3 Biochemical properties and functions of annexins

Ca^{2+} -dependent phospholipid binding is shared by all annexins. However, individual members differ in their Ca^{2+} sensitivity and phospholipid headgroup (phosphatidylserine, phosphatidylinositol) specificity (Raynal and Pollard, 1994). Additional features of annexins were revealed in *in vitro* studies of annexin A5 and annexin B12. These annexins exhibit a Ca^{2+} -independent binding to negatively charged phospholipids under low pH conditions. In these studies it has been proposed that protonation of a certain residue could induce a reversible conformational change in the protein and lead to insertion into phospholipid bilayers (Köhler *et al.*, 1997; Isas *et al.*, 2000).

Although annexins have been known for more than 20 years their function remains elusive. A role in regulation of membrane-cytoskeleton dynamics has been suggested (Alvarez-Martinez *et al.*, 1997; Gerke and Moss, 1997; Babiychuk *et al.*, 1999). Since some annexins bind actin, an involvement in exocytosis (Chasserot-Golaz *et al.*, 1996; Rosales and Ernst, 1997; Iino *et al.*, 2000; Caohuy and Pollard, 2001; Salzer *et al.*, 2002), in endocytosis (Futter *et al.*, 1993; Grewal *et al.*, 2000) and phagocytosis (Diakonova *et al.*, 1997; Majeed *et al.*, 1998; Pittis and Garcia, 1999) has been proposed. Furthermore, annexins could participate in signaling events since, for example, annexin A6 is found in association with activated PKC- α (Schmitz- Pfeiffer *et al.*,

1998) and annexin A7 interacts with GTP and catalyzes its hydrolysis mediating thus the Ca^{2+} /GTP signal during exocytotic membrane fusion (Caohuy *et al.*, 1996). Recently, mutant mice have been generated that either overexpress or lack a specific annexin. These studies showed that overexpression of annexin A6 in the heart causes cardiac hypertrophy in mice (Gunteski-Hamblin *et al.*, 1996) whereas a mouse strain lacking this protein is rather mildly affected and suffers from an increase in myocyte contractility and faster diastolic Ca^{2+} removal from the cytoplasm (Song *et al.*, 2002). Mouse mutants lacking annexin A7 were reported by two groups. Whereas in one case the knockout mice were inviable and even in the heterozygous condition animals suffered from a defect in Ca^{2+} signal transduction and in insulin secretion (Srivastava *et al.*, 1999), in the other case annexin A7 (-/-) mice were viable and exhibited an altered cell shortening-frequency relationship when cardiomyocytes were stimulated with high frequencies (Herr *et al.*, 2001).

1.4 *Dictyostelium discoideum* annexin

Dictyostelium cells harbor an annexin gene, which gives rise to two isoforms of approximately 47 and 51 kDa. At the time of its discovery this protein exhibited highest homology to annexin A7 (synexin) and hence it was called annexin 7 / synexin (Döring *et al.*, 1991). This homology extended not only along the annexin core domain but also throughout the amino terminal region, which is unusually long in these two proteins. Moreover, the amino terminal sequences of both proteins are subject to differential splicing yielding two isoforms (Bonfils *et al.*, 1994; Magendzo *et al.*, 1991a; Magendzo *et al.*, 1991b; Selbert *et al.*, 1996). With the description of further annexins phylogenetic studies became feasible and allowed a new classification of the annexin proteins. This placed *Dictyostelium* annexin together with the *Neurospora* protein into a separate group and is now called annexin C1 (proposed by Reginald Morgan and Maria-Pilar Fernandez, 1999).

1.5 The aim of the work

Dictyostelium discoideum annexin was previously described and characterized by Döring *et al.* (1995). A *Dictyostelium* mutant in which the annexin gene was inactivated has been generated

(SYN⁻). The mutant cells were nearly indistinguishable from wild type cells under normal laboratory conditions. Only development was noticeably affected and retarded by more than four hours. The cells were able to undergo development and to form fruiting bodies containing viable spores. However, only a limited number of the cells participated in fruiting body formation. Furthermore the fruiting bodies were significantly smaller. When the processes that involved membrane trafficking such as phagocytosis, exocytosis, pinocytosis and secretion were tested, a significant impairment was observed when the Ca²⁺ concentrations in the surrounding medium were strongly reduced, suggesting that annexin is involved in maintaining Ca²⁺ homeostasis (Döring *et al.*, 1995).

This study was initiated to answer further questions regarding the cellular and subcellular localization of *Dictyostelium* annexin, its dynamic behaviour and possible interactions with other proteins.

To get further insight into the *in vivo* role of *Dictyostelium* annexin we have made use of a GFP-tagged annexin fusion protein and studied its involvement in cellular processes in *Dictyostelium* *in vivo* and *in vitro*, with emphasis on processes like pinocytosis, phagocytosis, osmoregulation and development. Also, we studied the role of full length annexin and its core domain as well as a mutated annexin variant in rescuing the previously described impairment in SYN⁻ development. To accomplish this, we have generated strains that express annexin as a full length annexin-GFP fusion, the annexin core domain fused to GFP, or a mutated variant of full length annexin fused to GFP as well. Moreover, the GFP-tag enabled easy visualization of fusion proteins in living and fixed cells.

The ability of some annexins (A5 and B12) to bind to phospholipid vesicles independently of Ca²⁺ but under low pH conditions have been reported (Köhler *et al.*, 1997; Isas *et al.*, 2000). We analyzed whether relocalization of annexin from the cytoplasm to the plasma membrane upon a decrease of the cytosolic pH could be observed as well *in vivo*.

Finally, in order to understand better the function of annexin, we focused also on the identification of its possible binding partners.

2. Material and Methods

1. Material

1.1 Laboratory materials

Cellophane sheet, Dry ease	Novex
Centrifuge tubes, 15 ml, 50 ml	Greiner
Coverslips (glass), Ø12 mm, Ø18 mm, Ø55 mm	Assistant
Corex tube, 15 ml, 50 ml	Corex
Cryo tube, 1 ml	Nunc
Electroporation cuvette, 2 mm electrode gap	Bio-Rad
Gel-drying frames	Novex
Hybridisation bag	Life technologies
Microcentrifuge tube, 1.5 ml, 2.2 ml	Sarstedt
Micropipette, 1-20 µl, 10-200 µl, 100-1,000 µl	Gilson
Micropipette tips	Greiner
Needles (sterile), 18G–27G Terumo,	Microlance
Nitrocellulose membrane, BA85	Schleicher and Schuell
Parafilm	American National Can
Pasteur pipette, 145 mm, 230 mm	Volac
PCR softtubes, 0.2 ml	Biozym
Petri dish (35 mm, 60 mm, 100 mm)	Falcon
Petri dish (90 mm)	Greiner
Plastic cuvette, semi-micro	Greiner
Plastic pipettes (sterile), 1 ml, 2 ml, 5 ml, 10 ml, 25 ml	Greiner
Quartz cuvette, Infracil	Hellma
Quartz cuvette, semi-micro	Perkin Elmer
Saran wrap	Dow
Scalpels (disposable), Nr. 10, 11, 15, 21	Feather
Slides, 76 x 26 mm	Menzel
Syringes (sterile), 1 ml, 5 ml, 10 ml, 20 ml	Amefa, Omnifix
Syringe filters (Acrodisc), 0.2 µm, 0.45 µm	Gelman Sciences
Tissue culture flasks, 25 cm ² , 75 cm ² , 175 cm ²	Nunc
Tissue culture dishes, 6 wells, 24 wells, 96 wells	Nunc
Whatman 3MM filter paper	Whatman
X-ray film, X-omat AR-5, 18 x 24 mm, 535 x 43 mm	Kodak

1.2 Instruments and equipments

Centrifuges (microcentrifuges):

Centrifuge 5417 C

Centrifuge Sigma B.

Cold centrifuge Biofuge fresco

Centrifuges (table-top, cooling, low speed):

Eppendorf

Braun Biotech Instruments

Heraeus Instruments

Centrifuge CS-6R	Beckman
Centrifuge RT7	Sorvall
Centrifuge Allegra 21R	Beckman
Centrifuges (cooling, high speed):	
Beckman Avanti J25	Beckman
Sorvall RC 5C plus	Sorvall
Centrifuge-rotors:	
JA-10	Beckman
JA-25.50	Beckman
SLA-1500	Sorvall
SLA-3000	Sorvall
SS-34	Sorvall
Electrophoresis power supply, Power-pac-200, -300	Bio-Rad
Electroporation unit, Gene-Pulser	Bio-Rad
Freezer (-80 °C)	Nunc
Freezer (-20 °C)	Siemens, Liebherr
Gel-documentation unit	MWG-Biotech
Heating block, DIGI-Block JR	NeoLab
Heating block, Dry-Block DB x 20	Techne
Ice machine	Ziegra
Incubators:	
Incubator, microbiological	Heraeus
Incubator with shaker, Lab-Therm	Kuehner
Laminar flow, Hera Safe (HS 12)	Heraeus
Magnetic stirrer, MR 3001 K	Heidolph
Microscopes:	
Light microscope, CH30	Olympus
Light microscope, DMIL	Leica
Light microscope, CK2	Olympus
Fluorescence microscope, DMR	Leica
Fluorescence microscope, 1X70	Olympus
Confocal laser scan microscope, DM/IRBE	Leica
Stereo microscope, MZFLIII	Leica
Stereomicroscope, SZ4045TR	Olympus
Oven, conventional	Heraeus
PCR machine, PCR-DNA Engine PTC-2000	MJ Research
pH-Meter	Knick
Refrigerator	Liebherr
Semi-dry blot apparatus, Trans-Blot SD	Bio-Rad
Shakers GFL	Kuehner
Sonicator, Ultra turrax T25 basic	IKA Labortechnik
Sonicator (water bath), Sonorex RK 52	Bandelin
Speed-vac concentrator, DNA 110	Savant

Spectrophotometer, Ultraspec 2000, UV/visible	Pharmacia Biotech
Ultracentrifuges:	
Optima TLX	Beckman
Optima L-70K	Beckman
Ultracentrifuge-rotors:	
TLA 45	Beckman
TLA 100.3	Beckman
SW 41	Beckman
UV- transilluminator, TFS-35 M	Faust
Vortex, REAX top	Heidolph
Waterbath	GFL
X-ray-film developing machine, FPM-100A	Fujifilm

1.3 Kits

Nucleobond AX	Macherey-Nagel
NucleoSpin Extract 2 in 1	Macherey-Nagel
Nucleotrap	Macherey-Nagel
Original TA Cloning	Invitrogen
pGEM-T Easy	Promega
Qiagen Midi- and Maxi-prep	Qiagen
Stratagene Prime It II	Stratagene

1.4 Enzymes, antibodies, substrates, inhibitors and antibiotics

Enzymes used in the molecular biology experiments:

Calf Intestinal Alkaline Phosphatase (CIAP)	Roche
Klenow fragment (DNA polymerase)	Roche
Lysozyme	Sigma
Restriction endonucleases	Amersham
Ribonuclease A (RNase A)	Sigma
T4 DNA ligase	Roche
<i>Taq</i> -polymerase	Roche

Primary antibodies:

Mouse anti-actin monoclonal antibody, Act 1-7	(Simpson <i>et al.</i> , 1984)
Mouse anti-GFP monoclonal antibody, K3-184-2	unpublished
Mouse anti-comitin monoclonal antibody 190-340-2	(Weiner <i>et al.</i> , 1993)
Mouse anti-CsA monoclonal antibody 33-294-17	(Bertholdt <i>et al.</i> , 1985)
Mouse anti-vacuolin monoclonal antibody 221-1-1	(Rauchenberger <i>et al.</i> , 1997)
Mouse anti-V/H ⁺ ATPase monoclonal antibody	(Jenne <i>et al.</i> , 1998)

Secondary antibodies:

Goat anti-mouse IgG, peroxidase conjugated	Sigma
--	-------

Sheep anti-mouse IgG, Cy3 conjugated Sigma

Substrates:

Hydrogen peroxide (H₂O₂) Sigma

Inhibitors:

Phenylmethylsulphonylfluoride (PMSF) Sigma

Sodium fluoride Sigma

Sodium orthovanadate Sigma

Antibiotics:

Ampicillin Gruenenthal

Blasticidin S ICN Biomedicals

Dihydrostreptomycinsulphate Sigma

Geneticin (G418) Life technologies

Tetracyclin Sigma

1.5 Chemicals and reagents

Most of the chemicals and reagents were obtained either from Sigma, Fluka, Difco, Merck, Roche, Roth or Serva. Those chemicals or reagents that were obtained from companies other than those mentioned here are listed below.

Acetic acid (98-100%)	Riedel-de-Haen
Acrylamide (Protogel: 30:0,8 AA/Bis-AA)	National Diagnostics
Agar-Agar (BRC-RG)	Biomatic
Agarose (Electrophoresis Grade)	Life technologies
Chloroform	Riedel-de-Haen
Ethanol	Riedel-de-Haen
Glycerine	Riedel-de-Haen
Glycine	Riedel-de-Haen
Isopropyl-β-D-thiogalactopyranoside (IPTG)	Loewe Biochemica
Methanol	Riedel-de-Haen
N- [2-Hydroxyethyl] piperazine-N'-2-	
-ethanesulfonic acid (HEPES)	Biomol
Nonidet P40	Fluka
Peptone	Oxoid
Sodium hydroxide	Riedel-de-Haen
TRIzol	Gibco BRL
Yeast extract	Oxoid

1.6 Media and buffers

All media and buffers were prepared with deionised water filtered through an ion-exchange unit

(Membra Pure). The media and buffers were sterilized by autoclaving at 120 °C and antibiotics were added to the media after cooling to approx. 50 °C. For making agar plates, a semi-automatic plate-pouring machine (Technomat) was used.

1.6.1 Media and buffers for *Dictyostelium* culture

<u>AX2-medium, pH 6.7:</u> (Claviez <i>et al.</i> , 1982)	7.15 g yeast extract 14.3 g peptone (proteose) 18.0 g maltose 0.486 g KH ₂ PO ₄ 0.616 g Na ₂ HPO ₄ ·2H ₂ O add H ₂ O to make 1 liter
<u>Phosphate agar plates, pH 6.0:</u>	9 g agar add Soerensen phosphate buffer, pH 6.0 to make 1 liter
<u>Salt solution:</u> (Bonner, 1947)	10 mM NaCl 10 mM KCl 2.7 mM CaCl ₂
<u>SM agar plates, pH 6.5:</u> (Sussman, 1951)	9 g agar 10 g peptone 10 g glucose 1 g yeast extract 1 g MgSO ₄ ·7H ₂ O 2.2 g KH ₂ PO ₄ 1 g K ₂ HPO ₄ add H ₂ O to make 1 liter
<u>Soerensen phosphate buffer, pH 6.0:</u> (Malchow <i>et al.</i> , 1972)	2 mM Na ₂ HPO ₄ 14.6 mM KH ₂ PO ₄

1.6.2 Media for *E. coli* culture

<u>LB medium, pH 7.4:</u> (Sambrook <i>et al.</i> , 1989)	10 g bacto-tryptone 5 g yeast extract 10 g NaCl adjust to pH 7.4 with 1 N NaOH add H ₂ O to make 1 liter
--	---

For LB agar plates, 0.9 % (w/v) agar was added to the LB medium and the medium was then autoclaved. For antibiotic selection of *E. coli* transformants, 50 mg/l ampicillin, kanamycin or chloramphenicol was added to the autoclaved medium after cooling it to approx. 50 °C. For blue/white selection of *E. coli* transformants, 10 µl 0.1 M IPTG and 30 µl X-gal solution (2 % in dimethylformamide) was plated per 90 mm plate and the plate was incubated at 37 °C for at least 30 min before using.

SOC medium, pH 7.0:
(Sambrook *et al.*, 1989)

20 g bacto-tryptone
5 g yeast extract
10 mM NaCl
2.5 mM KCl
dissolve in 900 ml deionised H₂O
adjust to pH 7.0 with 1 N NaOH
The medium was autoclaved, cooled to approx. 50 °C
and then the following solutions, which were
separately sterilized by filtration (glucose) or
autoclaving, were added:
10 mM MgCl₂·6H₂O
10 mM MgSO₄·7H₂O
20 mM Glucose
add H₂O to make 1 liter

1.6.3. Buffers and other solutions

The buffers and solutions that were commonly used during the course of this study are mentioned below.

10 x NCP-Puffer (pH 8.0):

12.1 g Tris/HCl
87.0 g NaCl
add H₂O to make 995 ml
add 5.0 ml Tween 20 after autoclaving

PBG (pH 7.4):

0.5 % bovine serum albumin
0.1 % gelatin (cold-water fish skin)
in 1 x PBS, pH 7.4

1 x PBS (pH 7.4):

8.0 g NaCl
0.2 g KH₂PO₄
1.15 g Na₂HPO₄
0.2 g KCl

dissolve in 900 ml deionised H₂O
 adjust to pH 7.4
 add H₂O to make 1 liter, autoclave

TE buffer (pH 8.0):

10 mM Tris/HCl, pH 8.0
 1 mM EDTA, pH 8.0

10 x TAE buffer (pH 8.3):

27.22 g Tris
 13.6 g sodium acetate
 3.72 g EDTA
 add H₂O to make 1 liter

1.7 Biological materialsBacterial strains:

<i>E. coli</i> DH5 α	Hanahan, 1983
<i>E. coli</i> XL1 blue	Bullock <i>et al.</i> , 1987
<i>Klebsiella aeorgenes</i>	Williams and Newell, 1976

Dictyostelium discoideum strain:

AX2-214

An axenically growing derivative of wild strain, NC-4 (Raper, 1935). Commonly referred to as AX2.

1.8 Plasmids

pDdA15gfp
 pDEX-RH
 pGEM-T Easy
 pUC
 pT7-7

Neujahr *et al.*, 1997
 Westphal *et al.*, 1997
 Promega
 Pharmacia
 Tabor, S. & Richardson, C. C. (1985)

1.9 Oligonucleotide primers

The oligonucleotide primers were designed on the basis of sequence information available and ordered for synthesis to Sigma. Following is a list of the primers used for PCR, sequence analysis or site directed mutagenesis during the course of the present investigation. The position and orientation of the primers are indicated in the text when discussed.

Name	Sequence	Analysis
AnnA1-AccI 5'	5'-CTGTCGACATGTCCTATCCACCAAACC-3'	Site dir. mut. & PCR
AnnA2-PstI 3'	5'-TCTGCAGTACCAATTTTACCTTCACCAGCTTTGTAGAGATC-3'	Site dir. mut. & Seq.
AnnB1-AccI 3'	5'-TGTCGACTTATGAGATAATATCTAATAATAATTTTTTG-3'	Site dir. mut. & PCR
AnnB2-PstI 5'	5'-GTAAAATTGGTACTGCAGAAAAGGAATTCATCAAAAATTCTC-3'	Site dir. mut. & Seq.
AnnCore-AccI 5'	5'-CTGTCGACGGATATCATCAA-3'	PCR
SP6 universal	5'-ATTTAGGTGACACTATAG-3'	Seq.
Syng1 3'	5'-CGCGGATCCTGAGATAATATCTAATAATAATTTT-3'	PCR
Syng1 5'	5'-CGCGGATCCATGTCCTATCCACCAAAC-3'	PCR
T7 universal	5'-TAATACGACTCACTATAGGG-3'	Seq.

2. Cell biological methods

2.1 Growth of *Dictyostelium*

2.1.1 Growth in liquid nutrient medium (Claviez *et al.*, 1982)

Dictyostelium discoideum AX2 and the derived transformants were grown in liquid AX2 medium containing dihydrostreptomycin (40 µg/ml) and other appropriate selective antibiotics at 21 °C either in a shaking-suspension in Erlenmeyer flasks with shaking at 160 rpm or on petri dishes. For all the cell biological works, cultures were harvested at a density of 3-5 x 10⁶ cells/ml.

2.1.2. Growth on SM agar plates

Dictyostelium cells were plated onto SM agar plates overlaid with *Klebsiella aerogenes* and incubated at 21 °C for 3-4 days until *Dictyostelium* plaques appeared on the bacterial lawns. To obtain single clones of *Dictyostelium*, 50-200 cells were suspended in 100 µl Soerensen phosphate buffer and plated onto *Klebsiella*-overlaid SM agar plates. Single plaques obtained after incubation at 21 °C for 3-4 days were picked up with sterile tooth-picks, transferred either to new *Klebsiella*-overlaid SM agar plates or to separate petri dishes with AX2 medium supplemented with dihydrostreptomycin (40 µg/ml) and ampicillin (50 µg/ml) (to eliminate the bacteria) and any other appropriate selective antibiotic (depending upon mutant).

2.2 Development of *Dictyostelium*

Development in *Dictyostelium* is induced by starvation. Cells grown to a density of $2-3 \times 10^6$ cells/ml were pelleted by centrifugation at 2,000 rpm (Sorvall RT7 centrifuge) for 2 min at 4°C and were washed two times in an equal volume of cold Soerensen phosphate buffer in order to remove all the nutrients present in the culture medium. 5×10^7 cells/ml were then resuspended in 3 ml Soerensen phosphate buffer and evenly distributed onto phosphate-buffered agar plates (90 mm) or water agar plates (90 mm). The plates were air dried and any excess liquid was carefully aspirated without disturbing the cell layer. The plates were then incubated at 21°C . Different stages of development were observed and the images were captured at indicated time points. For development in suspension culture, the cells were resuspended in Soerensen phosphate buffer at a density of 1×10^7 cells/ml and were shaken at 160 rpm and 21°C for desired time periods.

2.3 Preservation of *Dictyostelium*

Dictyostelium cells were allowed to grow in AX2 medium to a density of $4-5 \times 10^6$ cells/ml. 9 ml of the dense grown culture were collected in a 15 ml Falcon tube on ice and supplemented with 1 ml horse serum and 1 ml DMSO. The contents were mixed by gentle pipetting, and aliquoted in cryotubes (1 ml). The aliquots were incubated on ice for 60 min, followed by incubation at -20°C for at least 2 hours. Finally, the aliquots were transferred to -80°C for long term storage.

For reviving the frozen *Dictyostelium* cells, an aliquot was taken out from -80°C and thawed immediately at 37°C in a waterbath. In order to remove DMSO, the cells were transferred to a Falcon tube containing 30 ml AX2 medium and centrifuged at 2,000 rpm (Sorvall RT7 centrifuge) for 2 min at 4°C . The cell pellet was resuspended in 10 ml of AX2 medium and 200 μl of the cell suspension was plated onto SM agar plates overlaid with *Klebsiella* while the remaining cell suspension was transferred into a 100-mm petri dish (Falcon) and antibiotics were added when appropriate. Cells in the petri dish were allowed to recover overnight at 21°C and the medium was changed the next day to remove the dead cells and the traces of DMSO, whereas, the SM agar plates coated with cell suspension and bacteria were incubated at 21°C until plaques of *Dictyostelium* cells started to appear.

2.4 Transformation of *Dictyostelium* cells by electroporation

The electroporation method for transformation of *Dictyostelium* cells described by de Hostos *et al.* (1993) was followed with little modifications. *Dictyostelium discoideum* cells were grown axenically in suspension culture to a density of $2-3 \times 10^6$ cells/ml. The cell suspension was incubated on ice for 20 min and centrifuged at 2,000 rpm (Sorvall RT7 centrifuge) for 2 min at 4 °C to collect the cells. The cells were then washed with an equal volume of ice-cold Soerensen phosphate buffer and afterwards with an equal volume of ice-cold electroporation-buffer. After washings, the cells were resuspended in electroporation- buffer at a density of 1×10^8 cells/ml. For electroporation, 20-25 µg of the plasmid DNA was added to 500 µl of the cell suspension and the cell-DNA mixture was transferred to a pre-chilled electroporation cuvette (2 mm electrode gap, Bio-Rad). Electroporation was performed with an electroporation unit (Gene Pulser, Bio-Rad) set at 0.9 kV and 3 µF without the pulse controller. After electroporation, the cells were immediately spread onto a 100-mm petri dish and were allowed to sit for 10 min at 21 °C. Thereafter, 1 ml of healing-solution was added dropwise onto the cells and the petri dish was incubated at 21 °C on a shaking platform at 50 rpm for 15 min. 10 ml of AX2 medium was added into the petri dish and the cells were allowed to recover overnight. The next day, the medium was replaced by the selection medium containing appropriate antibiotic. To select for stable transformants, selection medium was replaced every 24-48 hr until the control plate (containing cells electroporated without any DNA) was clear of live cells.

Electroporation-buffer:

100 ml 0.1 M potassium phosphate buffer
17.12 g sucrose
add distilled H₂O to make 1 litre
autoclave

0.1 M Potassium phosphate buffer:

170 ml 0.1 M KH₂PO₄
30 ml 0.1 M K₂HPO₄
adjust to pH 6.1

Healing-solution:

150 µl 0.1 MgCl₂
150 µl 0.1 CaCl₂
10 ml electroporation-buffer

2.5 Endocytosis and exocytosis assays

Fluid-phase endocytosis assays were performed according to the methods of Aubry *et al.* (1994). Fluid-phase efflux assays were performed as described using TRITC-dextran (Buczynski, 1997). Briefly, *Dictyostelium* cells were grown to $< 5 \times 10^6$ cell/ml. The cells were centrifuged and resuspended at 5×10^6 /ml in fresh axenic medium at 21°C and incubated for 15 min on a shaker to allow cells to recuperate. Then TRITC-dextran was added to a final concentration of 2 mg/ml. Samples were withdrawn at different time intervals and the cells were pelleted after incubating for 3 min with 100 µl of trypan blue (2 mg/ml) to remove non-specifically bound marker. The pellet was resuspended in phosphate buffer and the fluorescence was measured using a fluorimeter (544 nm excitation/574 nm emission). For fluid-phase exocytosis assays, cells were pulsed with TRITC-dextran (2 mg/ml) for 2 hours, washed and resuspended in fresh axenic medium. Fluorescence from the marker remaining in the cells was measured at different time intervals as explained above.

Phagocytosis was performed according to Maniak *et al.* (1995). Briefly, *Dictyostelium* cells were grown to $< 5 \times 10^6$ /ml over 5 generations in axenic medium. Cells were centrifuged and resuspended at 2×10^6 /ml in fresh axenic medium at 21 °C. TRITC-labeled yeast cells prepared according to Material and Methods 5.3 were added in a 5 fold excess (10^9 yeast cells/ml stock). Cells were incubated on a rotary shaker at 160 rpm. Samples were taken at different intervals and the fluorescence of non internalized yeasts was quenched by incubating for 3 min with 100 µl trypan blue (2 mg/ml). Cells were centrifuged again, resuspended in phosphate buffer and the fluorescence was measured using a fluorimeter (544 nm excitation/574 nm emission).

3. Molecular biological methods

3.1 Purification of plasmid DNA

In general, for small cultures (3 ml) of *E. coli* transformants, the boiling method described by Holmes and Quigley (1981) was used to extract plasmid DNA. This method is good for screening

a large number of clones simultaneously for the desired recombinant plasmid. Briefly, single transformants were picked up from the culture plate and were grown overnight in 3 ml of LB media containing suitable antibiotic. Next day, the overnight grown *E. coli* cells were pelleted by centrifugation at 6,000 rpm in a microcentrifuge for 3-5 min. The pellet was then resuspended completely in 250 µl STET/lysozyme buffer and the suspension was incubated at room temperature for 10 min to lyse the bacterial cells. The bacterial lysate was boiled at 100 °C for 1 min and was then centrifuged in an eppendorf centrifuge at maximum speed for 15 min at room temperature. The plasmid DNA present in the supernatant was precipitated by adding an equal volume of isopropanol and incubating at room temperature for 10 min. The precipitated DNA was pelleted in the eppendorf centrifuge at 12,000 rpm for 15 min and the DNA pellet was washed with 70 % ethanol, dried in a speed-vac concentrator and finally resuspended in 40 µl TE, pH 8.0 containing RNase A at 1 µg/ml.

STET/lysozyme buffer, pH 8.0:

50 mM Tris/HCl, pH 8.0

50 mM EDTA

0.5 % Triton X-100

8.0 % Sucrose Add lysozyme at 1 mg/ml at the time of use.

Alternatively, for pure plasmid preparations in small and large scales (for sequencing, PCR or transformations), kits provided either by Macherey-Nagel (Nucleobond AX kit for small scale plasmid preparations) or by Qiagen (Qiagen Midi- and Maxi-Prep kit for large scale plasmid preparations) were used. These kits have the following approach: first overnight culture of bacteria containing the plasmid is pelleted and the cells are lysed by alkaline lysis. The freed plasmid DNA is then adsorbed on a silica matrix, washed with ethanol, and then eluted with TE, pH 8.0 or water. This method avoids the requirement of caesium chloride or phenol-chloroform steps during purification.

3.2 Digestion with restriction enzymes

All restriction enzymes were obtained from NEB, Amersham or Life Technologies and the

digestions were performed in the buffer systems and temperature conditions as recommended by the manufacturers. The plasmid DNA was digested for 1-2 hr.

3.3 Dephosphorylation of DNA fragments

To avoid self-ligation of the vector having blunt ends or that has been digested with a single restriction enzyme, 5' ends of the linearised plasmids were dephosphorylated by calf-intestinal alkaline phosphatase (CIAP). Briefly, in a 50 μ l reaction volume, 1-5 μ g of the linearised vector-DNA was incubated with 1 U calf-intestinal alkaline phosphatase in CIAP-buffer (provided by the manufacturer) at 37 $^{\circ}$ C for 30 min. The reaction was stopped by heat-inactivating the enzyme at 65 $^{\circ}$ C for 10 min. The dephosphorylated DNA was extracted once with phenol-chloroform and precipitated with 2 vol. ethanol and 1/10 vol. 2 M sodium acetate, pH 5.2.

3.4 Setting up of ligation reactions

A DNA fragment and the appropriate linearised plasmid were mixed in approximately equimolar amounts. T4 DNA ligase and ATP were added as indicated below and the ligation reaction was left overnight at 10-12 $^{\circ}$ C.

Ligation reaction

Linearised vector DNA (200-400 ng)
DNA fragment
4 μ l 5x ligation buffer
1 μ l 0.1 M ATP
1.5 U T4 Ligase
and water to make up to 20 μ l.

5 x Ligation buffer

Supplied with the enzyme
by manufacturers

3.5 PCR and generation of mutations by PCR-based site directed mutagenesis

For polymerase chain reaction (PCR) plasmid carrying annexin C1 cDNA (pT7-7) was used. *Dictyostelium* annexin C1 sequence carrying a mutation at the position 293 where aspartic acid (D) was replaced by alanine (A) was generated from wild type cDNA by PCR-based site directed mutagenesis. In two separate PCR reactions using the primers AnnA1-AccI and AnnA2-PstI in the first and AnnB2-PstI and AnnB1-AccI in the second, two halves of the annexin cDNA carrying wanted mutation are generated. The products of both steps were used as a template for a

new round of PCR in which AnnA1-AccI and AnnB1-AccI were used as the forward and reverse primers, respectively. PCR products were cloned into the pGEM-T easy vector and verified by sequencing.

PCR conditions:

Reaction-mix (50 μ l final volume):

1 μ l template (50-200 ng DNA)
1 μ l 5' primer (5 pmol/ μ l)
1 μ l 3' primer (5 pmol/ μ l)
1 μ l dNTP-mix (10 mM)
5 μ l 10x PCR buffer
1 μ l Taq polymerase (1 U/ μ l)
40 μ l H₂O

Reaction programme:

1-step 92 °C for 2 min
2-step 30 cycles of-
92 °C for 1 min
51 °C for 1 min
72 °C for 2 min
3-step 72 °C for 10 min
4-step 4 °C till end

3.6 DNA agarose gel electrophoresis

Agarose gel electrophoresis was performed according to the method described by Sambrook *et al.* (1989) to resolve and purify the DNA fragments. Electrophoresis was performed with 0.7 % (w/v) agarose gels or with 1 % (w/v) agarose gels in 1 x TAE buffer submerged in a horizontal electrophoresis tank containing 1 x TAE buffer at 1-5 V/cm. The percentage of agarose in the gel was dependent on size of fragments to be resolved. DNA-size marker was always loaded along with the DNA samples in order to estimate the size of the resolved DNA fragments in the samples. The gel was run until the bromophenol blue dye present in the DNA-loading buffer had migrated the appropriate distance through the gel. The gel was examined under UV light at 302 nm and was photographed using a gel-documentation system (MWG-Biotech).

DNA-size marker:

1 kb DNA Ladder (Life Technologies): 12,216; 11,198; 10,180; 9,162; 8,144; 7,126;
6,108; 5,090; 4,072; 3,054; 2,036; 1,636; 1,018;
506; 396; 344; 298; 220; 201; 154; 134; 75 bp

3.7 Recovery of DNA fragments from agarose gel

DNA fragments from restriction enzyme digests or from PCR reactions were separated by agarose gel electrophoresis and the gel piece containing the desired DNA fragment was carefully and quickly excised while observing the ethidium bromide stained gel under a UV transilluminator. The DNA fragment was then purified from the excised gel piece using the Macherey-Nagel gel elution kit (NucleoSpin Extract 2 in 1), following the method described by the manufacturers or by centrifugation through the glass wool followed by DNA precipitation.

3.8 Transformation of *E. coli*

3.8.1 Standard protocol for the preparation and transformation of competent cells

(Inoue *et al.*, 1990)

Preparation of competent *E. coli* cells by SEM:

An overnight grown culture of *E. coli* (0.5 ml) was inoculated into 250 ml LB medium and incubated at 18 °C, with shaking 250 rpm until an OD₆₀₀ of 0.4-0.6 was obtained. The bacteria were then incubated on ice for 10 minutes and pelleted at 4 °C for 10 min at 4,000 rpm (Beckman Avanti J25, rotor JA-25.50). The bacterial pellet was resuspended in 80 ml of ice-cold TB, incubated on ice for 10 min and spun down as above. The cells pellet was gently resuspended in 20 ml of TB and DMSO was added with gentle swirling to a final concentration of 7 %. After incubating on ice for 10 min, the cell suspension was aliquoted 200 µl/tube. The aliquots were then quickly frozen in a dry ice/ethanol bath and immediately stored at -80 °C.

Standard protocol for SEM transformation:

Plasmid DNA (~50-100 ng of a ligase reaction or ~10 ng of a supercoiled plasmid) was mixed with 100-200 µl of CaCl₂-competent *E. coli* cells and incubated on ice for 30 min. The cells were then heat-shocked at 42 °C for 45 s and immediately transferred to ice for 2 minutes. The cells were then mixed with 1 ml of pre-warmed (at 37 °C) SOC medium and incubated at 37 °C with

shaking at ~150 rpm for 45 min. Finally, the cells were pelleted at 20 °C for 30 s at 3,000 rpm, 2. the bacterial pellet was resuspended in 100-200 µl of SOC medium and plated onto selection plates. The transformants were allowed to grow overnight at 37 °C.

TB buffer:

10 mM HEPES

15 mM CaCl₂

250 mM KCl

adjust pH to 6.7 with KOH

dissolve MnCl₂ to have a final concentration of 55 mM in TB buffer

all salts should be added as solids

Sterilized by filtration through 0.45 µm filter and stored at 4 °C

3.8.2 Transformation of *E. coli* cells by electroporation

Preparation of electroporation-competent *E. coli* cells:

An overnight grown culture of *E. coli* (5 ml) was inoculated into 1,000 ml of LB medium and incubated at 37 °C with shaking at 250 rpm until an OD₆₀₀ of 0.4-0.6 was obtained. The culture was then incubated on ice for 15-20 min. Thereafter, the culture was transferred to pre-chilled 500-ml centrifuge bottles (Beckman) and the cells were pelleted by centrifugation at 4,200 rpm (Beckman Avanti J25, rotor JA-10) for 20 min at 4 °C. The bacterial pellet was washed twice with an equal volume of ice-cold water and the cells were resuspended in 40 ml of ice-cold 10 % glycerol, transferred to a pre-chilled 50-ml centrifuge tube and centrifuged at 3,000 rpm (Beckman Avanti J25, rotor JA-25.50) for 10 min at 4 °C. Finally, the cells were resuspended in an equal volume of 10 % chilled glycerol and aliquoted (50-100 µl) in 1.5-ml eppendorf tubes that have been placed in a dry ice/ethanol bath. The frozen aliquots were immediately transferred to -80 °C for long-term storage.

Transformation of electroporation-competent *E. coli* cells:

Plasmid DNA (~20 ng dissolved in 5-10 µl ddH₂O) was mixed with 50-100 µl electroporation-competent *E. coli* cells. The transformation mix was transferred to a 2 mm BioRad electroporation cuvette (pre-chilled) and the cuvette was incubated on ice for 10 min. The DNA

was then electroporated into competent *E. coli* cells using an electroporation unit (Gene Pulser, Bio-rad) set at 2.5 KV, 25 μ F, 200 Ω . Immediately after electroporation, 1 ml of pre-warmed (37 $^{\circ}$ C) SOC medium was added onto the transformed cells and the cells were incubated at 37 $^{\circ}$ C with shaking at \sim 150 rpm for 45 min. Finally, the cells were pelleted at 20 $^{\circ}$ C for 30 s at 3,000 rpm, the bacterial pellet was resuspended in 100-200 μ l of SOC medium and plated onto selection plates. The transformants were allowed to grow overnight at 37 $^{\circ}$ C.

3.9 Glycerol stock of bacterial cultures

Glycerol stocks of all the bacterial strains/transformants were prepared for long-term storage. The culture was grown overnight in LB medium with or without the selective antibiotic (depending upon the bacterial transformation). 850 μ l of overnight culture was added to 150 μ l of sterile glycerol in a 1.5 ml microcentrifuge tube, mixed well by vortexing and the tube was frozen on dry ice and stored at -80° C.

Alternatively, 950 μ l of overnight culture was mixed with 70 μ l of DMSO in a 1.5 ml microcentrifuge tube and stored at -80° C.

3.10 Construction of vectors

3.10.1 Vectors for expression of annexin as GFP-fusion proteins

Vectors were constructed that allowed expression of GFP fused to C- or N-terminus of annexin in *Dictyostelium* cells under the control of the actin-15 promoter. Full length annexin was amplified using the cDNA as source with appropriate primers carrying add-on BamHI-linkers or AccI-linkers. The PCR product was digested with BamHI or AccI and cloned into similarly cut pDdA15gfp (Neujahr *et al.*, 1997) or ClaI cut pDEX-RH (Westphal *et al.*, 1997) expression vectors. GFP was fused to the C- or N-terminus of *Dictyostelium* annexin, respectively. The full length annexin carrying the mutation in its core domain was generated as previously described (Material and Methods 3.5) and cloned into ClaI cut pDEX-RH vector with GFP on its N-terminal. For analysis of the function of annexin core domain, annexin cDNA was used for PCR

reaction with appropriate primers carrying add-on AccI linkers and the PCR product was cloned in ClaI cut pDEX-RH vector. GFP was fused to N-terminus of annexin core. Single colonies expressing annexin-GFP were further analysed. The resulting vectors were introduced into AX2 or SYN⁻ (Döring *et al.*, 1995) cells by electroporation. Since SYN⁻ cells already had G418 resistance, pUC vector carrying blasticidin resistance was introduced simultaneously. After selection for growth in the presence of G418 or G418 and blasticidin, GFP-expressing transformants were confirmed by visual inspection under a fluorescence microscope. Furthermore, the size of expressed fusion protein was confirmed as well by Western blot.

3.11 DNA sequencing

Sequence of the PCR-amplified products or plasmid DNA was performed at the sequencing facility of the Centre for Molecular Medicine, University of Cologne, Cologne by the modified dideoxy nucleotide termination method using a Perkin Elmer ABI prism 377 DNA sequencer.

3.12 Computer analyses

Sequencing analysis, homology searches, structural predictions and multiple alignment of protein sequences were performed using the University of Wisconsin GCG software package (Devereux *et al.*, 1984) and Expasy Tools software, accessible on the world-wide web.

4. Biochemical methods

4.1 Preparation of total protein from *Dictyostelium*

1×10^7 to 5×10^8 *Dictyostelium* cells either vegetative or at different stages of development were washed once in Soerensen phosphate buffer. Total protein was prepared by lysing the pellet of cells in 500 μ l 1 x SDS sample buffer. Equal amounts of protein (equivalent to 2×10^5 to 1×10^7 cells/lane) were loaded onto discontinuous SDS-polyacrylamide gels.

4.2 Subcellular fractionation

2×10^7 cells were resuspended in 1 ml of the lysis buffer and opened by sonication. Cytosol and membranes were separated by centrifugation at 10,000 x g for 1 hour at 4 °C. Membrane pellet was afterwards two times washed in lysis buffer at 10, 000 x g for 15 min. Supernatant was further centrifuged at 100,000 x g for 1 hour at 4 °C. Obtained pellet was then washed as described and supernatant was collected. For the fractionation of membranes on sucrose gradient 8×10^8 cells were washed in Soerensen phosphate buffer and resuspended in a HEPES buffer. The cells were opened by sonication, nuclei were removed by centrifugation at 720 x g and, after separation of membranes from the cytosol by centrifugation at 100,000 x g for 1 hour, the membrane pellet was loaded onto sucrose step gradient (2.45 M, 1.45 M, 1.32 M, 1.16 M, 0.88 M sucrose in HEPES buffer, pH 7.4). The gradients were centrifuged at 100,000 x g in a SW41 rotor (Beckman Coulter, Munich, FRG) for 18 hours at 4 °C. Fractions were afterwards collected, corresponding to the layers of different density, checked for alkaline phosphatase activity as plasma membrane marker (Loomis, 1969), acid phosphatase activity as lysosomal marker (Loomis and Kuspa, 1984) and comitin as Golgi marker (Weiner *et al.*, 1993). The fractions were separated by SDS PAGE followed by immunoblotting.

Lysis buffer

30 mM Tris-HCl, pH 7.0
0.5 mM PMSF
5 mM benzamidine
30 % sucrose
2 mM DTT

HEPES buffer

30 mM HEPES, pH 7.4
0.5 mM PMSF
5 mM benzamidine
2 mM DTT

4.3 Triton X-100 extraction of *Dictyostelium* cells

For preparation of the Triton X-100 insoluble fraction growth phase AX2 and annexin-GFP expressing *Dictyostelium* cells were washed and resuspended in lysis buffer and lysed with 1 % Triton X-100 in the presence or absence of 100 μ M CaCl₂ for 15 min on ice. The Triton X-100-insoluble material which included cytoskeleton associated proteins was pelleted at 4 °C for 10 min

at 14,000 x g. The supernatant was carefully collected and the pellet was washed twice and finally resuspended in lysis buffer. Proteins of the Triton X-100-soluble and -insoluble fractions were extracted in 2 x SDS sample buffer and resolved on SDS-polyacrylamide gels. The resolved proteins were blotted onto a nitrocellulose membrane and the blot was subsequently probed with anti annexin mAb 185-447-3 (Döring *et al.*, 1995) and anti actin Act 1-7 antibody (Simpson *et al.*, 1984).

Lysis buffer

10 mM HEPES, pH 7.4

138 mM KCl

3 mM MgCl₂

Protease inhibitor cocktail (10 µg/ml of each inhibitor, Roche)

4.4 Gelfiltration

Analytical gel filtration employed the SMART System™ (Amersham Biosciences). The Superdex® 200 PC 3.2/30 column equilibrated in 100 mM NaCl in 0,33 x PBS pH 7.4, buffer, operated at a flow rate of 6 ml/h. Thyreoglobulin (669 kDa), ferritin (440 kDa), aldolase (158 kDa), ovalbumin (43 kDa) and chymotrypsinogen (25 kDa) were used for Mw calibration. 10 µg of each protein was loaded onto the column. Before loading, all the samples (the cells were previously opened by sonication) and standards were purified by centrifugation at 4 °C, for 1 hour at 100,000 x g. The gel filtration technique is a method to separate proteins according to their molecular mass. The principle of the gel filtration theory is that proteins occupy a volume directly proportional to their molecular mass, and that they will diffuse and be separated through a gel with different rates depending on their ability to enter the pores of the gel matrix. Because the pore accessibility depends not only on the molecular mass but also on the size of the molecule, proteins will be separated according to their molecular mass and size. It is therefore possible that two proteins, even with the same molecular mass, but with a completely different folding that leads to a different shape, volume and finally accessibility to the gel pore, can be successfully separated by a gel filtration experiment. The samples were subsequently analyzed by Western blotting.

4.5 Isolation of phagosomes

Phagosomes from AX2 cells and cells expressing annexin-GFP were prepared as described (Maniak *et al.*, 1995) with some modifications. Cells were washed twice in Soerensen phosphate buffer, resuspended at 4×10^6 cells/ml in nutrient medium and allowed to recover for 30 minutes at 21 °C. Carboxylated para magnetic beads of 1-2 µm diameter (Polysciences Europe GmbH, Eppelheim, FRG) were then added in a ratio of 100 beads per cell. The suspension was shaken for 10 minutes and phagocytosis was stopped by centrifugation at 720 x g at 4 °C and by washing three times with ice-cold Soerensen phosphate buffer. The pellet was resuspended to a cell density of 5×10^7 /ml in homogenization buffer. Cells were opened

by three cycles of freezing in liquid nitrogen and thawing on ice. Phagosomes were separated from the lysate by magnetic extraction and washed three times in homogenization buffer. For determination of the protein concentration, phagosomes were kept at 95 °C for 5 minutes in lysis buffer and for SDS-PAGE and immunoblotting in 2 x SDS sample buffer. The beads were removed by centrifugation.

Homogenisation buffer

30 mM Tris-HCl, pH 8.0
30 % sucrose
3 mM DTT
3 mM benzamidine
0.5 mM PMSF

Lysis buffer

20 mM Tris-HCl, pH 8.0
0.1 % SDS
1 mM DTT
10 mM EDTA
0.5 mM PMSF

4.6 Immunoprecipitation experiments

300 ml of dense Dictyostelium shaking culture (5×10^6 cells / ml) was centrifuged at 2 000 x g for 3 min at 4 °C. The cell pellet was washed twice in Soerensen phosphate buffer and resuspended finally in immunoprecipitation (IP) buffer. The volume of the buffer depended on the obtained amount of cells (for 1 g of the cell pellet 2 ml of the buffer was used). The cells were than opened by sonication. The cell lysate was prior immunoprecipitation pre-cleared with Protein sepharose A beads for 30 min and not opened cells and proteins non specifically bound to the beads were removed by centrifugation (2,000 x g , for 3 min, at 4 °C). Cleared cell lysate was than incubated with chosen anti body for 3-4 hours at 4 °C and the sepharose A beads were

subsequently added. After incubation for 30–60 min the samples were centrifuged for 3 min at 2,000 x g and the beads pellet was washed several times in the IP buffer. Finally, the samples were resuspended in the SDS-sample buffer and subsequently resolves by SDS-PAGE (see the next chapter).

Immunoprecipitation buffer:

0.33 x PBS

2 mM benzamidine

4 mM DTT

0.5 mM PMSF

(Triton X-100 was added after the sonication to the final concentration of 0.5 %)

4.7 2D gel electrophoresis

Two dimensional electrophoresis (2D-electrophoresis) is a widely used method for the analysis of complex protein mixtures extracted from cells, tissue or other biological samples. The technique separates proteins according to two independent properties in two discrete steps: The first dimension is an isoelectric focusing which separates proteins according to their isoelectric point (pI); the second dimension is an SDS-PAGE which separates proteins according to their molecular weights. Thus, every spot in 2D-electrophoresis provides information about protein's pI and molecular weight. Because the pI of unphosphorylated and phosphorylated proteins is different, whereas the molecular masses are only marginally different, this method allows also the detection of this covalent modification.

For isoelectric focusing, Multiphor II system (Amersham Biosciences) was used. The procedure was performed as described in the manual supplied by manufacturer. Shortly, 5×10^6 cells were pelleted, washed twice in Soerensen phosphate buffer and finally resuspended in 2D-lysis buffer. DTT and IPG buffers were added to the mixture at a final concentration of 2 % (v/v) immediately prior to use. Subsequently, a trace of bromphenol blue was added to the sample. Prior this step, IPG strips (pI 3-10, 7 cm, Amersham Biosciences) were rehydrated (in an IPG-strip tray) in the rehydration buffer over night at room temperature. To minimize evaporation and urea crystallization, mineral oil was applied to cover the surface of the strip. The rehydrated IPG strips were cleaned afterwards with water and transferred to adjacent grooves of the aligner in the

immobiline dry strip tray. The strips were placed with the acidic (pointed) end at the top of the tray near the anode, and the blunt end positioned at the bottom of the tray near the cathode. The electrodes and the sample cups were carefully positioned and the samples were loaded into the sample cups. To avoid urea crystallization, a drop of mineral oil was applied to cover the surface. Isoelectric focusing was performed with a program described below. After finished first dimension, the IPG strips were washed with water and incubated with SDS-equilibration buffer for 20 min at room temperature. The second dimension was done as described in Material and Methods 4.8. Western blotting (see Material and Methods 4.9) and immunodetection (Material and Methods 4.10) followed.

2D-lysis buffer:

8 M urea
4 % W/V CHAPS
2 % DTT
40 mM Tris-HCl, pH 8.0
2 % IPG buffer
1 mM sodium orthovanadate
10 mM sodium fluoride
5 mM sodium pyrophosphate
10 mM β glycerophosphate
1 x complete mini protease inhibitor

SDS-equilibration buffer:

6 M urea
30 % (v/v) glycerol
2 % SDS (w/v)
2 % DTT
50 mM Tris-HCl, pH 8.8

Rehydration buffer:

8 M urea
4 % w/v CHAPS
1 % IPG buffer
2 % DTT

Isoelectric focusing:

10 min 150 V
90 min 150 V
30 min 300 V
4 hours 300 V
10 min 3500 V
30 min 3000 V
16 hours 3000 V, at 16 °C

4.8 SDS-polyacrylamide gel electrophoresis

SDS-polyacrylamide gel electrophoresis (SDS-PAGE) was performed using the discontinuous buffer system of (Laemmli, 1970). Discontinuous polyacrylamide gels (10-15 % resolving gel, 5 % stacking gel) were prepared using glass plates of 10 cm x 7.5 cm dimensions and spacers of 0.5 mm thickness. A 12-well comb was generally used for formation of the wells in the stacking

gel. The composition of 12 resolving and 12 stacking gels is given in the table below. Samples were mixed with suitable volumes of SDS sample buffer, denatured by heating at 95 °C for 5 min and loaded into the wells in the stacking gel. A molecular weight marker, which was run simultaneously on the same gel in an adjacent well, was used as a standard to establish the apparent molecular weights of proteins resolved on SDS- polyacrylamide gels. The molecular weight markers were prepared according to manufacturer's specifications. After loading the samples onto the gel, electrophoresis was performed in 1 x gel-running buffer at a constant voltage of 100-150 V until the bromophenol blue dye front had reached the bottom edge of the gel or had just run out of the gel. After the electrophoresis, the resolved proteins in the gel were transferred onto a nitrocellulose membrane.

Components	<u>Resolving gel</u>			<u>Stacking gel</u>
	10 %	12 %	15 %	5 %
Acrylamide/Bisacrylamide (30:0.8) [ml]:	19.7	23.6	30	4.08
1.5 M Tris/HCl, pH 8.8 [ml]:	16	16	16	-
0.5 M Tris/HCl, pH 6.8 [ml]:	-	-	-	2.4
10 % SDS [μl]:	590	590	590	240
TEMED [μl]:	23	23	23	20
10 % APS [μl]:	240	240	240	360
Deionised H ₂ O [ml]:	23.5	19.6	13.2	17.16

2 x SDS-sample buffer:

100 (mM) Tris/HCl, pH 6.8
 4 (% v/v) SDS
 20 (% v/v) glycerine
 0.2 (% v/v) bromophenol blue
 4 (% v/v) β-mercaptoethanol

Molecular weight markers:

94, 67, 43, 30, 20.1, 14.4 kD

4.9 Western blotting using the semi-dry method

The proteins resolved by SDS-PAGE were electrophoretically transferred from the gel to a nitrocellulose membrane by the method described by Towbin *et al.* (1979) with little modifications. The transfer was performed using Towbin's buffer in a semi-dry blot apparatus

(Bio-Rad) at a constant voltage of 10 V for 45-90 min. The instructions provided along with the semi-dry apparatus were followed in order to set up the transfer.

Transfer buffer:

39 mM glycine,
48 mM Tris/HCl, pH 8.3
and 10 % methanol

4.10 Immunodetection of membrane-bound proteins

The Western blot was immersed in blocking buffer and the blocking was performed with gentle agitation either overnight at 4 °C or for 30 min. to 1 hour at room temperature.

After blocking, the blot was incubated at room temperature with gentle agitation with hybridoma supernatant for 1-2 h. After incubation with primary antibody, the blot was washed 5-6 times with 1 x NCP at room temperature for 5 min each with repeated agitation.

Following washings, the blot was incubated for 1 hr at room temperature with an appropriate dilution (in 1 x NCP) of horse radish peroxidase-conjugated secondary antibody directed against the primary antibody. After incubation with secondary antibody, the blot was washed as described above. After washings, enhanced chemi-luminescence (ECL) detection system was used. For this, the blot was incubated in ECL-detection-solution for 1-2 min and then wrapped in saran wrap after removing the excess ECL-detection solution. A X-ray film was exposed to the wrapped membrane for 1-30 min and the film was developed to observe the immunolabelled protein.

ECL-detection solution:

2 ml 1 M Tris/HCl, pH 8.0
200 µl 250 mM 3-aminonaphthylhydrazide in DMSO
89 µl 90 mM p-Coumaric acid in DMSO
18 ml deionised H₂O
6.1 µl 30 % H₂O₂ (added just before using)

Blocking buffer :

5 % milk powder in 1 x
NCP

5. Immunological methods

5.1 Indirect immunofluorescence of *Dictyostelium* cells

5.1.1 Preparation of *Dictyostelium* cells

Dictyostelium cells were grown in shaking culture to a density of $2-4 \times 10^6$ cells/ml. The desired amount of cells was collected in a centrifuge tube, cells were then washed two times in Soerensen phosphate buffer and finally resuspended in the same buffer at a density of 1×10^6 cells/ml. Around 300 μ l of the cell suspension was then pipetted onto the coverslips and cells were allowed to attach for 20 min. Thereafter, cells attached onto the coverslip were fixed immediately as described below.

5.1.2 Methanol fixation

After the cells attached to the coverslip, the supernatant was aspirated and the coverslip was dipped instantaneously into pre-chilled (-20°C) methanol in a petri dish and incubated at -20°C for 10 min. The coverslip was then taken out from methanol and placed on a parafilm covered glass plate resting in a humid box with the cell-surface facing upwards. This was followed by 3 washings with 500 μ l of PBS-Gly for 5 min each than 2 washings with 500 μ l of PBG for 15 min each and immunolabelling as described in section 5.1.3.

PBS-Gly, pH 7.4
0.1 M Gly
in 1 x PBS, pH 7.4

PBG, pH 7.4:
0.5 % bovine serum albumin
0.1 % gelatin (cold-water fish skin)
in 1 x PBS, pH 7.4

5.1.3 Immunolabelling of fixed cells

Coverslips containing the fixed cells were incubated with 200 μ l of the desired dilution (in PBG) of primary antibody for 1-2 hr in a humid box at room temperature. After incubation, the excess unattached antibody was removed by washing the coverslip 6 times with PBG for 5 min each.

Now the coverslip was incubated for 30 min with 200 μ l of a proper dilution (in PBG) of Cy3-conjugated secondary antibody. Following this incubation, two washings with PBG for 5 min each followed by three washings with PBS-Gly for 5 min each were performed. After washings, the coverslip was mounted onto a glass slide (see sections, 5.1.4).

5.1.4 Mounting of coverslips

After immunolabelling of the fixed cells, the coverslip was swirled once in deionised water and the extra water was soaked off on a soft tissue paper. Now a drop of gelvatol was placed to the middle of a clean glass slide and the coverslip was mounted (with the cell-surface facing downwards) onto the drop of gelvatol, taking care not to trap any air-bubble between the coverslip and the glass slide. Mounted slides were then stored overnight in the dark at 4 $^{\circ}$ C. Thereafter, the mounted slides were observed under a fluorescence microscope or confocal laser scanning microscope.

Gelvatol:

2.4 g of polyvinyl alcohol (Mw 30,000-70,000; Sigma) was added to 6 g of glycerol in a 50 ml centrifuge tube and mixed by stirring. To the mixture, 6 ml of distilled water was added and the mixture was incubated at room temperature. After several hours of incubation at room temperature, 12 ml of 0.2 M Tris/HCl, pH 8.5, was added and the mixture was heated to 50 $^{\circ}$ C for 10 min with occasional mixing to completely dissolve polyvinyl alcohol. The solution was centrifuged at 5,100 rpm for 15 min. After centrifugation, 2.5 % of diazabicyclo octane (DABCO), an anti-oxidant agent, was added to reduce the bleaching of the fluorescence. The solution was aliquoted in 1.5 ml microcentrifuge tubes and stored at -20 $^{\circ}$ C.

5.2 Immunolabelling of GFP-annexin expressing *Dictyostelium* cells fixed during phagocytosis

To correlate the localization of annexin with the organization of the actin cytoskeleton during the process of phagocytosis, GFP-annexin expressing cells were fixed during phagocytosis and immunolabelled with anti-actin monoclonal antibody (Act 1-7). Briefly, cells were prepared as explained in sections 5.1.1. After the cells had adhered to the glass coverslip, the Soerensen

phosphate buffer on the coverslip was replaced with 400 μ l of a suspension containing heat-killed yeast cells diluted 1:10 in Soerensen phosphate buffer. Cells were incubated with yeast for 20 min. Thereafter, the buffer on the coverslips was carefully aspirated and the cells were immediately fixed by the methanol fixation method (see sections, 5.1.2). After fixation and usual washings, either the coverslip was directly mounted onto a glass slide or the cells were first immunolabelled with anti-actin monoclonal antibody (Act 1-7) as described in section 5.1.3, before mounting onto a glass slide.

Preparation of heat-killed yeast cells:

Five grams of dry yeast *Saccharomyces cerevisiae* (Sigma) were suspended in 50 ml of PBS in a 100 ml Erlenmeyer flask and incubated for 30 min in a boiling waterbath with stirring. After boiling, the yeast cells were washed five times with PBS, followed by two washings with Soerensen phosphate buffer. The yeast cells were then finally resuspended in Soerensen phosphate buffer at a concentration of 1×10^9 yeast cells/ml. Aliquots of 1 ml and 20 ml were made and stored at -20°C .

TRITC-labelling of heat-killed yeast cells :

For labelling, the pellet of 2×10^{10} heat-killed yeast cells were resuspended in 20 ml of 50 mM Na_2HPO_4 , pH 9.2, containing 2 mg of TRITC (Sigma) and incubated for 30 min at 37°C on a rotary shaker. After washing twice with 50 mM Na_2HPO_4 , pH 9.2, and four times with Soerensen phosphate buffer, aliquots of 1×10^9 yeast cells/ml were frozen at -20°C .

6. Microscopy

Visual inspection of *Dictyostelium* cells expressing annexin was performed using an inverted fluorescence microscope (Olympus IX70). Confocal images of immunolabelled specimens were obtained with confocal laser scanning microscope TCS-SP (Leica) equipped with a 63 x PL Fluotar 1.32 oil immersion objective. A 488-nm argon-ion laser for excitation of GFP fluorescence and a 568-nm krypton-ion laser for excitation of Cy3 or TRITC fluorescence were

used. For simultaneous acquisition of GFP and Cy3 fluorescence, the green and red contributions to the emission signal were acquired separately using the appropriate wavelength settings for each photomultiplier. The images from green and red channels were independently attributed with colour codes and then superimposed using the accompanying software.

6.1 Live cell imaging of *Dictyostelium* cells expressing GFP-annexin

To record the distribution of annexin-GFP in living cells, cells were grown to a density of $2-3 \times 10^6$ cells/ml, washed in Soerensen phosphate buffer and resuspended at a density of 1×10^7 cells/ml. The cells were then starved for about 1 hr with shaking. Starvation facilitated observation as it allowed the cells to digest endocytosed nutrient medium, which is autofluorescent. For observation, cells were initially diluted in Soerensen phosphate buffer at 1×10^6 cells/ml and then 500 μ l of the cell suspension were transferred onto a 18 mm glass coverslip glued to a plastic rim of the same size. Cells were allowed to adhere to the glass coverslip for 10-15 min and confocal images were obtained and processed as described above.

6.1.2 Live cell imaging of GFP-annexin during pinocytosis

For analysis of dynamics of GFP-annexin during pinocytosis, coverslips containing GFP-annexin expressing cells were prepared as described above. After the cells had adhered to the glass coverslips, confocal images were obtained as explained above.

6.1.3 Manipulation of the cytoplasmic pH of GFP-annexin expressing living cells

For manipulation of the cytoplasmic pH, half of the volume (0.25 ml) was replaced by 20 mM MES buffer, pH 6.0, containing 40 mM propionic acid (20 mM final concentration), or by 0.25 ml of 20 mM Tris-HCl buffer, pH 8.0, containing 20 mM ammonium chloride. The effect of propionic acid was reversed by removing 0.25 ml of the MES buffer, pH 6.0, and adding the same volume of ammonium chloride in Tris-HCl buffer, pH 8.0. The procedure was repeated twice to achieve a final concentration of 10 mM ammonium chloride and a buffer pH of 7.3 ± 0.1

(Hanakam *et al.*, 1996). Confocal sections were obtained by scanning at different intervals in one plane using a 488-nm argon-ion laser for GFP fluorescence and a 568-nm krypton-ion laser for TRITC fluorescence using a Leica TCS-SP laser scanning microscope with a 63 x PL Fluotar 1.32 oil-immersion objective (Leica Lasertechnik GmbH, Heidelberg, FRG).

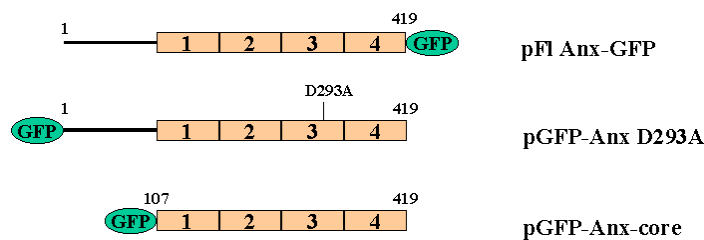
6.2 Microscopy of agar plates

To determine development of *Dictyostelium* on phosphate agar plates an Olympus SZ-045TR stereo microscope was used or Leica MZFIII stereo microscope. Images were captured with a JAI CV-M10 or Hitachi HV-C20A CCD video camera and for processing images Adobe Photoshop was used.

1. Biochemical studies

1.1. Expression of the full length annexin, a mutated annexin and the annexin core as GFP fusion proteins in AX2 and SYN⁻ cells

The SYN⁻ cells (Döring *et al.*, 1995) were stably transformed with the pDdA15-GFP vector into which the full length annexin cDNA had been cloned (pFl Anx-GFP) in order to express annexin tagged C-terminally with GFP, Fl Anx-GFP (Fig. 3). Since the vector was carrying the G418 resistance cassette which had been used to generate the mutant cells, SYN⁻ cells were simultaneously transformed with a pUC vector carrying a blasticidin resistance cassette to allow selection of the transformants. The transformants (RES) were confirmed visually by testing the fluorescence of the green fluorescent protein (not shown) and by Western blot analysis (Fig. 4). In addition, wild-type AX2 cells were stably transformed with pFl Anx-GFP (Fig. 3). In whole cell homogenates of transformants a monoclonal antibody raised against the annexin core domain (Döring *et al.*, 1995) recognized the GFP fusion protein (74 kDa) as well as both isoforms (47 and 51 kDa) of the endogenous protein (Fig. 4A).



	<i>Fl Anx-GFP</i>	<i>GFP-Anx D293A</i>	<i>GFP-Anx-core</i>
<i>AX2</i>	AX2-Anx-GFP	AX2 D293A	AX2-core
<i>SYN⁻</i>	RES	SYN ⁻ D293A	SYN ⁻ -core

Fig. 3. Schematic description of the constructs used for transformations and the obtained cell lines. The full length annexin cDNA was cloned into the pDdA15-GFP vector in order to express C-terminally GFP-tagged annexin (Fl Anx-GFP). The wild type AX2 and SYN⁻ cells were transformed with the described vector and two cell lines were obtained, AX2-Anx-GFP and RES, respectively (Table). The annexin full length cDNA carrying a mutation in the third annexin repeat, where aspartic acid at the position 293 was replaced with alanine,

as indicated in the scheme (GFP-Anx D293A) was cloned into the pDEX-RH vector. The strains obtained by transformation of this construct into the AX2 and SYN^- cells were named AX2 D293A and SYN^- D293A, respectively. Finally, the annexin core domain was cloned into the pDEX-RH vector (GFP-Anx-core). The cells (AX2 and SYN^-) in which this vector was introduced expressed the annexin core carrying GFP at its N-terminus and were called AX2-core and SYN^- -core.

Furthermore, SYN^- cells were transformed with pDEX-RH vector in which GFP was fused with annexin cDNA carrying a mutation in its core domain at the position 293 where aspartic acid was replaced by alanine (pGFP-Anx D293A, Fig. 3 and Fig. 4B). The mutation was generated by site directed mutagenesis (Material and Methods 3.5). Finally, the annexin core domain was fused at its N-terminus to GFP using the pDEX-RH vector (pGFP-Anx-core) and introduced into AX2 and SYN^- cells (Fig. 3 and Fig. 4B). SYN^- cells were simultaneously co-transformed with pUC-*bsr* vector to allow the selection of the transformants. The monoclonal anti annexin antibody 185-447-3 recognized in homogenates of these cells a protein of approximately 64 kDa corresponding to the size of the fusion of the annexin core domain and GFP. In wild type cells endogenous protein was detected as well. The expression level of GFP-fusion proteins is similar to the one of the endogenous protein (Fig. 4B).

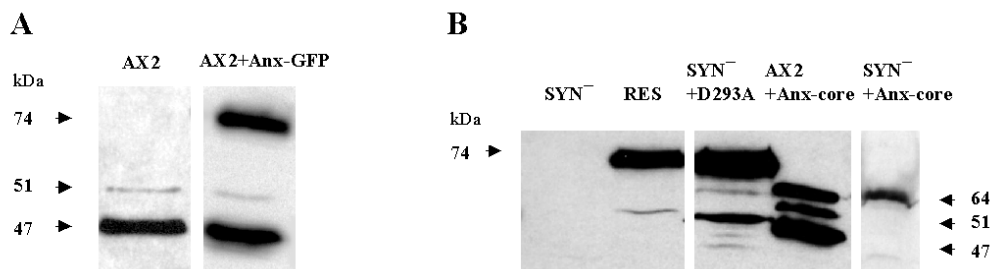


Fig. 4. Expression of annexin-GFP fusion proteins in wild type and mutant cells. Total cellular extracts from *D. discoideum* strains AX2, AX2+Anx-GFP, SYN^- , RES, SYN^- D293A and AX2+GFP-Anx-core (5×10^5 cells per lane) were separated by SDS-PAGE (12 % acrylamide). Monoclonal antibody 185-447-3 raised against the annexin core domain was used for detection of annexin in all strains. The antibody recognizes the 47 and 51 kDa isoform as well the annexin-GFP fusion proteins. The additional bands detected in SYN^- +D293A cells represent degradation products of the GFP-Anx D293A protein .

1.2 Subcellular localization of endogenous annexin and the various annexin GFP-fusion proteins

In methanol-fixed AX2 cells expressing annexin-GFP the plasma membrane is the most prominently labeled structure. The GFP-fluorescence is also present throughout the cytoplasm where it is diffusely distributed and also present on internal membranes and in the nucleus (Fig. 5B). This distribution resembles the one described previously for endogenous annexin (Fig. 5A) using monoclonal antibodies (Döring *et al.*, 1995). In all other strains (SYN⁻ D293A, SYN⁻-core and AX2-core), the annexin fusion proteins showed the same localization as endogenous annexin in AX2 wild type cells (Fig. 5.C-F, respectively).

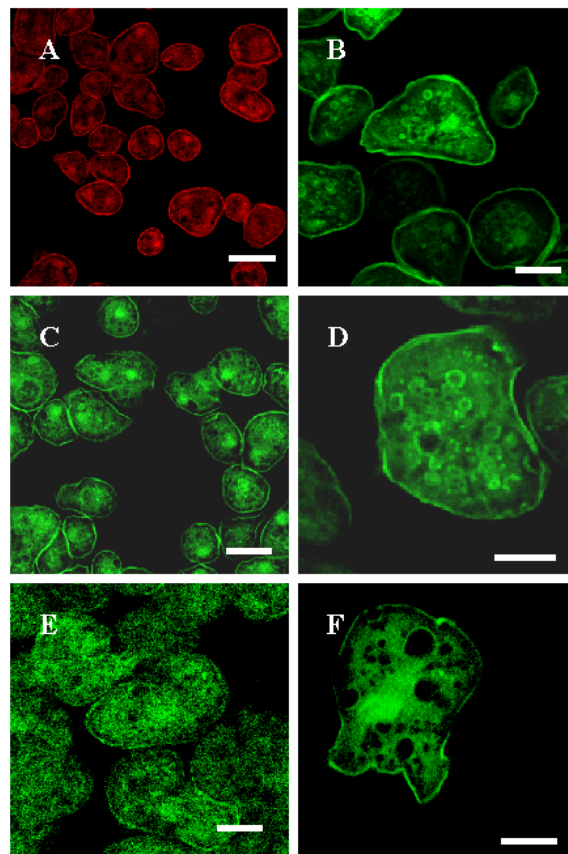


Fig. 5. Localization of annexin-GFP protein in *D. discoideum*. AX2 cells (A) grown in shaking culture were harvested at a density of $2-3 \times 10^6$, washed twice with Soerensen phosphate buffer, pH 6.0, and fixed with methanol ($-20\text{ }^{\circ}\text{C}$). Staining was done with mAb 185-338-1 followed by incubation with Cy3 labelled secondary antibody. AX2-Anx-GFP cells (B), AX2-core (F), SYN⁻ D293A cells (C and higher magnification in D) and SYN⁻-core (E)

were harvested at the same time point, washed and fixed with cold methanol. Bar, 6 μm (A and C), 2 μm (D), 3 μm (B and E) and 4 μm (F). Analysis was done by confocal microscopy.

In order to test whether the previously described subcellular distribution of annexin could be confirmed in cell fractionation experiments we separated cytosol and membranes by centrifugation. The cytosol fraction was obtained by centrifugation at 100,000 x g. The fraction which contained microsomes and vesicles was obtained by centrifugation at 100,000 x g (P_{10}) and the cytoskeleton and plasma membrane fraction was obtained by centrifugation at 10,000 x g (P_{100}). We found endogenous annexin, annexin-GFP and GFP-Anx D293A in the cytosolic and in the membrane fractions. The membrane pellet obtained from wild type cells by centrifugation at 100,000 x g contained lesser amounts of annexin when compared with the supernatant fractions and the fraction obtained by centrifugation at 10,000 x g (Fig. 6A). The P_{10} and P_{100} fractions from SYN^- D293A and RES cells (Fig. 6B) and AX2+Anx-GFP cells (Fig. 6A) showed nearly comparable amounts of annexin which were however lower than the one in the supernatant fractions (Fig. 6B). Furthermore, in AX2-core and SYN^- -core strains annexin core domain was observed in slightly higher amounts in the P_{100} fractions when compared with S and P_{10} fractions (Fig. 6C). This distribution of annexin and various annexin GFP-fusion proteins confirmed observations obtained by confocal microscopy (Fig. 5).

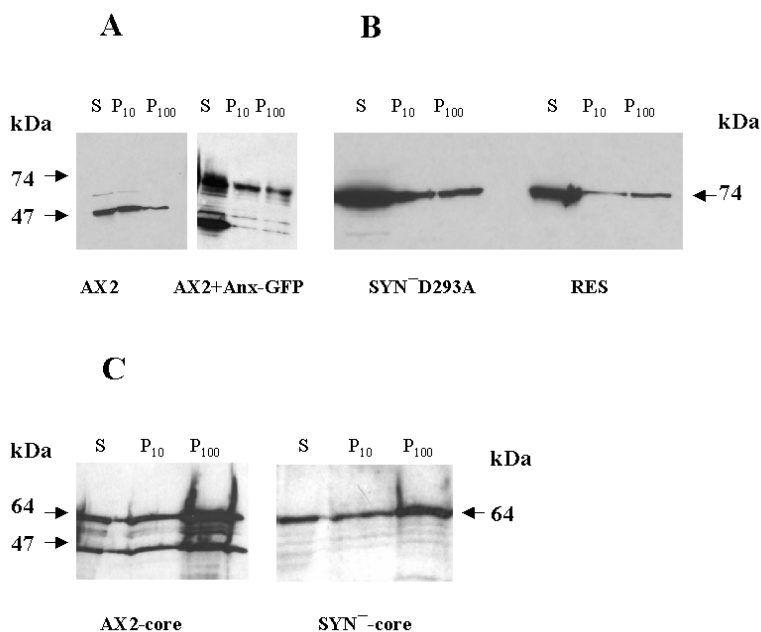


Fig. 6. (Previous page) **Analysis of annexin and annexin-GFP distribution by cell fractionation experiments.** 1×10^7 cells were opened by sonication and nuclei were removed by centrifugation at 720 x g. The supernatant was fractionated into soluble (S) and membrane fractions (P_{10} and P_{100}). Supernatant fraction (S) was obtained by centrifugation at 100,000 x g and P_{10} and P_{100} were obtained by centrifugation at 10,000 x g and 100,000 x g, respectively. (A, B and C). The blot was probed with anti annexin antibody mAb 185-447-3 and the detection was done as described in Material and Methods (4.10).

1.3 Association of annexin with intracellular membranes

The GFP fluorescence revealed an association of annexin with intracellular membranes (Fig. 5). To identify these membranes we performed co-immunostaining with antibodies specific for the A subunit of the V/H^+ -ATPase, a protein specific for membranes of the contractile vacuole and on early endosomes of *D. discoideum* (Jenne *et al.*, 1998; Clarke *et al.*, 2002; Maniak, 2003). The results indicated an overlapping localization at some but not all V/H^+ -ATPase positive structures. Furthermore, annexin occasionally co-localized with vacuolin, a marker for late stage endosomes (Rauchenberger *et al.*, 1997) (Fig. 7).

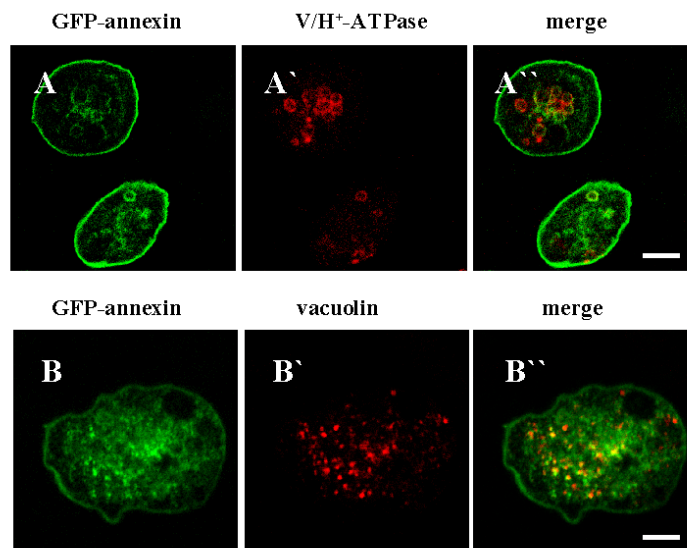


Fig. 7. Co-localization of annexin with V/H^+ -ATPase and vacuolin. Co-immunostaining of fixed cells expressing annexin-GFP with mAb 221-35-2 recognizing the A subunit of the V/H^+ -ATPase (A''), a marker for contractile vacuoles and endo/lysosomes, showed localization of annexin at these structures. Annexin co-localizes as well with vacuolin, a marker for vacuoles of the post-lysosomal compartment (B''). The immunostaining was performed with mAb 221-1-1. Bar, 5 μ m (A) and 1,5 μ m (B). The analysis was done by confocal microscopy.

Further fractionation of membranes in a discontinuous sucrose gradient confirmed the immunofluorescence data and showed that both the endogenous protein and annexin-GFP co-distributed throughout the gradient and were present in the plasma membrane fraction, the Golgi fraction and in fractions containing endosomes and lysosomes (Fig. 8C, D; fractions 5-8). Annexin-GFP was present to a lesser extent in the ER fraction (Fig. 8C, D; fractions 9 and 10). For control, we examined the distribution of comitin, which corresponded to the published pattern and was mainly present in fractions containing Golgi and ER membranes (Weiner *et al.*, 1993).

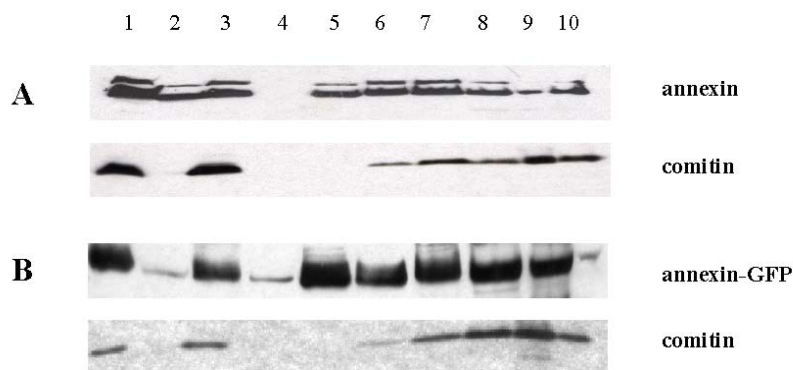


Fig. 8. Analysis of annexin and annexin-GFP distribution by separation of membranes on a discontinuous sucrose gradient. Membranes of wild type cells (A) and of cells expressing annexin-GFP (B) were separated by sucrose density gradient centrifugation (Material and Methods 4.2). Immunoblotting was performed with mAb 185-447-3 for detection of annexin and annexin-GFP. For comparison the comitin recognizing mAb 190-340-3 was used. Comitin is a protein mainly present in Golgi and ER-membrane containing fractions (Weiner *et al.*, 1993). Detection was done as described for Fig. 4. Lane 1, cell homogenates; 2, cytosol; 3, total membranes; 4, gradient supernatant; 5, plasma membrane; 6, Golgi; 7, 8, 9, endosomes, lysosomes; 10, ER.

Since the contractile vacuole complex is the major osmoregulatory organelle of the cell, we studied a possible role of annexin in osmoregulation and compared the growth of wild type, SYN^- cells and cells overexpressing annexin in the presence of 30 mM NaCl or 115 mM sorbitol. The complete absence of annexin had no influence on growth under hyperosmotic conditions as the SYN^- mutant was affected in the same fashion as wild type cells (Fig. 9A, B). AX2 cells expressing annexin-GFP in addition to the endogenous protein showed the highest sensitivity to

hyperosmotic conditions when cultivated in the presence of sorbitol (Fig. 9A). Increased concentration of NaCl in nutrient medium affected all the tested strains in the same manner (Fig. 9B).

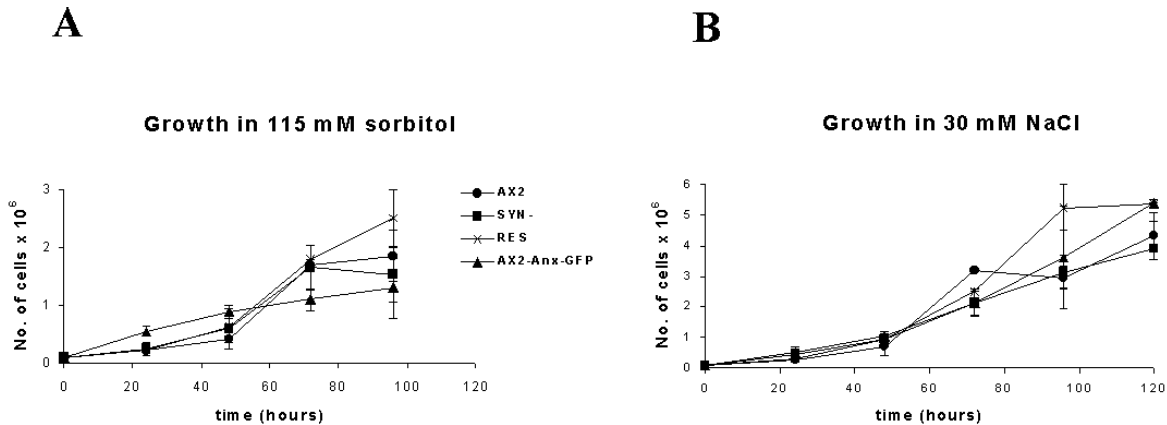


Fig. 9. Growth under osmotic shock condition. Cells were grown in the presence of 115 mM sorbitol (A) or 30 mM NaCl (B). The starting density was 1×10^5 cells/ml and the cells were counted every 24 hours during several days. AX2 wild type cells, SYN⁻ mutants, SYN⁻ mutants re-expressing annexin-GFP (RES) and wild type AX2 cells expressing annexin-GFP (AX2-Anx-GFP) were studied. The data are the average of three independent experiments. The error bars represent the standard deviation from the average values.

1.4 Gelfiltration experiments

Previous experiments led to the suggestion that annexins can form multimers (Creutz *et al.*, 1979; Zaks and Creutz, 1991). Therefore we analyzed the molecular mass of annexin-GFP by gelfiltration chromatography. AX2-Anx-GFP cells were lysed and cells cytosol was prepared by centrifugation at 100,000 x g. Fractions were collected and analyzed by SDS-PAGE followed by Western blotting. According to the calibration curve obtained the annexin-GFP had an apparent molecular mass of approximately 79 kDa that was neglectably higher than the expected 74 kDa (Fig. 10). The continuous annexin elution showed the presence of the protein already in the 126 kDa fraction. The most prominent accumulation of annexin-GFP was noticed in a fraction with the molecular mass of approximately 79 kDa. Although the experiment was performed in the presence of high salt (Materials and Methods 4.4), annexin was detected as well in fractions with much smaller molecular masses. This could be due to the interaction of the protein with the

column matrix. Our finding is in disagreement with results reported by Creutz *et al.* (1979), who showed that annexin VII underwent self association *in vitro*. Our experiment pointed to the possibility that annexin is present in the cell cytosol as a monomer and to the likelihood that it can form complexes with smallprotein(s). Comparison with the elution profile of actin confirmed confirmed that annexin is not present in high molecular weight complexes in our experiments. The actin peak in lower molecular weight fractions overlapped with annexin.

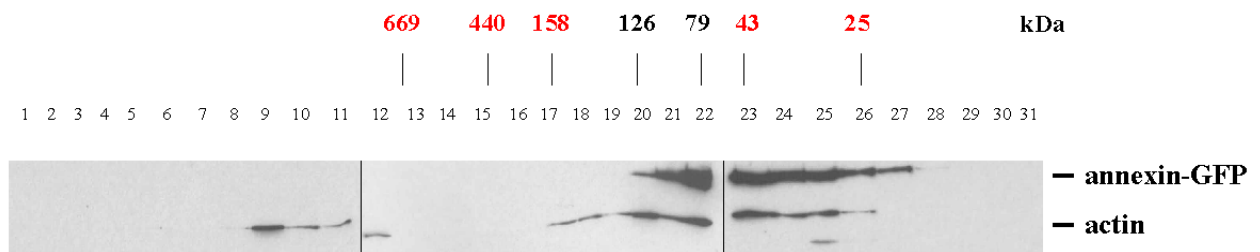


Fig. 10. Annexin-GFP is present in the cell cytosol as a monomer. The gel filtration experiments were performed with the supernatant obtained by centrifugation of the total cell lysate from AX2-Anx-GFP cells at 100,000 x g (Material and Methods 4.4). One peak of a molecular weight of about 79 kDa (fraction 22) was detected (Material and Methods 4.8) when the fractions were separated by SDS-PAGE, and the membranes were probed with monoclonal anti-annexin antibody 185-447-3. The same membranes were immunostained afterwards with an anti actin antibody (mAb Act 1-7).

1.5 Annexin associates with the Triton X-100 insoluble fraction in the presence of Ca^{2+}

Several annexins, most notably annexin XIIIb, were reported to be present in the Triton X-100 insoluble membrane subdomains (Lafont *et al.*, 1998). For annexin A2 it was shown, that it translocates to the Triton X-100 insoluble cytoskeleton upon stimulation of chromaffin cells with nicotine and in the presence of $1 \mu\text{M Ca}^{2+}$ (Sagot *et al.*, 1997). Furthermore, annexin A6 is recruited upon polarization of mammary epithelial cells to the Triton X-100 insoluble fraction. When we lysed the cells in the presence of 1 % Triton X-100 and analyzed the distribution of the protein, we found the endogenous protein and annexin-GFP exclusively in the cytosolic fraction (Fig. 11A). Addition of $100 \mu\text{M Ca}^{2+}$ to the lysis buffer led to enrichment of annexin in the Triton X-100 insoluble pellet of AX2 and AX2-Anx-GFP cells, whereas in the corresponding

supernatant fractions it was present in a lesser amount. Annexin D293A having a mutation in one of the proposed high affinity Ca^{2+} -binding sites (Weng *et al.*, 1993, Huber *et al.*, 1990) showed a slightly different behavior from endogenous annexin and annexin-GFP. It remained mainly in the supernatant although low amount of the protein was present in the pellet fraction (Fig. 11B). When $100 \mu\text{M Ca}^{2+}$ was added to the lysate of $\text{SYN}^- \text{D293A}$ cells mAb 185-447-3 recognized a prominent protein band in the Triton X-100 insoluble pellet (Fig. 11B). The supernatant fraction contained a higher amount of annexin when compared with the corresponding supernatant fractions obtained from AX2 and AX2-Anx-GFP cells (Fig. 11A). The high amount of annexin that remained in the cytosol fraction after addition of $100 \mu\text{M Ca}^{2+}$ could be due to the mutation in the proposed high affinity Ca^{2+} -binding site ($\text{SYN}^- \text{D293A}$), suggesting that an intact Ca^{2+} -binding site is necessary for the association of annexin with Triton X-100 insoluble fraction. The control staining for actin showed correct loading as it is normally enriched in the Triton X-100 insoluble fraction (Fig. 11A, B).

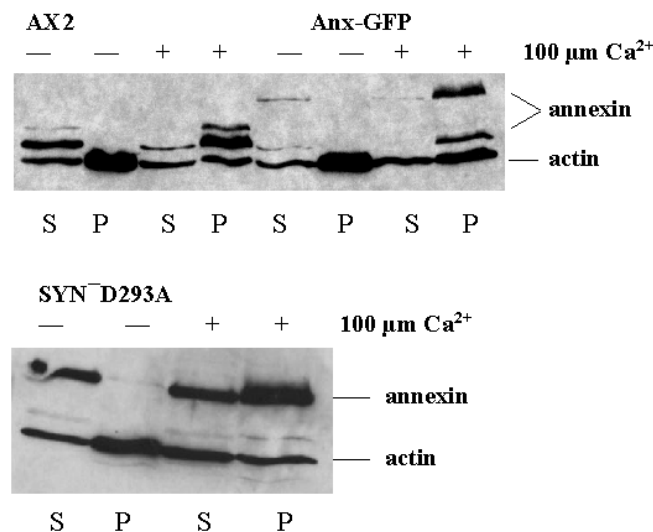


Fig. 11. Annexin is found in the Triton X-100 insoluble fraction in the presence of $100 \mu\text{M Ca}^{2+}$. AX2 wild type cells, AX2-Anx-GFP, and $\text{SYN}^- \text{D293A}$ cells were lysed in the presence of 1 % Triton X-100 (with or without $100 \mu\text{M CaCl}_2$) and pelleted by centrifugation at $14,000 \times g$ for 10 min (Material and Methods 4.3). Soluble fractions (S) and Triton insoluble pellet fractions (P) of all strains were resolved by SDS-PAGE (12 % acrylamide), blotted to nitrocellulose and the blots were immunolabelled with mAb 185-447-3. Detection was with enhanced chemiluminescence. The actin distribution was tested for control.

1.6 pH-dependent shuttling of annexin between cytoplasm and plasma membrane and effect of pH value of the medium on the growth of *Dictyostelium* cells

For annexin B12 it has been reported that it undergoes a conformational change at low pH which then allows an insertion of the protein into a membrane (Langen *et al.*, 1998a; Langen *et al.*, 1998b). Working with *D. discoideum* allowed us to test this proposal directly *in vivo*.

The intracellular pH can easily be manipulated in *D. discoideum* by subjecting cells to buffers of different pH in the presence of a weak acid or base. Propionic acid and ammonia can diffuse through the plasma membrane in the undissociated state and alter the pH of the cytoplasm after dissociation within the cell (Inouye, 1989). In living *D. discoideum* cells, that were kept in Soerensen phosphate buffer, pH 6.0, or MES buffer, pH 6.0, annexin-GFP was present in the cytosol and in the nucleus (Fig. 12A, B). Although clearly visible in fixed cells, membrane staining was not noted in living cells when viewed in a confocal microscope. However, after addition of propionic acid adjusted to the same pH (pH 6.0), annexin-GFP was enriched at the plasma membrane (Fig. 12C). This re-localization was reversible and increasing the pH by the addition of ammonium chloride lead to re-localization of the protein back to the cytosol (Fig. 12D). Previous studies by Hanakam *et al.* (1996) had shown that such a behaviour is not mediated by the GFP tag, since GFP does not change its localization upon changing of pH value. The same experiment was performed with SYN⁻ D293A cells (Fig. 12E-H). The mutant showed no differences when compared with the AX2-Anx-GFP strain, suggesting that the mutation in the Ca²⁺-binding site did not affect this behavior.

We studied the re-localization also at the biochemical level when appropriate buffers were added to wild type cells and cells expressing annexin-GFP prior to fractionation. When AX2 cells (Fig. 12I-1) and AX2-Anx-GFP cells (Fig.12J-1) were resuspended in MES buffer, pH 6.0, subsequently opened by sonication and the cell lysates centrifuged at 100,000 x g, annexin could be detected in the cytosolic fraction (S) and in the membrane pellet fraction (P) in comparable amounts. Upon treatment with propionic acid annexin could not be detected in the supernatant from AX2 cells (Fig. 12I-2) and it was exclusively present in the membrane fraction (P). In contrast to the endogenous protein, annexin-GFP, probably due to its overexpression, could still

be observed in the supernatant (cytosolic fraction) although in a lower amount than in the membrane pellet fraction (Fig. 12J-2).

To test the biological relevance of this behavior for the cells, we followed the growth of wild type cells, SYN⁻ and AX2-Anx-GFP cells in axenic medium of a different pH. We found however that all three strains showed normal growth behavior under standard laboratory conditions (nutrient medium, pH 6.7) and when subjected to slightly lower pH (pH 6.0). The growth was impaired when the pH of the medium was high (pH 8.0) and all the strains were affected in the same manner (Fig. 13).

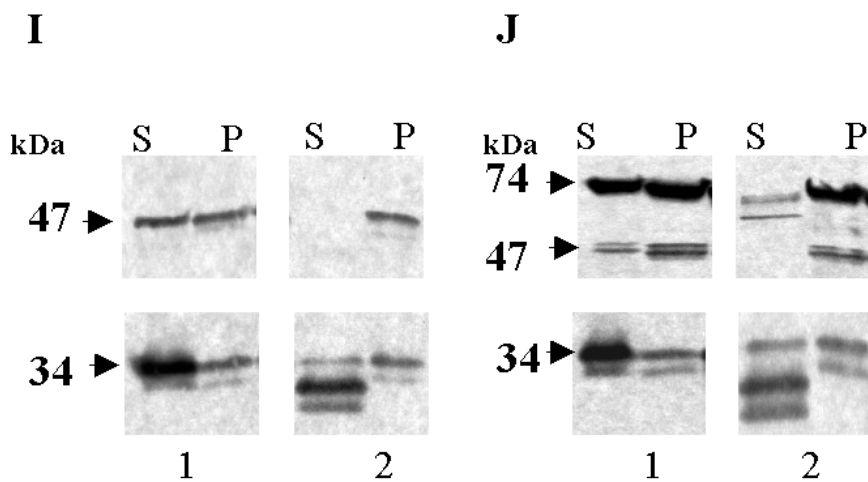
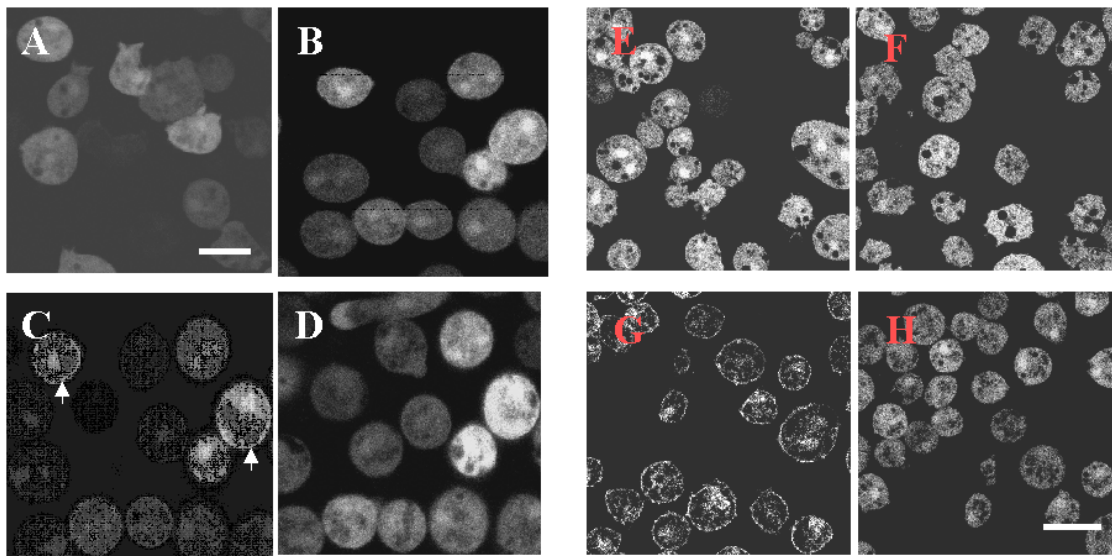


Fig. 12. (Previous page) **Decrease of the intracellular pH induces translocation of annexin-GFP to the plasma membrane *in vivo*.** Living *Dictyostelium* AX2 cells expressing annexin-GFP (A) and SYN⁻ D293A cells (E) in Soerensen phosphate buffer, pH 6.0, or in MES buffer, pH 6.0, (B, F respectively) showed an overall distribution of annexin-GFP. Lowering of the intracellular pH by propionic acid (described in Material and Methods 6.1.3) results in fast translocation of the protein to the plasma membrane (C, G). The rise of the pH by addition of ammonium chloride brought the protein back to the cytosol (D, H). Bar, 5 μ m. The images were taken by a confocal microscope. (I) and (J) show the same experiment done with AX2 (I) and AX2-Anx-GFP cells (J) followed by cell fractionation. The cell supernatant (S) and pellet (P) were separated by centrifugation at 100,000 x g. The treatment with MES buffer is shown in I-1 and J-1 and the relocation upon the treatment with propionic acid in I-2 and J-2. Immunoblots were performed with mAb 185-447-3. Detection was done as described in Material and Methods 4.10. A monoclonal antibody which recognizes the 34 kDa subunit of actin capping protein cap 32/34 (135-409-16) was used for control.

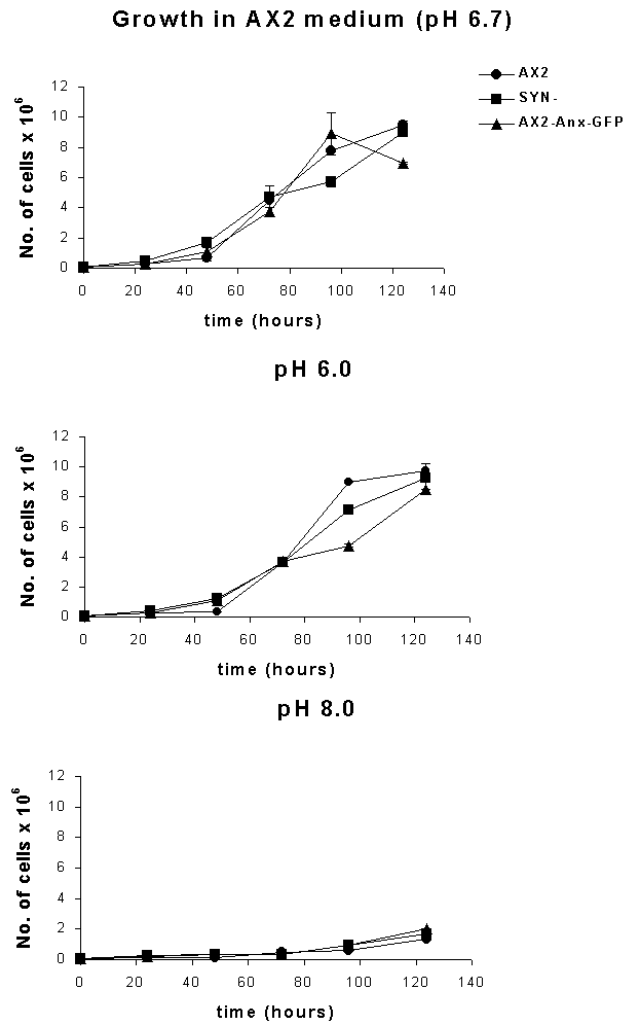


Fig. 13. (Previous page) **Growth under different pH-conditions.** The starting density was 1×10^5 cells/ml and the cell number was determined by counting every 24 hours for several days. Under standard laboratory conditions (pH of the medium is 6.7) all the strains showed normal growth and comparable behavior (A). A slightly lower pH (6.0) had no influence (B) whereas increased pH of the medium (8.0) impaired the growth of all the strains in the same fashion (C). All values are the average of three independently performed experiments and the error bars represent the standard deviation from the average values.

1.7 Detection of annexin binding partners

The gelfiltration experiments (Results 1.3) suggested that annexin might form complexes with some small protein(s) in the cytosol. In order to detect possible binding partners we performed immunoprecipitation experiments using monoclonal anti-GFP antibody, K3-184-2 (unpublished data) for precipitation of GFP tagged annexin from AX2-Anx-GFP and RES cells (Material and Methods 4.6). The immunoprecipitated protein samples were resolved by SDS-PAGE, the gel subsequently silver-stained (data not shown) and the protein bands were dissected from the gels in order to be analysed by MALDI MS. In order to confirm that annexin-GFP was successfully immunoprecipitated, we performed in parallel Western blotting experiments (Fig. 12A, B). The anti-annexin antibody recognized annexin-GFP in the samples obtained from AX2-Anx-GFP cells. A control experiment was performed with SYN⁻ cells and, as expected, only IgG heavy and light chains could be observed when the membrane was immunostained with mAb 185-447-3. In the gel, which was silver-stained, one weak protein band that was smaller than the IgG light chain and that was unique in AX2-Anx-

GFP samples (data not shown) was excised and further analyzed by MALDI MS. Protein sequencing and further similarity searches revealed a small, 20 kDa Ca²⁺-binding protein CBP2 (Fig. 12C) which contains four consensus sequences all predicted to bind Ca²⁺ and that are typical for Ca²⁺-binding EF-hand domains (André *et al.*, 1996).

In addition, the same experiment was performed with RES cells. mAb-185-447-3 recognized annexin-GFP while in AX2 cells that were used as a control just immunoglobulin chains could be seen. Two prominent protein bands unique for the RES sample were detected by silver staining (not shown) and excised for further processing by MALDI MS. Both protein bands had molecular weights lower than the IgG light chains. MALDI analysis identified both samples as DdPEF-2 protein (Fig. 12C). The sample with the lower molecular mass represented a degradation product of DdPEF-2. This penta EF-hand protein was recently described by

Ohkouchi *et al.* (2001). Comparison with the canonical EF-hand sequence suggested that EF-4 and EF-5 do not bind Ca^{2+} due to the presence of unfavorable residues at the Ca^{2+} -coordinating positions while sequences in EF-1, EF-2 and EF-3 match with a 13-residue consensus pattern the EF-hand motif (Ohkouchi *et al.*, 2001).

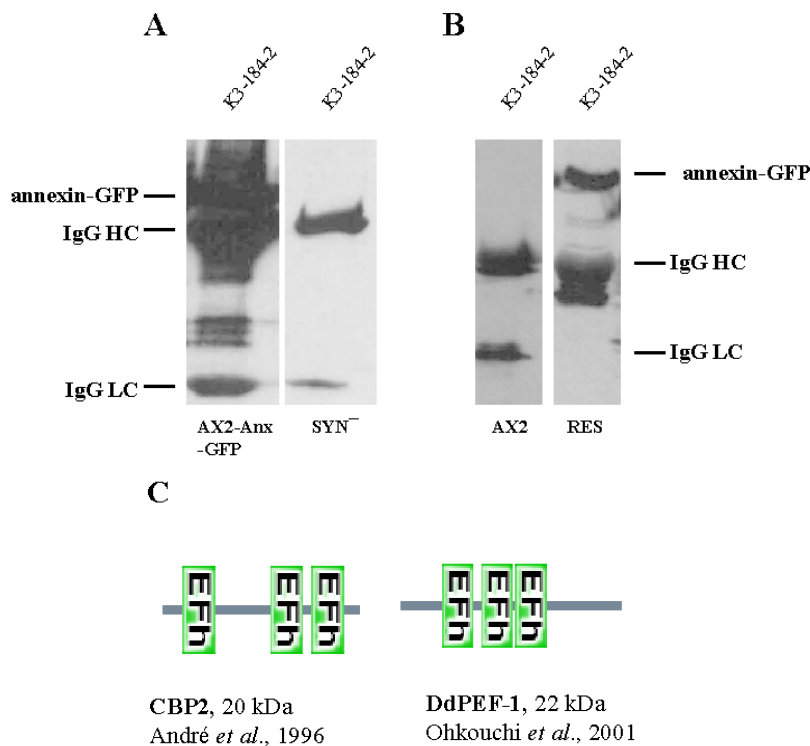


Fig. 14. Immunoprecipitation of annexin and co-immunoprecipitation of annexin binding partners. Cell lines expressing annexin-GFP (AX2-Anx-GFP (A) and RES (B)) were used for the assay. For control AX2 and SYN⁻ cells were used (B, A respectively). The experiment was performed as described in Material and Methods 4.7 using mAb K3-184-2. The samples were resolved in 15 % (A) and 12 % (B) SDS-PAGE gels. After Western blotting, nitrocellulose membranes were immunolabeled with mAb 185-447-3 for detection of annexin, and subsequently enhanced chemiluminescence was performed (Material and Methods 4.10). IgG HC (heavy chain), IgG LC (light chain). (C) Schematic description of the two proteins co-immunoprecipitated with annexin and identified by MALDI MS.

2. Localization of annexin during pinocytosis and phagocytosis

Although earlier studies with SYN⁻ cells had not shown significant differences in the uptake of [³H] dextran and latex beads (Döring *et al.*, 1995), taking advantage of the annexin-GFP protein

we followed the protein *in vivo* during pinocytosis. We observed an enrichment of annexin-GFP at the tips of plasma membrane protrusions of newly formed pinosomes (Fig. 15A, time points 5, 10 and 15 seconds). Within seconds, the protein dissociated from the place of previous accumulation (Fig. 15A, time points 20 and 25 seconds) and was no longer enriched on pinosomes when the TRITC-dextran was entirely engulfed. The loss of annexin C1 resulted in a slightly higher and faster rate of pinocytosis and slightly faster rate of exocytosis of TRITC-dextran when compared with AX2 cells (Fig. 15B, C).

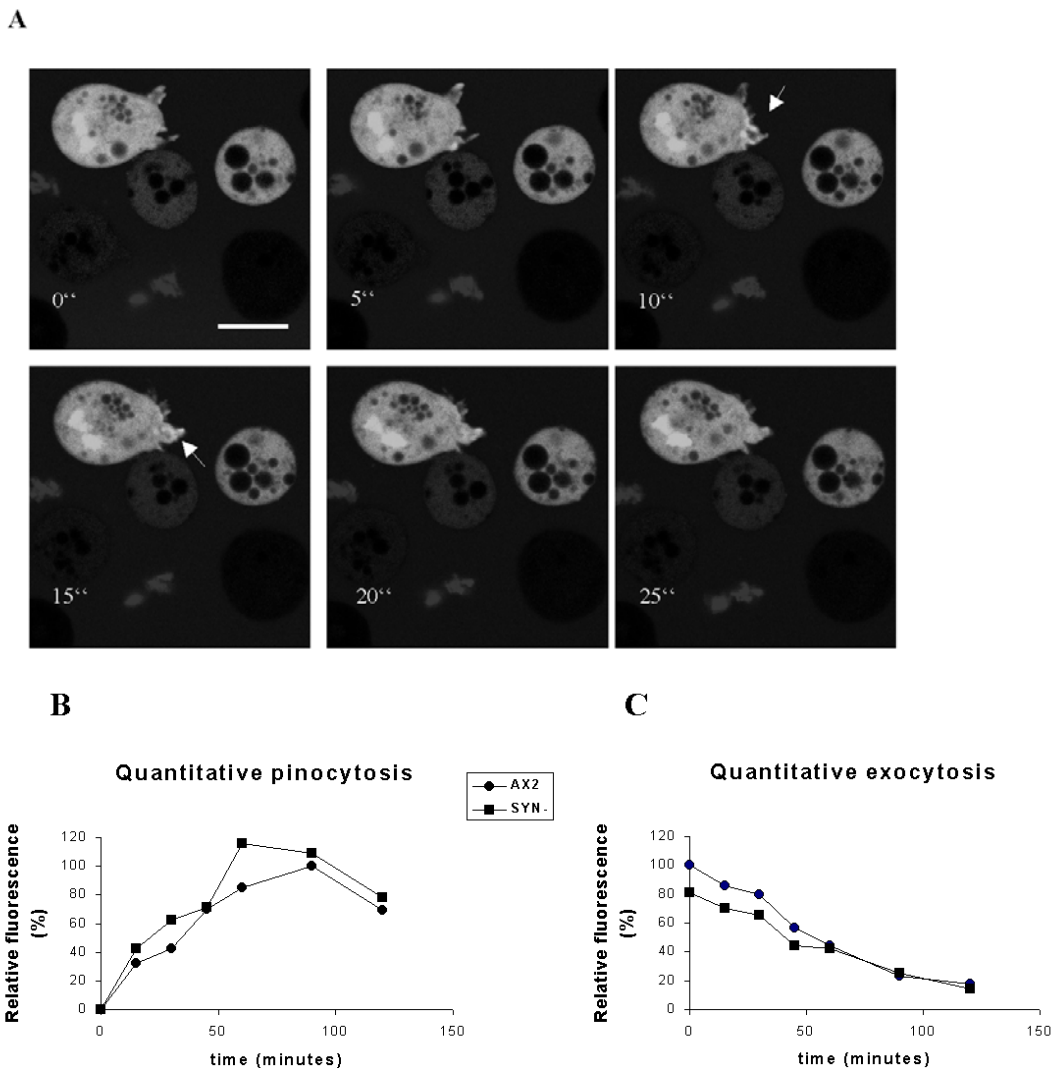


Fig. 15. Annexin transiently accumulates at the tips of plasma membrane protrusions of newly formed pinosomes. The loss of annexin in SYN⁻ cells does not affect pinocytosis and exocytosis. (A) *Dictyostelium* cells were allowed to attach onto coverslips. After 15 minutes the medium was carefully aspirated and replaced with

Soerensen phosphate buffer containing 1 mg/ml TRITC-dextran. Transient enrichment of annexin-GFP fusion protein was observed at the time point of 5, 10 and 15 seconds (A). Within seconds, the protein then dissociated from the place of previous accumulation (time points 20 and 25 seconds) and was not enriched on pinosomes when the TRITC-dextran was entirely engulfed. Bar, 10 μ m. For the quantitative pinocytosis (B) and exocytosis (C) assay, cells were prepared as described (Materials and Methods 2.5). All the values are calculated relative to maximum values for AX2 cells with the highest value taken as 100 %. The samples were taken during a period of 120 minutes. A typical experiment is shown in each case.

Behavior during pinocytosis was distinctly different from phagocytosis where endogenous annexin and annexin-GFP were present on the phagosomes during engulfment of a yeast particle (Fig. 16A, D) and stayed on the phagosome after internalization (Fig.16E, H). Because of the presence of annexin at the plasma membrane, it was difficult to distinguish in fixed cells an accumulation of annexin at the base of a future phagosome upon an attachment of a yeast particle, whereas co-immunostaining for actin clearly showed that actin was attracted to these sites (Fig. 16G, H). Once a yeast particle was completely engulfed, no actin staining was detected anymore (Fig. 16G, H), whereas annexin stayed on the phagosomal membrane for longer (Fig. 16E, H). The same behavior we observed with the endogenous annexin in AX2 cells (Fig. 16I). The monoclonal antibody 185-447-3 prominently labeled phagosomal membranes and the phagocytic cup.

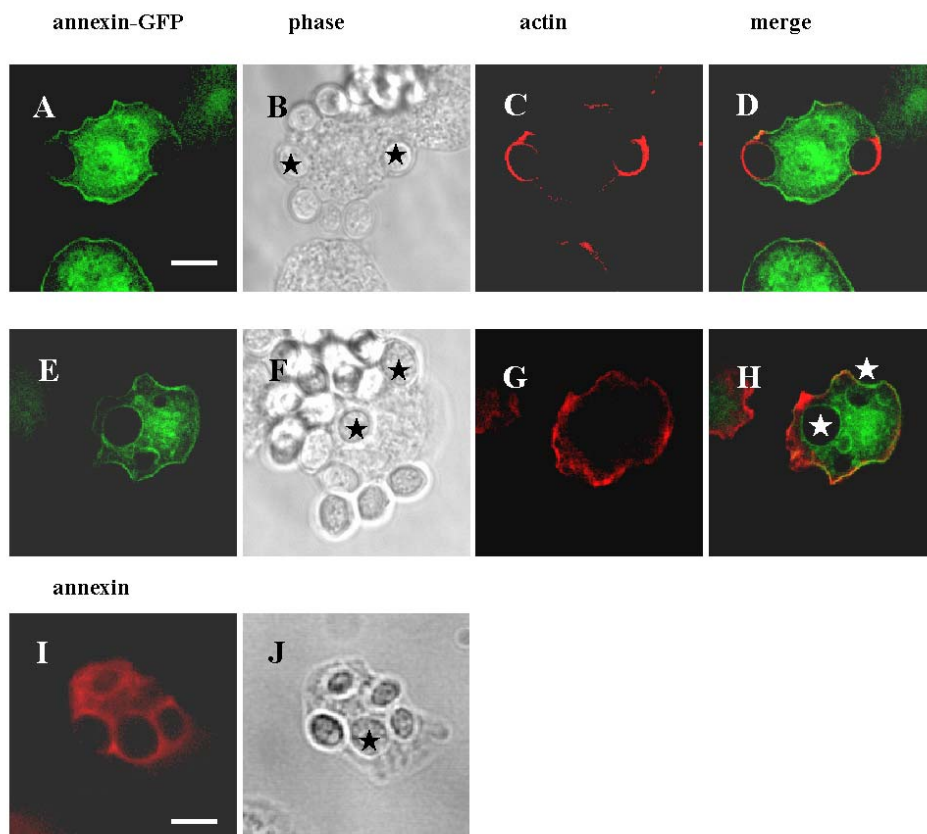


Fig. 16. (Previous page) **Annexin is found on late phagosomal membranes in immunofluorescence studies.** AX2 cells or AX2 cells expressing annexin-GFP were seeded on coverslips and allowed to attach for 20 minutes. After attachment, the cells were incubated for 15 minutes with unlabeled yeast cells and fixed afterwards. Fixed AX2 cells were subsequently incubated with mAb 185-338-1 (Döring *et al.*, 1995) for detection of annexin. Actin was detected using mAb Act-1-7. Asterisks indicate yeast particles. The images were taken by a confocal microscope. A-D represent the beginning phase of the engulfment of yeast particles, with B as the phase contrast image. E-H, completely engulfed yeast particle, with F as the phase contrast image. I and J, fixed wild type cells during phagocytosis, immunolabeled with mAb 185-338-1 (I), J phase contrast. Bar, 4 μ m (I, J) and 6 μ m (A-H).

Isolation of phagosomes from AX2 cells (Fig. 17A) and cells overexpressing annexin-GFP (Fig. 17B) confirmed the finding that annexin is present on phagosomes. Since the cells were allowed to perform phagocytosis for 10 minutes, the obtained phagosomes could be designated as late phagosomes (Furukawa and Fechheimer, 1994). After ten minutes, the phagocytosis of paramagnetic beads was stopped by incubation of the cells on ice, and the cells were opened by three cycles of freezing in liquid nitrogen and thawing on ice (Material and Methods 4.5). Total cell homogenate and several subsequent washing steps were collected and used afterwards for Western blot analysis. Annexin was detected in whole cell homogenates of AX2 and AX2-Anx-GFP cells (Fig. 17A, B, respectively) and its amount was declining during the washing steps resulting in the absence of annexin (Fig. 17A) or almost no annexin-GFP (Fig. 17B) in the samples of the third washing step. We concluded that annexin not being involved in phagocytosis was completely removed during this procedure and that the protein which we could detect in the phagosomal fraction was specifically bound to phagosomal membranes. Immunostaining for comitin (Schreiner *et al.*, 2002) and α -actinin (Furukawa and Fechheimer, 1994) was used as a positive control since both proteins were previously described to localize on phagosomes. Control experiments with cells expressing GFP proved that the GFP tag was not responsible for the localization of the fusion protein on phagosomes (data not shown).

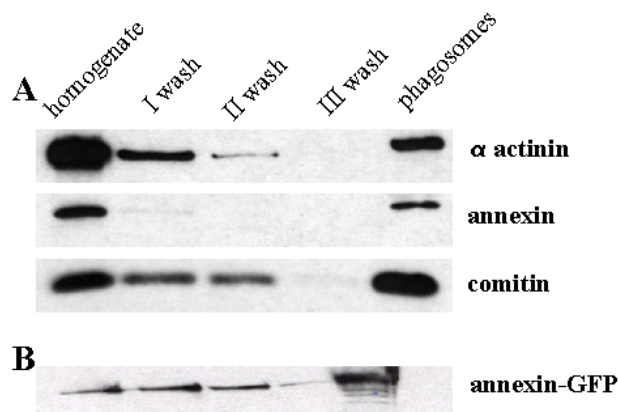


Fig. 17. (Previous page) **Enrichment of annexin on phagosomes after 10 minutes of incubation of AX2 cells and AX2 cells expressing annexin-GFP with magnetic beads.** After magnetic extraction of phagocytosed paramagnetic beads, proteins present on the phagosomal membrane were solubilized in SDS sample buffer and resolved on 12 % acrylamide gels after removal of the beads by short centrifugation. Phagosomes from AX2 cells are shown in (A) and from annexin-GFP expressing cells in (B). Control stainings were performed using monoclonal anti α -actinin (47-62-17) and anti comitin (190-340-3) antibody.

Our findings that *D. discoideum* annexin is involved in phagocytosis are in agreement with data obtained for annexins a1-a5 present on phagosomes from J774 macrophages and for annexins a7 and a11 found on phagosomes from macrophage-like cells (Diakonova *et al.*, 1997; Pittis and Garcia, 1999, respectively). In order to investigate which consequence the absence of annexin had, we performed a quantitative phagocytosis assay with SYN^- cells. It had been previously reported that SYN^- mutant behaved like wild type cells when uptake of latex beads was measured (Döring *et al.*, 1995). Here we tested the uptake of yeast cells which involves a different receptor in order to screen for possible defects (Vogel *et al.*, 1980). The SYN^- cells exhibited a slightly higher incorporation rate of yeast particles than AX2 cells (Fig. 18). Furthermore, the mutant was phagocytosing faster although mutant and wild type reached the same level of uptake after 90 minutes. In accordance with this finding was the observation that AX2-Anx-GFP cells were much slower than AX2 and SYN^- cells in phagocytosing yeast particles. In addition, they never managed to achieve the same level of uptake as AX2 and SYN^- cells. This finding suggested an inhibitory effect of annexin on phagocytosis.

Although numerous reports point to a presence and a role of different annexins in phagosome maturation, their exact function in this process remains to be solved. However, it has been reported by Bennett *et al.* (1995) that annexin A5 could inhibit the uptake of apoptotic vascular smooth muscle cells by normal smooth muscle cell monolayers in a dose-dependent and Ca^{2+} -dependent manner. Furthermore, annexin A6 is reported to have a role in the remodeling of the spectrin-actin cytoskeleton by targeting the action of the calpain protease to regions of the cytoskeleton that must be freed, so scission can release endocytic vesicles (Kamal *et al.*, 1998). Caohuy and Pollard (2001) were studying the process of exocytosis and found that phosphorylation of annexin A7 by PKC enhances the Ca^{2+} -dependent membrane fusion and this event is closely correlated with the levels of catecholamine secretion.

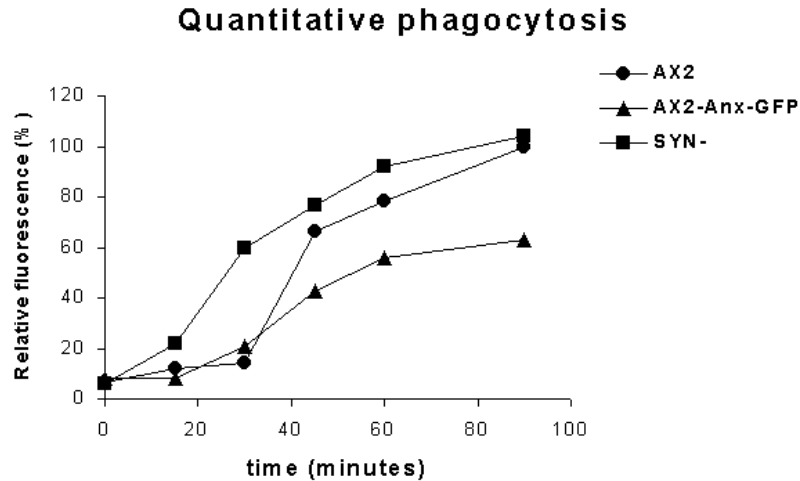


Fig. 18. Phagocytosis of TRITC labeled yeast cells. For the quantitative phagocytosis assay, cells were prepared as described (Material and Methods 2.5). The samples were taken during a period of 90 minutes. All the values are calculated relative to the maximal value for AX2 cells with the highest value taken as 100 %. The results of a typical experiment are shown.

3. Phosphorylation of annexin

Annexins are long known to be phosphorylated. Annexin A2 was previously reported to be a substrate for v-src protein kinase and the tyrosine kinase activity of the epidermal growth factor receptor (EGFR) is known to phosphorylate annexin A1 (Rothhut, 1997). Furthermore, annexins A7 and A11 are reported to be phosphorylated on tyrosine residues *in vitro* by the Ca^{2+} -dependent tyrosine kinase Pyk-2, the src tyrosine kinase and the epidermal growth factor receptor kinase although physiological consequences of these phosphorylations remain to be elucidated (Furge *et al.*, 1999). In addition, many annexins can be phosphorylated on serine and threonine residues and annexin A2 (Sarafian *et al.*, 1991; Delouche *et al.*, 1997) and A7 (Caohuy and Pollard, 2001) have been reported to be a substrate of protein kinase C (PKC).

In order to see whether *D. discoideum* annexin could also represent a target for protein kinases, we analyzed the annexin sequence with the help of the ScanProsite program (<http://us.expasy.org/tools/scanprosite>). The prediction pointed to 13 putative phosphorylation

sites. Ten of those were predicted to be serine, two threonine and one tyrosine phosphorylation sites (data not shown). Comparison of the annexin C1 sequence and the predicted phosphorylation sites with corresponding sequences of human annexin A7 and a mouse homologue Anxa7 revealed that two serine residues are conserved and were predicted to be phosphorylated in all three proteins. In *Dictyostelium* annexin these residues were Ser-177 and Ser-246.

Dictyostelium discoideum annexin C1 is a basic protein with an isoelectric point of around 8.1. In order to identify possible charge isomers, we performed 2D gel electrophoresis and resolved the AX2 cell lysate in the first dimension with a the pH range from 3 to 10 followed by SDS-PAGE (12 % gel) in the second dimension. Although this approach does not allow conclusions which and how many of the putative phosphorylation sites are in fact modified it gives an information about the presence and amount of phosphorylated proteins. 2D gel analysis revealed that annexin was mainly present at its isoelectric point (8.1). However, a significant amount of protein was detected at a more neutral pH (7.46 and 6.81) showing the existence of charge isomers of annexin modified by negative charge and suggesting its possible phosphorylation (Fig. 19).

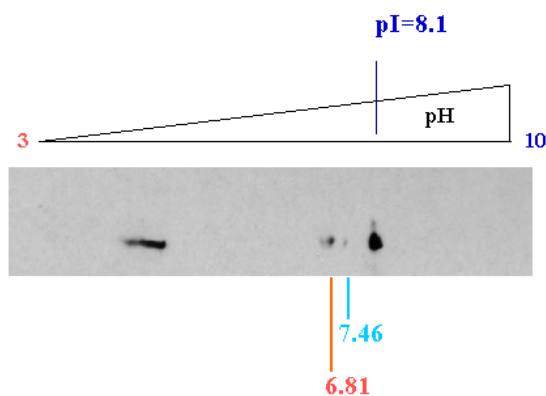


Fig. 19. Analysis of annexin by 2D gel electrophoresis. The experiment was performed as described in Material and Methods 4.7. Cells were lysed in 2D lysis-buffer in the presence of phosphatase inhibitors. The proteins were separated according to their isoelectric points in the first dimension and according to molecular masses in the second (SDS-PAGE). The immunostaining was done with mAb 185-447-3 and detection with enhanced chemiluminescence (Material and Methods 4.10). Isoelectric point is shown in dark blue (pI=8.1) and charge isomers in light blue (7.46) and red (6.81). The first dimension separation is shown as an increase of pH from pH 3.0 to pH 10.0.

4. Development of SYN⁻ cells

4.1 Development on phosphate agar palates

Deprived of nutrients, *D. discoideum* undergoes a developmental program that lasts about 24 hours and starts with the formation of aggregates which undergo morphological changes before culminating into a fruiting body (Fig. 20).

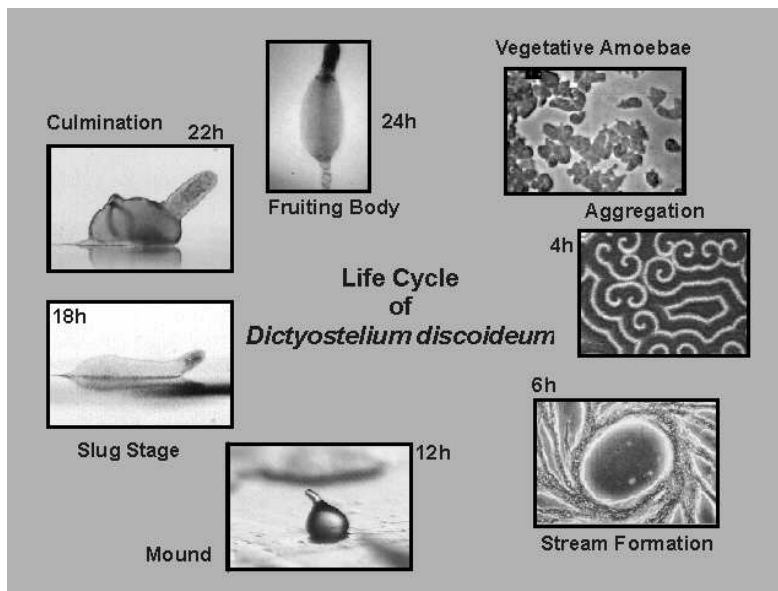


Fig. 20. Life cycle of *Dictyostelium discoideum*. After 4 hours of starvation cells start to aggregate. *Dictyostelium* form during development mounds and slugs and developments ends with formation of culminants and spores containing fruiting bodies. The picture is taken from the Institute for Zoology, Munich homepage: <http://www.zi.biologie.uni-muenchen.de/zoologie/dicty/dicty.html>

The SYN⁻ mutant showed a delay of 3 to 4 hours in development when compared with wild-type AX2 cells (Döring *et al.*, 1995). Furthermore, only few aggregates developed into mature fruiting bodies. These structures were however smaller than wild type fruiting bodies (Fig. 21E). In order to rescue the impairment in development and to characterize the part of the annexin gene that was responsible for this particular phenotype, several cell lines were established (Results 1.1). When transfected into SYN⁻ cells, the full length annexin-GFP protein completely rescued the

developmental defect (Fig. 21D), proving the biological activity of the fusion protein (strain RES). AX2 cells overexpressing annexin exhibited normal development on phosphate agar plates (Fig. 21C).

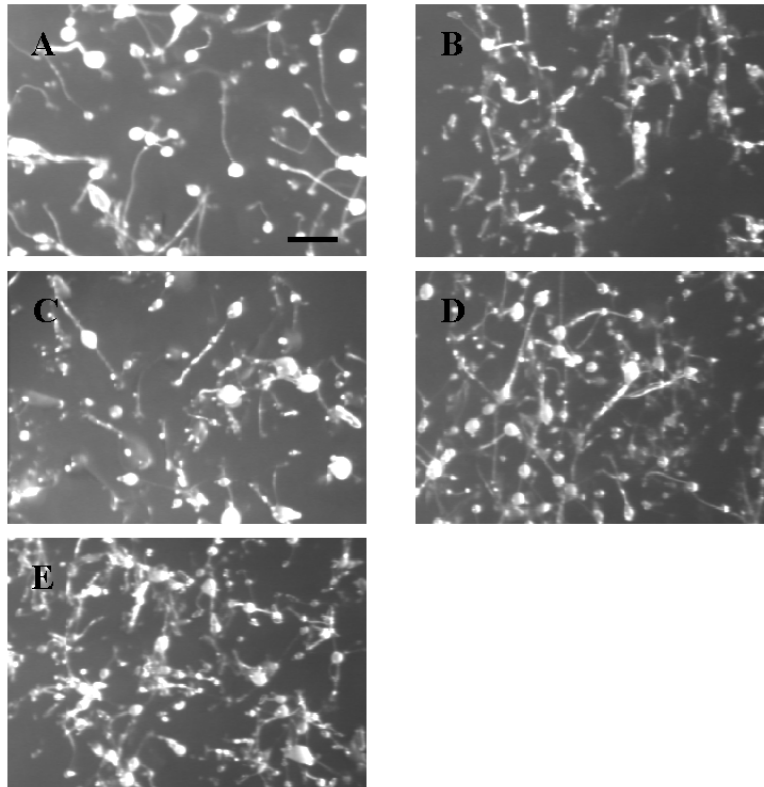


Fig. 21. Annexin-GFP is functional in *D. discoideum* and rescues the development of the annexin minus mutant, SYN^- . (A) AX2 wild type, (B) SYN^- cells, AX2 cells expressing annexin-GFP (C), and (D) SYN^- cells expressing annexin-GFP. Axenically grown cells were washed, plated on phosphate agar plates at a density of 1×10^8 cells and allowed to develop at $21^\circ C$. Photographs were taken after 23 hours with an Olympus SZ-045TR stereo microscope. Wild-type cells (A) and cells over-expressing annexin (C) uniformly developed into fruiting bodies, while SYN^- cells formed aggregates and mounds (B) and after prolonged incubation of 28 hours occasionally fruiting bodies (E). Annexin-GFP completely rescued the defect in development of the SYN^- cells (D). Bar, 5 mm.

We examined as well SYN^- D293A and AX2 D293A cells and mutant and wild type cells expressing the annexin core for development (Fig. 22). When these strains were allowed to develop on phosphate agar plates, they showed an even longer delay in development when compared to AX2 cells than the SYN^- mutant. The SYN^- D293A mutant formed aggregates after 23 hours (Fig. 22A) and after 48 hours only few of those aggregates developed into small fruiting bodies with short stalks (Fig. 22B). Wild type cells expressing D293A annexin were as

well impaired but they were developing faster than $\text{SYN}^- \text{D293A}$, forming the culminants after 23 hours (Fig. 22C) and completely finishing development after 38 hours (Fig. 22D). Similar to the $\text{SYN}^- \text{D293A}$ strain not all of the culminants developed into fruiting bodies. The most striking impairment we observed with SYN^- cells expressing the annexin core domain ($\text{SYN}^- \text{-core}$). These cells started to move towards aggregation centers after 23 hours (Fig. 22E) and after 38 hours they formed aggregates (Fig. 22F). Fruiting bodies could also be observed occasionally. Expression of the annexin core did not have an inhibitory effect on the development of AX2 cells, but the fruiting bodies that could be observed after 23 hours (Fig. 22G) were noticeably smaller when compared with the fruiting bodies of AX2 cells (Fig. 22H). Furthermore, as already

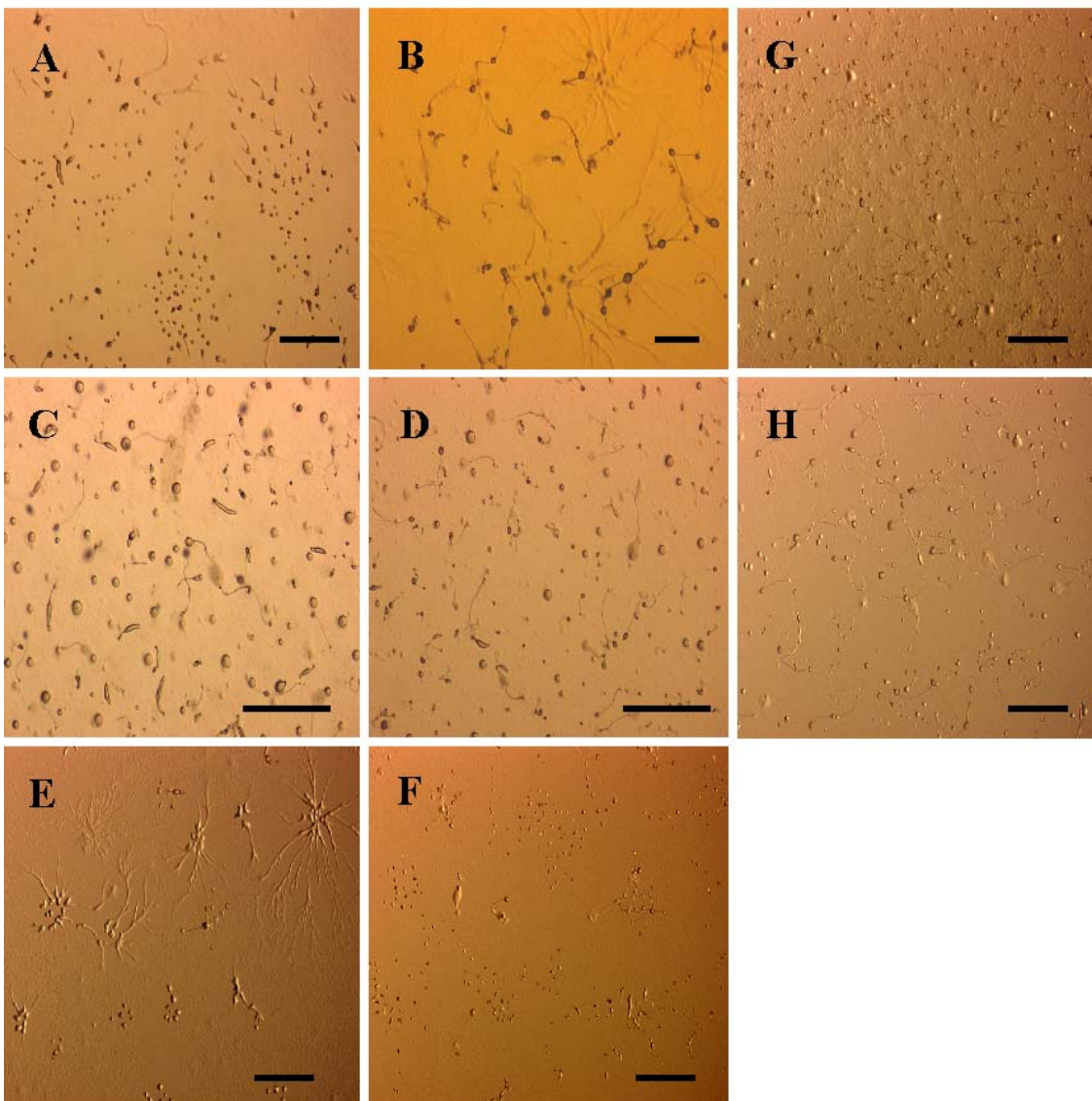


Fig. 22. (Previous page) **Expression of the D293A mutated annexin and the annexin core domain have a negative effect on the development of wild type and SYN⁻ cells.** The cells were prepared as described for Fig. 21. (A, B) SYN⁻ D293A cells after 23 and 48h, respectively, (C, D) AX2 D293A cells after 23 and 48h, respectively, (E, F) SYN⁻-core cells after 23 and 38h, respectively, (G) AX2-core cells, (H) AX2 cells. The pictures were take after 23 hours (unless noted otherwise in the text) with a Leica MZFLIII stereo microscope. Bar, 25 mm (note that some bars have different sizes).

observed with previously described cell lines (AX2 D293A, SYN⁻ D293A and SYN⁻-core), not all culminants gave rise to mature fruiting bodies.

All the results obtained in experiments with development on phosphate agar plates are summarized in Table 1.

Cell line (1 x 10 ⁸ cells)	Hours needed for (full) development	Hours of delay	Phenotype
AX2	23-24	/	normal
SYN⁻	27	3-4	few fruiting bodies
RES	23-24	/	normal
AX2-Anx- GFP	23-24	/	normal
SYN⁻ D293A	48	25	few, small fruiting bodies with short stalks
AX2 D293A	38	15	few fruiting bodies
AX2-core	23-24	/	small fruiting bodies
SYN⁻-core	more than 48	more than 25	forming aggregates and seldom fruiting bodies

Table 1. Comparison of development of different cell lines. All the defects in development and resulting phenotypes are presented. The most striking impairment showed SYN⁻-core cells being not able to complete their development.

Furthermore, we were interested to see whether the impairment in development of SYN⁻ and SYN⁻ D293A cells could be detected using specific markers for development. For this purpose

Dictyostelium cells were starved for 10 hours in Soerensen phosphate buffer in shaking culture. Samples were taken every two hours, cells were lysed and subsequently resolved by SDS-PAGE (Fig. 23). As a protein marker for early development the contact site A glycoprotein (csA) was used (Coates and Harwood, 2001). csA was first detected during aggregation of the cells which occurs at around six hours under the conditions used. The protein amount further increases strongly during development. AX2 wild type, AX2 expressing Anx-GFP as well as SYN⁻ cells expressing Anx-GFP showed the same pattern of csA accumulation, whereas in SYN⁻ cells csA was first detected at 10 hours of development indicating a developmental delay of four hours. By contrast, in SYN⁻ D293A cells no csA protein was detected even at 10 hours of starvation confirming the strong impairment of development in this strain. In developing SYN⁻-core and AX2-core cells csA was detected at 10 hours of development. These strains had the same pattern of csA expression like SYN⁻ cells although they showed more severe impairment in development on phosphate agar plates than the SYN⁻ mutant (Fig. 22E-H). In addition, when compared with SYN⁻ D293A, SYN⁻-core cells showed slower development on phosphate agar plates although csA was detected at 10 hours of development and in the SYN⁻ D293A not (Fig. 23). The same membranes were tested with Act 1-7 antibody as a control for equal loading (not shown).

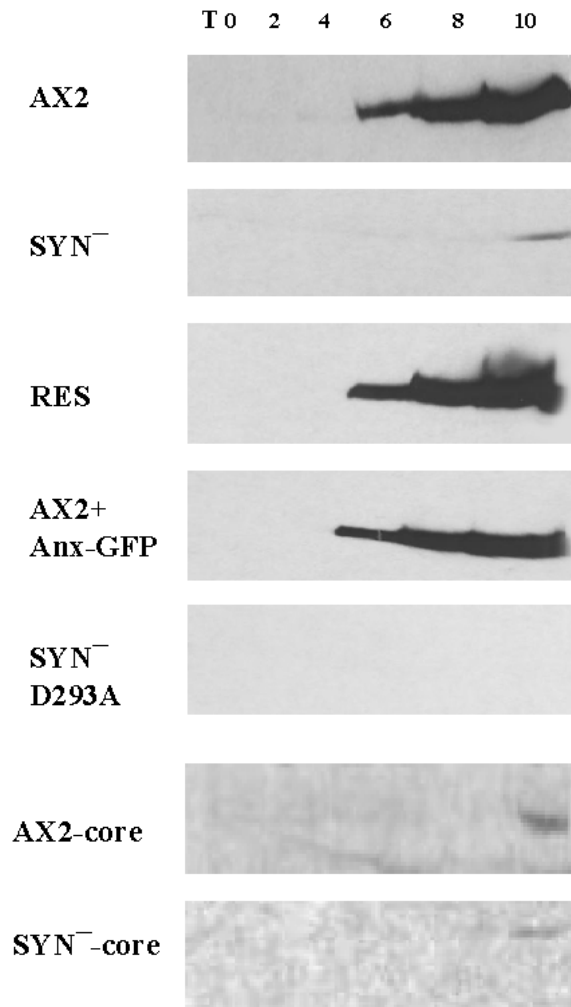


Fig. 23. SYN⁻ D293A cells showed complete deficiency of the early development marker csA. 1×10^7 cells/ml were incubated for 10 hours in Soerensen phosphate buffer, pH 6.0. The samples were collected every 2 hours and the protein resolved afterwards by SDS-PAGE. The Western blot analysis was performed as described in Material and Methods 4.9 and 4.10. The membranes were probed with anti contact site A antibody (mAb 33-294-17).

4.2 Localization of annexin in slugs and fruiting bodies

Annexin C1 is present during all stages of *D. discoideum* development in similar amounts (Döring *et al.*, 1995). For studying the localization of annexin during development, slugs and forming fruiting bodies were fixed with methanol (Fig. 24). Both, endogenous annexin and

annexin-GFP showed an overall distribution in slugs (Fig. 24G, I). The green fluorescence was observed, similar to vegetative cells, at membranes of single cells within the slug and was diffusely present in the cytosol. For visualizing the distribution of endogenous annexin in slugs mAb 185-338-1 was used. Similar to annexin-GFP, the endogenous protein localized to the plasma membrane and was present in the cytoplasm. The staining of nuclei was observed in addition. Furthermore, annexin was present in the prespore and the prestalk cells of the developing fruiting bodies (Fig. 24B, E, K). Although under the control of a different promoter than endogenous annexin, annexin-GFP correctly distributed to both cell types.

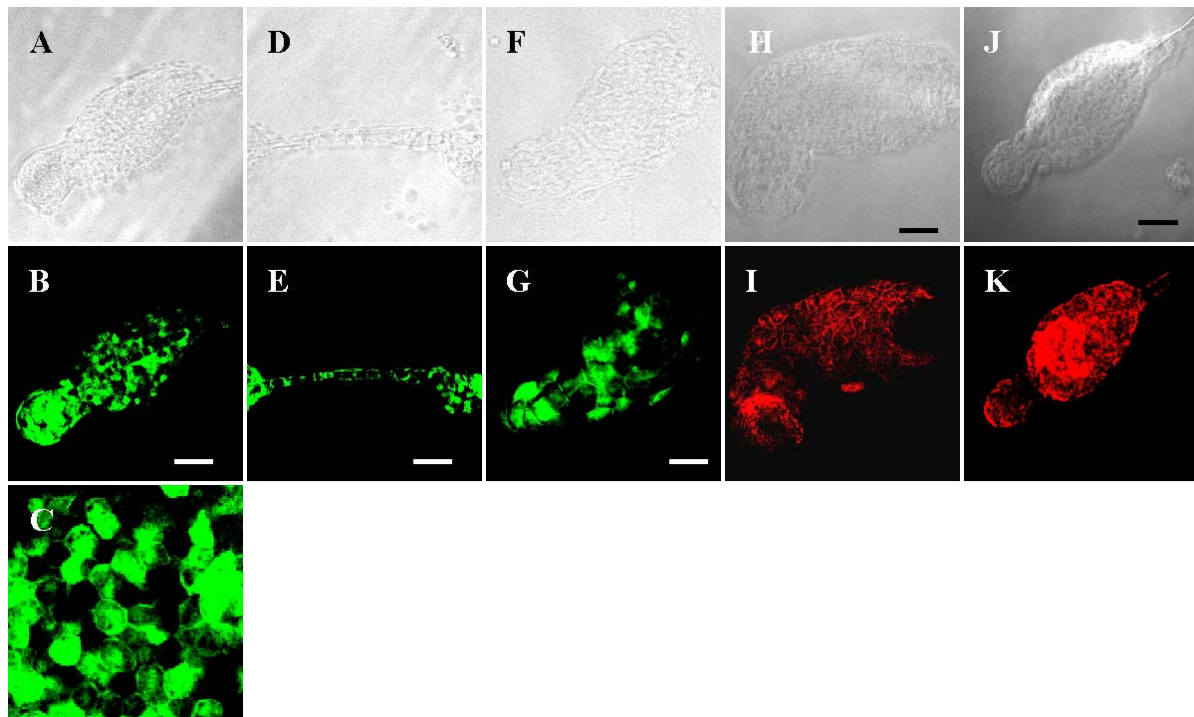


Fig. 24. Localization of annexin in slugs and forming fruiting bodies. After developing on phosphate agar plates (Material and Methods 2.2) slugs and fruiting bodies were carefully resuspended in Soerensen phosphate buffer, allowed for 20 min to settle and attach onto the coverslips and fixed in cold methanol (Material and Methods 5.1.2). (A, D, F, H, J) Phase contrast. (A-G) Cells expressing annexin-GFP and (H-K) wild type cells. (F, G, H, I) Slugs and (A, B, J, K) fruiting bodies. (C) Detail, prespore cells of the fruiting body shown in (B). (D, E) The stalk of the fruiting body. The endogenous protein was detected with mAb 185-338-1. Immunofluorescence was performed as described in Material and Methods 5.1.3. Images were taken by confocal microscopy. Bar, 18 μm (A, B), 17 μm (D, E), 7 μm (F, G), 9 μm (H, I), 10 μm (J, K).

The localization of annexin and annexin-GFP in the single cells within fruiting bodies was in the cytosol and on the plasma membrane of the single cells and was not altered when compared with vegetative cells (Fig. 4).

Unlike annexin-GFP, D293A annexin did not rescue the delayed development of SYN^- cells. Moreover, it provoked even a bigger impairment and longer delay in development. However, when we inspected fixed fruiting bodies for its localization the protein was correctly distributed, residing in the spore and the stalk cells (Fig. 25B, D). Single spore and stalk cells within fruiting bodies had D293A annexin present on their membranes and in the cytosol (Fig. 25) as it has been seen in the SYN^- D293A vegetative cells (Fig. 4C, D). Also, D293A annexin showed an overall distribution in the slugs formed from AX2 D293A cells (Fig. 25H). Within single cells, it was situated on the cell membranes and in the cell cytoplasm. The finding obtained from the studies of fruiting bodies from SYN^- D293A cells that D293A annexin is present in both, spore cells and stalk cells and that it had an unchanged localization within the cells was additionally confirmed by examination of fruiting bodies that consisted of AX2 D293A cells (Fig. 25F).

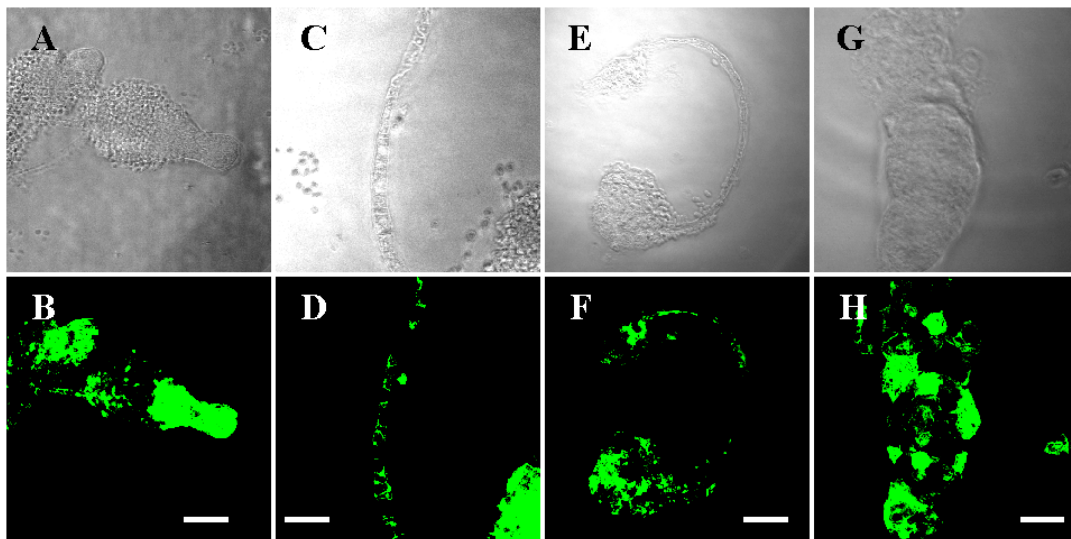


Fig. 25. (Previous page) **Localization of D293A annexin in slugs and forming fruiting bodies.** Preparation of slugs and fruiting bodies were done as described for Fig. 24. (A, C, E, G) Phase contrast. (A-D) SYN^- D293A cells and (E-H) AX2 D293A cells. (G, H) Slugs and (A, B, E, F) fruiting bodies. (C, D) The stalk of the fruiting body. Immunofluorescence was performed as described in Material and Methods 5.1.3. Images were taken by a confocal microscope. Bar, 22 μm (A, B), 15 μm (C, D), 24 μm (E, F), 12 μm (G, H).

4. Discussion

Annexins are an evolutionarily conserved multigene family with an increasing number of family members. They are present throughout animal and plant kingdom. In general each species harbors several annexin genes which can be co-expressed in cells and tissues. The conservation of their structure and their biochemical properties further complicates the analysis of their *in vivo* function. In fact, the knock out mice, that have been established recently, have given only limited information on the functions of annexins. In general, inactivation of a particular gene did not interfere with viability and fertility of these animals. A loss of annexin A6 was associated with increased mechanical properties in isolated cardiomyocytes that are due to altered Ca^{2+} -handling (Song *et al.*, 2002). Cardiomyocytes isolated from annexin A7 knock-out mice have an altered frequency induced shortening, which might result from an altered cellular Ca^{2+} homeostasis (Herr *et al.*, 2001). Recently described annexin A1 knock-out mice are more sensitive to inflammatory and other environmental stimuli, which resulted in a more intense inflammatory response (Hannon *et al.*, 2003). These findings support the notion that annexin A1 is a mediator of glucocorticoid action in inflammation. Taken together, the relatively mild effects might be due to the presence of other annexin proteins taking over the function of the missing protein.

Organisms harboring a single annexin gene therefore appear to be uniquely suited to study the role of annexins. It might well be that a single annexin performs all the tasks that are normally carried out by a set of annexin proteins in an organism. Alternatively, it takes over that role, which is the most essential one. In general, annexin does not appear to be essential for eukaryotic life because *Saccharomyces cerevisiae* and *Schizosaccharomyces pombe* can exist without this protein. By contrast, *Dictyostelium* harbors annexin(s). Unlike yeast, *Dictyostelium* exists as a unicellular and multicellular organism and undergoes a developmental cycle in which the cells differentiate into at least two cell types, prespore and prestalk cells. In addition to the developmental aspects, *Dictyostelium* offers a wide range of techniques for analysis of cell biological aspects.

1.1 Subcellular localization of *Dictyostelium* annexin C1

Dictyostelium harbors an annexin gene which gives rise to two isoforms. These two isoforms differ by a short insertion in the unusually long amino terminal domain which is composed of GYPPQQ repeats. The additional exon adds four extra copies of this repeat (Greenwood and Tsang, 1991).

It is known for different annexins that they show different subcellular distributions but they often reside in a cytosolic and a membrane-associated pool with a switch between the two pools regulated by Ca^{2+} . In most cases, the plasma membrane and membranes of the biosynthetic or the endocytic pathway are the target membranes for different annexins (Zoblack *et al.*, 2001; Recher *et al.*, 2000) suggesting a role for annexins in membrane trafficking. For some annexins (annexin A1 and annexin A2) it was shown that removal of the unique N-terminal domain resulted in a change of intracellular localization (Rescher *et al.*, 2000; Eberhard *et al.*, 2001) which could reflect distinct functions of the two species.

Immunofluorescence studies of *Dictyostelium* cell lines expressing either annexin, Anx-D293A or annexin core as GFP fusion proteins (Fig. 3) revealed subcellular localizations of these fusion proteins (Fig. 5B-F) essentially consistent with that of the endogenous one (Döring *et al.*, 1995; Fig. 5A). Annexin localized diffusely in the cytoplasm of the cells and stained prominently plasma membranes and cell nuclei. Interestingly, the core domain fused to GFP showed the same localization as the full length protein strongly suggesting that the core domain is responsible for the proper targeting of the protein to different compartments of the cell. Closer inspection of the cells revealed the presence of the protein also on internal membranes.

This finding was supported by the subcellular fractionation experiments (Fig. 6) in which annexin was detected in the cell cytosol, microsomes, vesicle fraction and cytoskeleton as well as plasma membrane fraction. The nature of the annexin-containing vesicles was partly revealed by co-immunostaining of cells expressing annexin-GFP with antibodies specific for the A subunit of the vacuolar V/H^+ -ATPase or with vacuolin specific antibodies and by cell fractionation experiments. The internal membranes partially overlapped with membranes that were positive for the vacuolar V/H^+ -ATPase. The vacuolar V/H^+ -ATPase is primarily found

in membranes of the contractile vacuole complex and in endosomal membranes in *Dictyostelium*. Membranes containing the V/H⁺-ATPase also fuse with phagosomes during phagosome maturation (Clarke *et al.*, 2002; Gotthardt *et al.*, 2002). Furthermore, annexin-GFP was present on vesicular structures positive for vacuolin, which is a marker for late stage endosomes (Maniak, 2003). Upon further fractionation of the membranes in a discontinuous sucrose gradient we confirmed the immunofluorescence data and showed that both the endogenous protein and annexin-GFP co-distributed throughout the gradient and were present in the plasma membrane fraction, the Golgi fraction and in fractions containing endosomes and lysosomes (Fig. 8). Annexin-GFP was present to a lesser extent in the ER fraction.

The annexin-endosome interactions have been already described for annexins A1, A2 and A6. For example, annexin A1 was found on early and multivesicular endosomes (Seemann *et al.*, 1996; Futter *et al.*, 1993). It had been proposed by Futter *et al.* (1993) that it mediates the inward vesiculation in multivesicular endosomes. Annexin A2 was also detected on early endosomes (Jost *et al.*, 1997) while annexin A6 was observed on different endosomal membranes such as the apical endocytic compartment and late endosomes in different cells, respectively (Ortega *et al.*, 1998; Pons *et al.*, 2000). However, the function of different annexins that correlates with their localization on endosomes remains still to be established.

1.2 Annexin localizes on pinosomes and phagosomes

Pinocytosis studies revealed that annexin accumulated also on pinosomes where it appeared to dissociate quickly once the pinosome was internalized (Fig. 15A). This behaviour was distinctly different from phagocytosis where annexin was present on phagosomes during engulfment of a particle and stayed on the phagosome after internalization (Fig. 16).

Although macropinocytosis, which we observe, and phagocytosis are similar processes both involving PIP₂, actin polymerization, and the accumulation of proteins like coronin, biochemically they appear to be distinct. Whereas phagocytosis is regulated by Rap1, RacC and myosin VII, pinocytosis involves profilin, LmpA and PKB (Cardelli, 2001). A different pattern of annexin association with these structures is therefore not unexpected. The behavior during endocytosis and phagocytosis has been also studied in detail for mammalian annexins

Anxa1, Anxa2, Anxa3, Anxa4 and Anxa5 in J744 mouse macrophages which resemble the professional phagocyte *Dictyostelium* in several aspects (Diakonova *et al.*, 1997). In these immuno electron microscopic studies annexins Anxa1, Anxa2, Anxa3, Anxa4 and Anxa5 were detected on early endosomes while annexin Anxa5 was also detected on late endosomal structures. All of the annexins were found on phagosomes. Anxa1, Anxa2, Anxa3 and Anxa5 were associated with phagosomes isolated at different time points. The amount of annexin Anxa4 increased at later times. Although these findings point to a role of the respective annexins in phagocytosis and phagosome maturation, the connection between annexins and phagocytosis remains to be solved.

Our findings for *Dictyostelium* annexin C1 are comparable to the ones obtained in mouse macrophages and the *Dictyostelium* annexin C1 protein thus has all the features observed for mouse annexins. Surprisingly, a loss of annexin C1 did not affect the efficiency of pinocytosis and exocytosis although SYN^- cells showed slightly higher and faster rate of pinocytosis and a faster rate of exocytosis when compared with AX2 cells. Similar, SYN^- exhibited a faster rate of phagocytosis when compared with wild type. In accordance with this finding is the observation that AX2-Anx-GFP cells were much slower than AX2 and SYN^- cells in phagocytosing yeast particles. Moreover, AX2-Anx-GFP cells never achieved the same level of uptake as AX2 and SYN^- cells. We conclude that annexin C1 has a moderate inhibitory effect on phago-, pino- and exocytosis.

1.3 Ca^{2+} -independent membrane binding of annexin C1

The single most important parameter regulating Ca^{2+} -independent membrane binding of annexins is the pH value chosen to analyze the interaction. Annexin A5 binds to and penetrates the bilayer of phosphatidylserine vesicles at pH 4.0 (Köhler *et al.*, 1997) and at pH 5.0 it can induce a leakage of the phosphatidylserine vesicles (Hoekstra *et al.*, 1993). At neutral pH, the presence of Ca^{2+} is necessary for the interaction with lipids (Köhler *et al.*, 1997). It was proposed by Beermann *et al.* (1998) when the acid-induced unfolding of the protein was analyzed that the described behavior is caused by a conformational change in the annexin A5 molecule, which

occurs between pH 4.6 and pH 4.0. Subsequent studies by Meers and Mealy (1993) and Sopkova *et al.* (1993, 1998, 1999, 2001) showed that this conformational change is characterized by the solvent exposure of the unique tryptophan residue in annexin A5 (Trp-187). A similar change can occur at neutral pH but it is then a consequence of the presence of Ca^{2+} . From the studies of annexin B12 a model emerged, which could explain events that follow the pH-dependent alteration in conformation. The pH-dependent alteration in conformation could be induced by the protonation of certain carboxylate residues found in or close to the loop of the helix-loop-helix motif. Upon deprotonation the protein could be driven back to the conformation which it has in solution (Langen *et al.*, 1998a; Langen *et al.*, 1998b). However, all these studies were done *in vitro* and at non physiological conditions (pH 4.0-5.0). With *Dictyostelium* as a model system and the use of annexin-GFP we could follow *in vivo* alterations in the annexin localization pattern upon the changes of the cytosolic pH. In living *Dictyostelium* cells annexin showed a different distribution when compared with methanol fixed cells. It was diffused in the cell cytoplasm and no obvious staining of internal membranes or plasma membrane could be seen. After decreasing the cytosolic pH by the addition of propionic acid, which was adjusted to pH 6.0, annexin-GFP translocated within seconds to the plasma membrane.

We speculate that this behavior *in vivo* could also occur upon hyperosmotic stress or hypoxia which leads to acidification of the cytosol (Pintsch *et al.*, 2001; Sartre *et al.*, 1989). Exposure of cells to high osmolarities evokes a variety of responses. Accumulation of compatible osmolytes raises the intracellular osmotic potential. Furthermore the synthesis of stress proteins protects cellular compartments facilitating repair and recovery (Kwon and Handler, 1995). However, this process is slow in both pro- and eukaryotes. Eukaryotes in addition show a quick change in their cell volume. *Dictyostelium* cells respond to osmotic stress by reducing their cell volume by 50 % within 5 min (Zischka *et al.*, 1999). In addition, progressive cytosol acidification is observed during hyperosmotic shock when the pH drops from 7.5 to 6.8 in 15 min (Pintsch *et al.*, 2001). We speculate that translocation of annexin C1 from the cytosol to the plasma membrane upon acidification of the cytosol can occur *in vivo* as a response to hyperosmotic stress. A similar behavior upon acidification of the cytosol was observed for *Dictyostelium* hisactophilins (Hanakam *et al.*, 1996). We speculate further that annexin C1 might penetrate the plasma

membrane and could induce a leakage of the cell as already reported for annexin A5. Annexin A5 can induce a leakage of the phosphatidylserine vesicles *in vitro* at pH 5.0 (Hoekstra *et al.*, 1993). This could explain the higher sensitivity to hyperosmotic conditions of the strain overexpressing annexin C1 (Results, Fig. 9A). Higher amounts of annexin in the cell could cause a bigger damage in the initial stage of hyperosmotic stress. The cell would then need longer time for repair and recovery.

Furthermore, acidification of the cytosol leads to inhibition of endocytosis, slowing down of vesicle mobility and depletion of the NTP pool indicating a general decrease in cellular activity (Pintsch *et al.*, 2001). In the present study we have shown moderate inhibition of phagocytosis in cells overexpressing annexin (Fig. 18) as well as an involvement of annexin in endocytosis (Fig. 15A) and its localization on endosomes and contractile vacuoles (Fig. 7). We further speculate that upon acidification of the cytosol, as a response to stress stimuli, annexin translocates quickly to the plasma membrane and plays a role in inhibition of endocytosis in this way indirectly participating in maintenance of cell homeostasis.

1.4 Nonlipid annexin ligands

Annexins are known for long to bind via their N-terminal domain to other proteins. Some of the typical binding partners are members of the EF hand superfamily which all possess a helix-loop-helix Ca^{2+} -binding motif. Annexins A1, A2 and A11 are reported to bind small EF hand proteins that belong to the S100 subfamily, S100A11, S100A10 and S100A6, respectively (Rety *et al.*, 1999; Rety *et al.*, 2000; Mailliard *et al.*, 1996; Tokumitsu *et al.*, 1992). In addition, sorcin that is described to interact with annexin A7, is as a well member of the EF hand superfamily like S100 proteins, but it contains five and not two (S100 proteins) helix-loop-helix motifs. Sorcin binds to the GYP-rich N-terminal domain of annexin A7 in a Ca^{2+} -dependent manner (Brownawell and Creutz, 1997) with the N-terminal domain of sorcin being necessary for the interaction (Verzili *et al.*, 2000).

In gel filtration experiments we showed that annexin C1 exists in the cytosol as a monomer. However, detection of the protein in fractions with a slightly higher molecular mass pointed to the existence of possible complexes with other protein(s). Immunoprecipitation experiments and

further MALDI MS analysis, protein sequencing followed by similarity searches revealed two possible binding partners of *Dictyostelium* annexin C1. The first one is a small, 20 kDa Ca^{2+} -binding protein named CBP2. CBP2 contains four consensus sequences all predicted to bind Ca^{2+} and all being typical for Ca^{2+} -binding EF-hand domains (André *et al.*, 1996). The second protein, DdPEF-2 (22-23 kDa), belongs to the penta EF-hand protein family and was recently described by Ohkouchi *et al.* (2001). Comparison with the canonical EF-hand sequence suggested that EF-4 and EF-5 do not bind Ca^{2+} due to the presence of unfavorable residues at the Ca^{2+} -coordinating positions, while sequences in EF-1, EF-2 and EF-3 match with a 13-residue consensus pattern of the EF-hand motif (Ohkouchi *et al.*, 2001). The subcellular localization of DdPEF-2 matches with the one of annexin supporting the assumption that they could interact *in vivo*. DdPEF-2 was found predominantly as cytosolic protein present in lesser amounts in the membrane pellet fractions. Moreover, DdPEF-2 shows similar behavior as annexin in the presence of Triton X-100, remaining exclusively in the Triton X-100 soluble fraction. Addition of Triton X-100 into the lysis buffer containing Ca^{2+} was not affecting the solubilization of DdPEF-2 (Ohkouchi *et al.*, 2001) neither had it an effect on the solubilization of annexin (Fig. 11).

One additional small protein belonging as well to the penta EF-hand protein family in *Dictyostelium* is DdPEF-1 (Ohkouchi *et al.*, 2001). DdPEF-1 is similar to DdPEF-2 present in the cells throughout development. The level of the DdPEF-2 gene transcript reached a peak after 4-8 hours of starvation and then decreased (12 hours of starvation) remaining at low levels in the later stages of development, whereas the level of DdPEF-1 gene transcript gradually increased. Based on this pattern of expression it might well be that we detected just DdPEF-2 as a binding partner since we used vegetative, but not developing cells for the assay. The expression pattern of DdPEF-1 opens the possibility that DdPEF-1 could interact with annexin in later stages of *Dictyostelium* development.

Annexin XIIIb (Lafont *et al.*, 1998) and annexin A2 (Sagot *et al.*, 1997) were reported to be present in the Triton X-100 insoluble membrane subdomains. Annexin A2 translocates to the Triton X-100 insoluble fraction upon stimulation of chromaffin cells with nicotine and as a function of Ca^{2+} . *Dictyostelium* annexin C1 associates with Triton X-100 insoluble material only in the presence of Ca^{2+} (Fig. 11). However, in the presence of Ca^{2+} annexin D293A did not

completely translocate to the Triton insoluble fraction and remained as well in the Triton X-100 soluble fraction. Considering the proposed high affinity for Ca^{2+} of this particular Ca^{2+} -binding site (Weng *et al.*, 1993, Huber *et al.*, 1990) and the previously described cooperation in binding of Ca^{2+} (Rosengarth *et al.*, 2001) we speculate that this particular substitution of aspartic acid at the position 293 with alanine reduced the protein's affinity for binding of Ca^{2+} and affected binding of Ca^{2+} to other Ca^{2+} -binding sites.

1.5 The role of annexin during development

Multicellularity and development are important features of *Dictyostelium*. The mechanism for generating multicellularity in *D. discoideum* differs significantly from the early steps of metazoan embryogenesis. Contrary to metazoans in *D. discoideum* growth and differentiation are well separated. Cells multiply first and then gather chemotactically to form a multicellular organism. However, subsequent processes depend on cell-cell communication in both systems, and basic processes such as differential cell sorting, pattern formation, stimulus-induced gene expression and cell-type specific regulation are common to *D. discoideum* and metazoans. The increased complexity of the organism, which is paralleled by an increased number of genes as compared to *S. cerevisiae* or *S. pombe* (Glöckner *et al.*, 2002) might require the presence of an annexin. In fact, the most obvious defect which we noted in the SYN^- mutant was a failure to undergo proper multicellular development. We conclude that annexin is not essential for viability of *Dictyostelium*, neither is its presence essential for membrane trafficking, however the loss of *Dictyostelium* annexin C1 affects development. This might be caused by its involvement in intracellular Ca^{2+} homeostasis. The fact which speaks in favor of this conclusion is that the $\text{SYN}^- \text{D293A}$ cells which expressed annexin with one of its high affinity Ca^{2+} -binding sites mutated were not rescued in their development. On the contrary, they showed an even longer delay in development when compared with the parental strain. However, the intact annexin core domain alone is not sufficient to compensate the described impairment, suggesting that the full length protein is necessary and the only factor able to rescue the impairment in development. Therefore, we speculate that the interaction of annexin with other protein(s) via its N-terminal domain might be of a crucial importance for *Dictyostelium* normal development. The annexin

literature contains a number of reports in which the expression of individual annexins is correlated with cell proliferation or differentiation. Annexin B12 from *Hydra vulgaris* is strictly confined to epithelial battery cells throughout tentacles while the second *Hydra* annexin is mainly located in the cytoplasm of nematocytes (Sopkova *et al.*, 1999). The annexin expressed earliest in Medaka fish embryogenesis (ortholog of annexin A11) appears transiently in the prechordal mesendoderm and hindbrain. The three other Medaka annexins (orthologs of annexins A1, A4 and A5) are expressed later in embryogenesis with their expression limited to liver, floor plate and skin (Osterloh *et al.*, 1998).

Dictyostelium cells undergo a relatively simple programme of multicellular development, which in many ways resemble animal development. It is known for *Dictyostelium* that high cytosolic Ca^{2+} concentration in prestalk cells is opposed to its low concentration in prespore cells from the earliest multicellular stages through the end of development (Cubitt *et al.*, 1995; Jaffe, 1997). Moreover, manipulations by which the cytosolic Ca^{2+} concentration can be raised, favor stalk cell formation (Maeda, 1970).

Under normal laboratory conditions, annexin C1 was observed in both prestalk and prespore cells of migrating slugs and its presence remained unaltered in stalk and spore cells of fruiting bodies. Its localization in spore and stalk cells was similar and did not differ from the one observed for the precursors of these cells. Even more, the distribution of annexin in differentiating cells did not differ from its distribution in vegetative cells. We concluded that association of annexin with the plasma membrane, its diffuse distribution in the cytosol and prominent nuclear localization is not changed during transition from unicellular to multicellular organism and stays unaltered till the end of development. This particular localization of annexin is not influenced by diverse patterns of differentiation of prestalk and prespore cells and is independent from changing intracellular Ca^{2+} concentrations directing cell fate.

1.6 Phosphorylation of annexin C1

Annexins are known to be targets for different kinases. Annexin A2 was isolated as a major substrate for v-src protein kinase and annexin A1 is phosphorylated by tyrosine kinase activity of

the epidermal growth factor receptor (Rothhut, 1997). Although these phosphorylations are known to occur *in vivo*, their physiological consequences have not been established. *In vitro* or *in situ* studies have revealed alterations in the Ca^{2+} -membrane binding of annexins A1 and A2 phosphorylated at Tyr-20 (by the EGF receptor kinase, De *et al.*, 1986) and Tyr-23 (by the src kinase, Glenney *et al.*, 1987), respectively. Tyrosine phosphorylated annexin A1 is more susceptible to N-terminal proteolysis, thus showing altered phospholipid vesicle binding and aggregation activities (Haigler *et al.*, 1992). Serine/threonine kinases have also been described to phosphorylate annexins. Phosphorylation sites again reside in the unique N-terminal domains of the annexins, and the modifications in some cases have been shown to affect biochemical properties of the annexins, in particular their affinity for Ca^{2+} and phospholipids (Gerke and Moss, 1997). PKC, for example, has long been known to phosphorylate a number of annexins, with annexin A5 being an exception as it can serve as a PKC inhibitor (Russo-Marie, 1999). In adrenal chromaffin cells nicotine stimulation leads to annexin A2 phosphorylation by PKC with activation of PKC being a prerequisite for regulated exocytosis (Delouche *et al.*, 1997).

We showed that *Dictyostelium* annexin C1 had several different charge isomers (Fig. 19). However, further studies are needed to elucidate whether these charge isomers represent phosphorylated annexin and if so which protein kinase is responsible for this modification *in vivo*, which amino acid residues are phosphorylated and how the phosphorylation influences localization and function of annexin C1.

Recently, new annexin gene sequence was obtained from *Dictyostelium* genome sequencing project. The new protein shows 30 % of identity with annexin C1. Although new annexin needs to be characterized we speculate that it could compensate the absence of annexin C1 in SYN^- cells what could further explain the fact that SYN^- cells did not show severe impairments. However, our first results (data not shown) pointed to its very low level of expression. We further speculate that this low level of expression is not sufficient for compensation of the role of annexin C1 in development. Further characterization of new annexin, its Ca^{2+} -binding affinity, its localization in the cell and its binding partners would as well lead to better understanding of annexin C1 function.

Summary

Annexins are big family of proteins which are binding to phospholipids in a Ca^{2+} -dependent manner. A lot is known about their distribution in the cells and tissues, their involvement in endocytosis and exocytosis, vesicular trafficking and rearrangement of the cytoskeleton. For several annexins mouse knock out models are established. However, loss of one particular annexin had relatively mild effects suggesting compensation of the lost annexin function by other annexins.

This study focused on *Dictyostelium discoideum* annexin C1, its dynamic behavior and possible interactions with other proteins. GFP-tagged full length annexin, a mutated form of annexin and the annexin core domain were used to study involvement of annexin in cellular processes *in vivo* and *in vitro*, with emphasis on processes like pinocytosis, phagocytosis, osmoregulation and development. *Dictyostelium* annexin C1 localizes in the cell cytosol and nucleus and on the plasma membrane. In the cytosol annexin is associated with internal membranes. Fractionation of membranes on discontinuous sucrose gradient showed that annexin C1 was present on plasma membrane, endosomal and lysosomal membranes, as well as in Golgi membranes and in a lesser amounts in ER fraction. In addition, co-immunostaining with several protein markers revealed annexin C1 in association with endosomes and contractile vacuoles. Although its localization on contractile vacuoles suggested a role in osmoregulation, mutant lacking annexin (SYN^-) behaved similar to wild type cells (AX2) under osmotic stress conditions. Despite the presence of annexin C1 on pinosomes and phagosomes the SYN^- mutant was not impaired in endocytosis and exocytosis when compared with AX2 and showed an increased rate of phagocytosis. In accordance with this is the decreased rate of phagocytosis observed with cells overexpressing annexin. Furthermore we observed *in vivo* translocation of annexin from the cytosol to the plasma membrane upon a decrease in cytosolic pH. This finding showed that the protein could bind to phospholipids in the absence of Ca^{2+} and was in accordance with previously published *in vitro* data for annexin A5 and B12.

We also found that annexin C1 associated with Triton X-100 insoluble pellet only in the presence of Ca^{2+} . A mutation in one Ca^{2+} -binding site in the third annexin repeat affected this behavior. Considering proposed high affinity for Ca^{2+} of this particular Ca^{2+} -binding site and the previously

described cooperation in binding of Ca^{2+} we speculate that his particular substitution of aspartic acid residue at the position 293 with alanine reduced protein affinity for binding of Ca^{2+} and eventually affected binding of Ca^{2+} to other Ca^{2+} -binding sites. Gel filtration and immunoprecipitation experiments revealed the presence of annexin C1 monomers in the cytoplasm and interactions with two small Ca^{2+} -binding proteins, CBP2 and DdPEF-2. Furthermore, we found annexin to be phosphorylated but the physiological role of phosphorylation is needed to be further studied in detail.

Taken together, annexin C1 is not crucial for the survival of *Dictyostelium*. In annexin minus mutant SYN^- however development was noticeably affected and was retarded by more than four hours and not all multicellular structures finally developed into fruiting bodies consisting of spore and stalk cells. Although all fusion proteins showed same localization in slugs, stalks and spore cells, impairment in development of SYN^- cells could only be rescued by the full length protein pointing out the crucial importance of annexin function for development.

Zusammenfassung

Annexine sind eine große Familie von Proteinen, die Phospholipide in Abhängigkeit von Kalziumionen binden. Viele Daten existieren über die Verteilung der Annexine in Zellen und Geweben und über deren Beteiligung an Exo- und Endozytose, Vesikeltransport und der Dynamik des Zytoskeletts. Verschiedene Annexin-Gene wurden in der Maus inaktiviert. Die relativ milden Phänotypen der einzelnen „Knock-Outs“ suggerieren jedoch Kompensationseffekte (eine zum Teil redundante Funktion) durch vorhandene andere Annexine. Der Fokus der vorliegenden Arbeit lag auf dem dynamischen Verhalten und den Protein-Protein-Interaktionen von Annexin C1 aus *Dictyostelium discoideum*. Annexin, eine mutierte Form von Annexin und die Annexin „core-domain“, wurden als GFP-Fusionsprotein zur Untersuchung der Rolle von Annexin bei zellulären Prozessen *in vivo* und *in vitro* verwendet. Das Augenmerk wurde hierbei auf die Pinozytose, Phagozytose, Osmoregulation und Entwicklung gelegt.

Dictyostelium Annexin C1 wurde im Zytosol, im Kern und an der Plasmamembran gefunden.

Im Zytosol wurde Annexin in Assoziation mit internen Membranen gefunden. Zellfraktionierungsexperimente mittels Saccharose-Dichtegradientenzentrifugation zeigten, dass Annexin C1 sowohl in der Plasmamembranfraktion als auch in endosomalen, lysosomalen und Golgi-Fractionen vorhanden war. In geringeren Mengen wurde es in der ER-Fraktion gefunden. Immunmarkierungen gegen verschiedene bekannte Proteine zeigten in der Fluoreszenzmikroskopie, dass Annexin C1 in Assoziation mit Endosomen und der kontraktilen Vakuole vorliegt.

Die Annexin C1-Lokalisierung an internen Membranen und die beobachtete Dynamik in der Lokalisierung in Antwort auf Veränderungen könnte eine Beeinträchtigung einer Vielzahl von membranassoziierten Prozessen nahelegen. Eine detaillierte Untersuchung der Osmoregulation, der Pinozytose und Phagozytose hat dies jedoch nicht gezeigt. Es wurde sogar eine verbesserte Phagozytoserate in SYN^- Zellen beobachtet. Dies lässt zumindest den Schluss zu, dass Annexin C1 eine Bedeutung für den Membranfluss besitzt.

Annexin C1 ist nicht essentiell zum Überleben von *Dictyostelium*. In einer Annexin defizienten Mutante SYN^- war jedoch der Entwicklungszyklus beeinflusst. Der Entwicklungszyklus war um mehr als vier Stunden verzögert.

Obwohl alle verwendeten Fusionsproteine eine identische Lokalisation in „slugs“, Stiel- und Sporenzellen aufwiesen, konnte ausschließlich das Vollängenfusionsprotein den Phänotyp der Mutanten aufheben. Dieser Befund weist auf die Bedeutung von Annexin für die Multizellularität hin.

Bibliography

Alvarez-Martinez, M. T., Porte, F., Liautard, J. P. & Sri Widada, J. Effects of profilin-annexin I association on some properties of both profilin and annexin I: modification of the inhibitory activity of profilin on actin polymerization and inhibition of the self-association of annexin I and its interactions with liposomes. *Biochim Biophys Acta* **1339**, 331-40 (1997).

Andre, B., Noegel, A. A. & Schleicher, M. *Dictyostelium discoideum* contains a family of calmodulin-related EF-hand proteins that are developmentally regulated. *FEBS Lett* **382**, 198-202 (1996).

Aubry, L., Klein, G., Martiel, J.-L. and Satre, M. Kinetics of endosomal pH evolution in *Dictyostelium discoideum* amoebae. Study by fluorescence spectroscopy. *J. Cell Sci.*, **105**, 861-866 (1994).

Babiychuk, E. B., Palstra, R. J., Schaller, J., Kampfer, U. & Draeger, A. Annexin VI participates in the formation of a reversible, membrane-cytoskeleton complex in smooth muscle cells. *J Biol Chem* **274**, 35191-5 (1999).

Becker, T., Weber, K. & Johnsson, N. Protein-protein recognition via short amphiphilic helices; a mutational analysis of the binding site of annexin II for p11. *Embo J* **9**, 4207-13 (1990).

Beermann ofm cap, B. B., Hinz, H. J., Hofmann, A. & Huber, R. Acid induced equilibrium unfolding of annexin V wild type shows two intermediate states. *FEBS Lett* **423**, 265-9 (1998).

Bennett, M. R., Gibson, D. F., Schwartz, S. M. & Tait, J. F. Binding and phagocytosis of apoptotic vascular smooth muscle cells is mediated in part by exposure of phosphatidylserine. *Circ Res* **77**, 1136-42 (1995).

Bertholdt, G., Stadler, J., Bozzaro, S., Fichtner, B. & Gerisch, G. Carbohydrate and other epitopes of the contact site A glycoprotein of *Dictyostelium discoideum* as characterized by monoclonal antibodies. *Cell Differ* **16**, 187-202 (1985).

Bonfils, C., Greenwood, M. & Tsang, A. Expression and characterization of a *Dictyostelium discoideum* annexin. *Mol Cell Biochem* **139**, 159-66 (1994).

Bonner, J.T. Evidence for the formation of cell aggregates by chemotaxis in development of the slime mold *Dictyostelium discoideum*. *J. Exp. Zool.*, **106**, 1-26 (1947).

Brownawell, A. M. & Creutz, C. E. Calcium-dependent binding of sorcin to the N-terminal domain of synexin (annexin VII). *J Biol Chem* **272**, 22182-90 (1997).

Buczynski, G., Grove, B., Nomura, A., Kleve, M., Bush, J., Firtel, R. A. & Cardelli, J. Inactivation of two *Dictyostelium discoideum* genes, DdPIK1 and DdPIK2, encoding proteins

related to mammalian phosphatidylinositol 3-kinases, results in defects in endocytosis, lysosome to postlysosome transport, and actin cytoskeleton organization. *J Cell Biol* **136**, 1271-86 (1997).

Bullock, W.O., Fernandez, J.M. and Short, J.M. XL1-blue: A high efficiency plasmid transforming recA *Escherichia coli* strain with beta-galactosidase selection. *BioTechniques* **5**, 376-378 (1987).

Campos, B., Mo, Y. D., Mealy, T. R., Li, C. W., Swairjo, M. A., Balch, C., Head, J. F., Retzinger, G., Dedman, J. R. & Seaton, B. A. Mutational and crystallographic analyses of interfacial residues in annexin V suggest direct interactions with phospholipid membrane components. *Biochemistry* **37**, 8004-10 (1998).

Campos, B., Wang, S., Retzinger, G. S., Kaetzel, M. A., Seaton, B. A., Karin, N. J., Johnson, J. D. & Dedman, J. R. Mutation of highly conserved arginine residues disrupts the structure and function of annexin V. *Arch Med Res* **30**, 360-7 (1999).

Caohuy, H. & Pollard, H. B. Activation of annexin 7 by protein kinase C *in vitro* and *in vivo*. *J Biol Chem* **276**, 12813-21 (2001).

Caohuy, H., Srivastava, M. & Pollard, H. B. Membrane fusion protein synexin (annexin VII) as a Ca²⁺/GTP sensor in exocytotic secretion. *Proc Natl Acad Sci U S A* **93**, 10797-802 (1996).

Cardelli, J. Phagocytosis and macropinocytosis in *Dictyostelium*: phosphoinositide-based processes, biochemically distinct. *Traffic* **2**, 311-20 (2001).

Chasserot-Golaz, S., Vitale, N., Sagot, I., Delouche, B., Dirrig, S., Pradel, L. A., Henry, J. P., Aunis, D. & Bader, M. F. Annexin II in exocytosis: catecholamine secretion requires the translocation of p36 to the subplasmalemmal region in chromaffin cells. *J Cell Biol* **133**, 1217-36 (1996).

Clarke, M., Kohler, J., Arana, Q., Liu, T., Heuser, J. & Gerisch, G. Dynamics of the vacuolar H(+)-ATPase in the contractile vacuole complex and the endosomal pathway of *Dictyostelium* cells. *J Cell Sci* **115**, 2893-905 (2002).

Claviez, M., Pagh, K., Maruta, H., Baltes, W., Fisher, P. and Gerisch, G. Electron microscopic mapping of monoclonal antibodies on the tail region of *Dictyostelium* myosin. *EMBO J.*, **1**, 1017-1022 (1982).

Coates, J. C. & Harwood, A. J. Cell-cell adhesion and signal transduction during *Dictyostelium* development. *J Cell Sci* **114**, 4349-58 (2001).

Creutz, C. E., Pazoles, C. J. & Pollard, H. B. Self-association of synexin in the presence of calcium. Correlation with synexin-induced membrane fusion and examination of the structure of synexin aggregates. *J Biol Chem* **254**, 553-8 (1979).

- Cubitt, A. B., Firtel, R. A., Fischer, G., Jaffe, L. F. & Miller, A. L. Patterns of free calcium in multicellular stages of *Dictyostelium* expressing jellyfish apoaequorin. *Development* **121**, 2291-301 (1995).
- Cubitt, A. B., Heim, R., Adams, S. R., Boyd, A. E., Gross, L. A. & Tsien, R. Y. Understanding, improving and using green fluorescent proteins. *Trends Biochem Sci* **20**, 448-55 (1995).
- De, B. K., Misono, K. S., Lukas, T. J., Mroczkowski, B. & Cohen, S. A calcium-dependent 35-kilodalton substrate for epidermal growth factor receptor/kinase isolated from normal tissue. *J Biol Chem* **261**, 13784-92 (1986).
- de Hostos, E. L., Rehfuess, C., Bradtke, B., Waddell, D. R., Albrecht, R., Murphy, J. & Gerisch, G. *Dictyostelium* mutants lacking the cytoskeletal protein coronin are defective in cytokinesis and cell motility. *J Cell Biol* **120**, 163-73 (1993).
- Delouche, B., Pradel, L. A. & Henry, J. P. Phosphorylation by protein kinase C of annexin 2 in chromaffin cells stimulated by nicotine. *J Neurochem* **68**, 1720-7 (1997).
- Devereux, J., P. Haeberli, and O. Smithies, A comprehensive set of sequence analysis programs for the VAX. *Nucleic Acids Res*, **12**, 387-95 (1984).
- Diakonova, M., Gerke, V., Ernst, J., Liautard, J. P., van der Vusse, G. & Griffiths, G. Localization of five annexins in J774 macrophages and on isolated phagosomes. *J Cell Sci* **110**, 1199-213 (1997).
- Doring, V., Schleicher, M. & Noegel, A. A. *Dictyostelium* annexin VII (synexin). cDNA sequence and isolation of a gene disruption mutant. *J Biol Chem* **266**, 17509-15 (1991).
- Doring, V., Veretout, F., Albrecht, R., Muhlbauer, B., Schlatterer, C., Schleicher, M. & Noegel, A. A. The in vivo role of annexin VII (synexin): characterization of an annexin VII-deficient *Dictyostelium* mutant indicates an involvement in Ca(2+)-regulated processes. *J Cell Sci* **108**, 2065-76 (1995).
- Eberhard, D. A., Karns, L. R., VandenBerg, S. R. & Creutz, C. E. Control of the nuclear-cytoplasmic partitioning of annexin II by a nuclear export signal and by p11 binding. *J Cell Sci* **114**, 3155-66 (2001).
- Furge, L. L., Chen, K. & Cohen, S. Annexin VII and annexin XI are tyrosine phosphorylated in peroxovanadate-treated dogs and in platelet-derived growth factor-treated rat vascular smooth muscle cells. *J Biol Chem* **274**, 33504-9 (1999).
- Furukawa, R. & Fechtmeier, M. Differential localization of alpha-actinin and the 30 kD actin-bundling protein in the cleavage furrow, phagocytic cup, and contractile vacuole of *Dictyostelium discoideum*. *Cell Motil Cytoskeleton* **29**, 46-56 (1994).

Futter, C. E., Felder, S., Schlessinger, J., Ullrich, A. & Hopkins, C. R. Annexin I is phosphorylated in the multivesicular body during the processing of the epidermal growth factor receptor. *J Cell Biol* **120**, 77-83 (1993).

Gerke, V. & Moss, S. E. Annexins and membrane dynamics. *Biochim Biophys Acta* **1357**, 129-54 (1997).

Gerke, V. & Moss, S. E. Annexins: from structure to function. *Physiol Rev* **82**, 331-71 (2002).

Glenney, J. R., Jr., Tack, B. & Powell, M. A. Calpactins: two distinct Ca⁺⁺-regulated phospholipid- and actin-binding proteins isolated from lung and placenta. *J Cell Biol* **104**, 503-11 (1987).

Glockner, G., Eichinger, L., Szafranski, K., Pachebat, J. A., Bankier, A. T., Dear, P. H., Lehmann, R., Baumgart, C., Parra, G., Abril, J. F., Guigo, R., Kumpf, K., Tunggal, B., Cox, E., Quail, M. A., Platzer, M., Rosenthal, A. & Noegel, A. A. Sequence and analysis of chromosome 2 of *Dictyostelium discoideum*. *Nature* **418**, 79-85 (2002).

Gotthardt, D., Warnatz, H. J., Henschel, O., Bruckert, F., Schleicher, M. & Soldati, T. High-resolution dissection of phagosome maturation reveals distinct membrane trafficking phases. *Mol Biol Cell* **13**, 3508-20 (2002).

Grewal, T., Heeren, J., Mewawala, D., Schnitgerhans, T., Wendt, D., Salomon, G., Enrich, C., Beisiegel, U. & Jackle, S. Annexin VI stimulates endocytosis and is involved in the trafficking of low density lipoprotein to the prelysosomal compartment. *J Biol Chem* **275**, 33806-13 (2000).

Gunteski-Hamblin, A. M., Song, G., Walsh, R. A., Frenzke, M., Boivin, G. P., Dorn, G. W., 2nd, Kaetzel, M. A., Horseman, N. D. & Dedman, J. R. Annexin VI overexpression targeted to heart alters cardiomyocyte function in transgenic mice. *Am J Physiol* **270**, 1091-100 (1996).

Haigler, H. T., Mangili, J. A., Gao, Y., Jones, J. & Horseman, N. D. Identification and characterization of columbid annexin Icp37. Insights into the evolution of annexin I phosphorylation sites. *J Biol Chem* **267**, 19123-9 (1992).

Hanahan, D. Studies on transformation of *Escherichia coli* with plasmids. *J Mol Biol* **166**, 557-80 (1983).

Hanakam, F., Albrecht, R., Eckerskorn, C., Matzner, M. & Gerisch, G. Myristoylated and non-myristoylated forms of the pH sensor protein hisactophilin II: intracellular shuttling to plasma membrane and nucleus monitored in real time by a fusion with green fluorescent protein. *Embo J* **15**, 2935-43 (1996).

Hannon, R., Croxtall, J. D., Getting, S. J., Roviezzo, F., Yona, S., Paul-Clark, M. J., Gavins, F. N., Perretti, M., Morris, J. F., Buckingham, J. C. & Flower, R. J. Aberrant inflammation and resistance to glucocorticoids in annexin 1^{-/-} mouse. *Faseb J* **17**, 253-5 (2003).

Herr, C., Smyth, N., Ullrich, S., Yun, F., Sasse, P., Hescheler, J., Fleischmann, B., Lasek, K., Brixius, K., Schwinger, R. H., Fassler, R., Schroder, R. & Noegel, A. A. Loss of annexin A7 leads to alterations in frequency-induced shortening of isolated murine cardiomyocytes. *Mol Cell Biol* **21**, 4119-28 (2001).

Hoekstra, D., Buist-Arkema, R., Klappe, K. & Reutelingsperger, C. P. Interaction of annexins with membranes: the N-terminus as a governing parameter as revealed with a chimeric annexin. *Biochemistry* **32**, 14194-202 (1993).

Hofmann, A., Raguene-Nicol, C., Favier-Perron, B., Mesonero, J., Huber, R., Russo-Marie, F. & Lewit-Bentley, A. The annexin A3-membrane interaction is modulated by an N-terminal tryptophan. *Biochemistry* **39**, 7712-21 (2000).

Holmes, D. S. & Quigley, M. A rapid boiling method for the preparation of bacterial plasmids. *Anal Biochem* **114**, 193-7 (1981).

Huber, R., Romisch, J. & Paques, E. P. The crystal and molecular structure of human annexin V, an anticoagulant protein that binds to calcium and membranes. *Embo J* **9**, 3867-74 (1990).

Iino, S., Sudo, T., Niwa, T., Fukasawa, T., Hidaka, H. & Niki, I. Annexin XI may be involved in Ca²⁺ - or GTP-gammaS-induced insulin secretion in the pancreatic beta-cell. *FEBS Lett* **479**, 46-50 (2000).

Inoue, H., Nojima, H. & Okayama, H. High efficiency transformation of *Escherichia coli* with plasmids. *Gene* **96**, 23-8 (1990).

Inouye, K. Control of cell type proportions by a secreted factor in *Dictyostelium discoideum*. *Development* **107**, 605-9 (1989).

Isas, J. M., Cartailier, J. P., Sokolov, Y., Patel, D. R., Langen, R., Luecke, H., Hall, J. E. & Haigler, H. T. Annexins V and XII insert into bilayers at mildly acidic pH and form ion channels. *Biochemistry* **39**, 3015-22 (2000).

Jaffe, L. F. Organization of early development by calcium patterns. *Bioessays* **21**, 657-67 (1999).

Jenne, N., Rauchenberger, R., Hacker, U., Kast, T. & Maniak, M. Targeted gene disruption reveals a role for vacuolin B in the late endocytic pathway and exocytosis. *J Cell Sci* **111**, 61-70 (1998).

Jost, M., Weber, K. & Gerke, V. Annexin II contains two types of Ca(2+)-binding sites. *Biochem J* **298**, 553-9 (1994).

Jost, M., Zeuschner, D., Seemann, J., Weber, K. & Gerke, V. Identification and characterization of a novel type of annexin-membrane interaction: Ca²⁺ is not required for the association of annexin II with early endosomes. *J Cell Sci* **110**, 221-8 (1997).

Kamal, A., Ying, Y. & Anderson, R. G. Annexin VI-mediated loss of spectrin during coated pit budding is coupled to delivery of LDL to lysosomes. *J Cell Biol* **142**, 937-47 (1998).

Kawasaki, H., Avila-Sakar, A., Creutz, C. E. & Kretsinger, R. H. The crystal structure of annexin VI indicates relative rotation of the two lobes upon membrane binding. *Biochim Biophys Acta* **1313**, 277-82 (1996).

Kohler, G., Hering, U., Zschornig, O. & Arnold, K. Annexin V interaction with phosphatidylserine-containing vesicles at low and neutral pH. *Biochemistry* **36**, 8189-94 (1997).

Kwon, H. M. & Handler, J. S. Cell volume regulated transporters of compatible osmolytes. *Curr Opin Cell Biol* **7**, 465-71 (1995).

Laemmli, U. K., Beguin, F. & Gujer-Kellenberger, G. A factor preventing the major head protein of bacteriophage T4 from random aggregation. *J Mol Biol* **47**, 69-85 (1970).

Lafont, F., Lecat, S., Verkade, P. & Simons, K. Annexin XIIIb associates with lipid microdomains to function in apical delivery. *J Cell Biol* **142**, 1413-27 (1998).

Langen, R., Isas, J. M., Hubbell, W. L. & Haigler, H. T. A transmembrane form of annexin XII detected by site-directed spin labeling. *Proc Natl Acad Sci U S A* **95**, 14060-5 (1998 a).

Langen, R., Isas, J. M., Luecke, H., Haigler, H. T. & Hubbell, W. L. Membrane-mediated assembly of annexins studied by site-directed spin labeling. *J Biol Chem* **273**, 22453-7 (1998 b).

Lewit-Bentley, A., Morera, S., Huber, R. & Bodo, G. The effect of metal binding on the structure of annexin V and implications for membrane binding. *Eur J Biochem* **210**, 73-7 (1992).

Loomis, W. F., Jr. Developmental regulation of alkaline phosphatase in *Dictyostelium discoideum*. *J Bacteriol* **100**, 417-22 (1969).

Loomis, W. F. & Kuspa, A. Biochemical and genetic analysis of pre-stalk specific acid phosphatase in *Dictyostelium*. *Dev Biol* **102**, 498-503 (1984).

Maeda, Y. Influence of ionic conditions on cell differentiation and morphogenesis of the cellular slime molds. *Dev Growth Differ* **12**, 217-27 (1970).

Magendzo, K., Shirvan, A., Cultraro, C., Srivastava, M., Pollard, H. B. & Burns, A. L. Alternative splicing of human synexin mRNA in brain, cardiac, and skeletal muscle alters the unique N-terminal domain. *J Biol Chem* **266**, 3228-32 (1991 a).

Magendzo, K., Shirvan, A., Pollard, H. B. & Burns, A. L. Tissue-regulated alternative splicing of synexin mRNA. *Ann N Y Acad Sci* **635**, 483-4 (1991 b).

Mailliard, W. S., Haigler, H. T. & Schlaepfer, D. D. Calcium-dependent binding of S100C to the N-terminal domain of annexin I. *J Biol Chem* **271**, 719-25 (1996).

Majeed, M., Perskvist, N., Ernst, J. D., Orselius, K. & Stendahl, O. Roles of calcium and annexins in phagocytosis and elimination of an attenuated strain of *Mycobacterium tuberculosis* in human neutrophils. *Microb Pathog* **24**, 309-20 (1998).

Malchow, D., Nagele, B., Schwarz, H. & Gerisch, G. Membrane-bound cyclic AMP phosphodiesterase in chemotactically responding cells of *Dictyostelium discoideum*. *Eur J Biochem* **28**, 136-42 (1972).

Maniak, M. Fusion and fission events in the endocytic pathway of *Dictyostelium*. *Traffic* **4**, 1-5 (2003).

Maniak, M., Rauchenberger, R., Albrecht, R., Murphy, J. & Gerisch, G. Coronin involved in phagocytosis: dynamics of particle-induced relocalization visualized by a green fluorescent protein Tag. *Cell* **83**, 915-24 (1995).

Meers, P. & Mealy, T. Relationship between annexin V tryptophan exposure, calcium, and phospholipid binding. *Biochemistry* **32**, 5411-8 (1993).

Neujahr, R., Heizer, C., Albrecht, R., Ecke, M., Schwartz, J. M., Weber, I. & Gerisch, G. Three-dimensional patterns and redistribution of myosin II and actin in mitotic *Dictyostelium* cells. *J Cell Biol* **139**, 1793-804 (1997).

Ohkouchi, S., Nishio, K., Maeda, M., Hitomi, K., Adachi, H. & Maki, M. Identification and characterization of two penta-EF-hand Ca(2+)-binding proteins in *Dictyostelium discoideum*. *J Biochem (Tokyo)* **130**, 207-15 (2001).

Ortega, D., Pol, A., Biermer, M., Jackle, S. & Enrich, C. Annexin VI defines an apical endocytic compartment in rat liver hepatocytes. *J Cell Sci* **111**, 261-9 (1998).

Osterloh, D., Wittbrodt, J. & Gerke, V. Characterization and developmentally regulated expression of four annexins in the killifish medaka. *DNA Cell Biol* **17**, 835-47 (1998).

Pintsch, T., Satre, M., Klein, G., Martin, J. B. & Schuster, S. C. Cytosolic acidification as a signal mediating hyperosmotic stress responses in *Dictyostelium discoideum*. *BMC Cell Biol* **2**, 9 (2001).

Pittis, M. G. & Garcia, R. C. Annexins VII and XI are present in a human macrophage-like cell line. Differential translocation on FcR-mediated phagocytosis. *J Leukoc Biol* **66**, 845-50 (1999).

Pons, M., Ihrke, G., Koch, S., Biermer, M., Pol, A., Grewal, T., Jackle, S. & Enrich, C. Late endocytic compartments are major sites of annexin VI localization in NRK fibroblasts and polarized WIF-B hepatoma cells. *Exp Cell Res* **257**, 33-47 (2000).

Raper, K.B. *Dictyostelium discoideum*, a new species of slime mould from decaying forest leaves. *J. Agr. Res.*, **50**, 135-147 (1935).

Rauchenberger, R., Hacker, U., Murphy, J., Niewohner, J. & Maniak, M. Coronin and vacuolin identify consecutive stages of a late, actin-coated endocytic compartment in *Dictyostelium*. *Curr Biol* **7**, 215-8 (1997).

Raynal, P. & Pollard, H. B. Annexins: the problem of assessing the biological role for a gene family of multifunctional calcium- and phospholipid-binding proteins. *Biochim Biophys Acta* **1197**, 63-93 (1994).

Rescher, U., Zobiack, N. & Gerke, V. Intact Ca(2+)-binding sites are required for targeting of annexin 1 to endosomal membranes in living HeLa cells. *J Cell Sci* **113**, 3931-8 (2000).

Rety, S., Osterloh, D., Arie, J. P., Tabaries, S., Seeman, J., Russo-Marie, F., Gerke, V. & Lewit-Bentley, A. Structural basis of the Ca(2+)-dependent association between S100C (S100A11) and its target, the N-terminal part of annexin I. *Structure Fold Des* **8**, 175-84 (2000).

Rety, S., Sopkova, J., Renouard, M., Osterloh, D., Gerke, V., Tabaries, S., Russo-Marie, F. & Lewit-Bentley, A. The crystal structure of a complex of p11 with the annexin II N-terminal peptide. *Nat Struct Biol* **6**, 89-95 (1999).

Rosales, J. L. & Ernst, J. D. Calcium-dependent neutrophil secretion: characterization and regulation by annexins. *J Immunol* **159**, 6195-202 (1997).

Rosengarth, A., Rosgen, J., Hinz, H. J. & Gerke, V. Folding energetics of ligand binding proteins II. Cooperative binding of Ca²⁺ to annexin I. *J Mol Biol* **306**, 825-35 (2001).

Rothhut, B. Participation of annexins in protein phosphorylation. *Cell Mol Life Sci* **53**, 522-6 (1997).

Russo-Marie, F. Annexin V and phospholipid metabolism. *Clin Chem Lab Med* **37**, 287-91 (1999).

Sagot, I., Regnouf, F., Henry, J. P. & Pradel, L. A. Translocation of cytosolic annexin 2 to a Triton-insoluble membrane subdomain upon nicotine stimulation of chromaffin cultured cells. *FEBS Lett* **410**, 229-34 (1997).

Salzer, U., Hinterdorfer, P., Hunger, U., Borken, C. & Prohaska, R. Ca(++)-dependent vesicle release from erythrocytes involves stomatin-specific lipid rafts, synexin (annexin VII), and sorcin. *Blood* **99**, 2569-77 (2002).

- Sambrook, J., Fritsch, E.F. and Maniatis, T. *Molecular Cloning: A Laboratory Manual*. 2nd ed. Cold Spring Harbor Laboratory Press, Cold Spring Harbor, New York (1989).
- Sarafian, T., Pradel, L. A., Henry, J. P., Aunis, D. & Bader, M. F. The participation of annexin II (calpactin I) in calcium-evoked exocytosis requires protein kinase C. *J Cell Biol* **114**, 1135-47 (1991).
- Schmitz-Peiffer, C., Browne, C. L., Walker, J. H. & Biden, T. J. Activated protein kinase C alpha associates with annexin VI from skeletal muscle. *Biochem J* **330**, 675-81 (1998).
- Seemann, J., Weber, K., Osborn, M., Parton, R. G. & Gerke, V. The association of annexin I with early endosomes is regulated by Ca²⁺ and requires an intact N-terminal domain. *Mol Biol Cell* **7**, 1359-74 (1996).
- Selbert, S., Fischer, P., Menke, A., Jockusch, H., Pongratz, D. & Noegel, A. A. Annexin VII relocalization as a result of dystrophin deficiency. *Exp Cell Res* **222**, 199-208 (1996).
- Simpson, P. A., Spudich, J. A. & Parham, P. Monoclonal antibodies prepared against *Dictyostelium* actin: characterization and interactions with actin. *J Cell Biol* **99**, 287-95 (1984).
- Song, G., Harding, S. E., Duchen, M. R., Tunwell, R., O'Gara, P., Hawkins, T. E. & Moss, S. E. Altered mechanical properties and intracellular calcium signaling in cardiomyocytes from annexin 6 null-mutant mice. *Faseb J* **16**, 622-4 (2002).
- Sopkova, J., Raguene-Nicol, C., Vincent, M., Chevalier, A., Lewit-Bentley, A., Russo-Marie, F. & Gallay, J. Ca(2+) and membrane binding to annexin 3 modulate the structure and dynamics of its N terminus and domain III. *Protein Sci* **11**, 1613-25 (2002).
- Sopkova, J., Renouard, M. & Lewit-Bentley, A. The crystal structure of a new high-calcium form of annexin V. *J Mol Biol* **234**, 816-25 (1993).
- Sopkova, J., Vincent, M., Takahashi, M., Lewit-Bentley, A. & Gallay, J. Conformational flexibility of domain III of annexin V studied by fluorescence of tryptophan 187 and circular dichroism: the effect of pH. *Biochemistry* **37**, 11962-70 (1998).
- Sopkova, J., Vincent, M., Takahashi, M., Lewit-Bentley, A. & Gallay, J. Conformational flexibility of domain III of annexin V at membrane/water interfaces. *Biochemistry* **38**, 5447-58 (1999).
- Sopkova-De Oliveira Santos, J., Vincent, M., Tabaries, S., Chevalier, A., Kerboeuf, D., Russo-Marie, F., Lewit-Bentley, A. & Gallay, J. Annexin A5 D226K structure and dynamics: identification of a molecular switch for the large-scale conformational change of domain III. *FEBS Lett* **493**, 122-8 (2001).

- Srivastava, M., Atwater, I., Glasman, M., Leighton, X., Goping, G., Caohuy, H., Miller, G., Pichel, J., Westphal, H., Mears, D., Rojas, E. & Pollard, H. B. Defects in inositol 1,4,5-trisphosphate receptor expression, Ca(2+) signaling, and insulin secretion in the *anx7(+/-)* knockout mouse. *Proc Natl Acad Sci U S A* **96**, 13783-8 (1999).
- Sussman, M. The origin of cellular heterogeneity in the slime molds, *Dictyosteliaceae*. *J. Exp. Zool.*, **118**, 407-417 (1951).
- Tabor, S. & Richardson, C. C. A bacteriophage T7 RNA polymerase/promoter system for controlled exclusive expression of specific genes. *Proc Natl Acad Sci U S A* **82**, 1074-8 (1985).
- Tokumitsu, H., Mizutani, A., Minami, H., Kobayashi, R. & Hidaka, H. A calyculin-associated protein is a newly identified member of the Ca²⁺/phospholipid-binding proteins, annexin family. *J Biol Chem* **267**, 8919-24 (1992).
- Towbin, H., Staehelin, T. & Gordon, J. Electrophoretic transfer of proteins from polyacrylamide gels to nitrocellulose sheets: procedure and some applications. *Proc Natl Acad Sci U S A* **76**, 4350-4 (1979).
- Verzili, D., Zamparelli, C., Mattei, B., Noegel, A. A. & Chiancone, E. The sorcin-annexin VII calcium-dependent interaction requires the sorcin N-terminal domain. *FEBS Lett* **471**, 197-200 (2000).
- Vogel, G., Thilo, L., Schwarz, H. & Steinhart, R. Mechanism of phagocytosis in *Dictyostelium discoideum*: phagocytosis is mediated by different recognition sites as disclosed by mutants with altered phagocytotic properties. *J Cell Biol* **86**, 456-65 (1980).
- Weiner, O. H., Murphy, J., Griffiths, G., Schleicher, M. & Noegel, A. A. The actin-binding protein comitin (p24) is a component of the Golgi apparatus. *J Cell Biol* **123**, 23-34 (1993).
- Weng, X., Luecke, H., Song, I. S., Kang, D. S., Kim, S. H. & Huber, R. Crystal structure of human annexin I at 2.5 Å resolution. *Protein Sci* **2**, 448-58 (1993).
- Westphal, M., Jungbluth, A., Heidecker, M., Muhlbauer, B., Heizer, C., Schwartz, J. M., Marriott, G. & Gerisch, G. Microfilament dynamics during cell movement and chemotaxis monitored using a GFP-actin fusion protein. *Curr Biol* **7**, 176-83 (1997).
- Williams, K. L. & Newell, P. C. A genetic study of aggregation in the cellular slime mould *Dictyostelium discoideum* using complementation analysis. *Genetics* **82**, 287-307 (1976).
- Zaks, W. J. & Creutz, C. E. Ca(2+)-dependent annexin self-association on membrane surfaces. *Biochemistry* **30**, 9607-15 (1991).

Zischka, H., Oehme, F., Pintsch, T., Ott, A., Keller, H., Kellermann, J. & Schuster, S. C. Rearrangement of cortex proteins constitutes an osmoprotective mechanism in *Dictyostelium*. *Embo J* **18**, 4241-9 (1999).

Erklärung

Ich versichere, dass ich die von mir vorgelegte Dissertation selbständig angefertigt, die benutzten Quellen und Hilfsmittel vollständig angegeben und die Stellen der Arbeit - einschließlich Tabellen und Abbildungen -, die anderen Werke im Wortlaut oder dem Sinn nach entnommen sind, in jedem Einzelfall als Entlehnung kenntlich gemacht habe; dass diese Dissertation noch keiner anderen Fakultät oder Universität zur Prüfung vorgelegen hat; dass sie noch nicht veröffentlicht ist, sowie, dass ich eine Veröffentlichung vor Abschluss des Promotionsverfahrens nicht vornehmen werde. Die Bestimmungen dieser Promotionsordnung sind mir bekannt. Die von mir vorgelegte Dissertation ist von Frau Prof. Dr. Angelika A. Noegel betreut worden.

Köln, den 20.11.2003

Marija Marko

Curriculum Vitae

Personal information

Name: Marko Marija
Address: Eythstr. 4
51103 Köln
Date of birth: 7.06.1974.
Place of birth: Yugoslavia, Serbia
Nationality: Serbian
Parents: Aleksandar Marko and Dragica Tasic-Marko

School education

1981-1989 Primary school
1989-1993 Grammar school (natural sciences)

University Studies:

1993-1999 Faculty of Biology, University Belgrade,
Dep. Molecular Biology and Physiology,
Experimental Biomedicine, major.

Graduated in May 1999. with average mark 9,09 (skale from 6 to 10). Final exam passed with highest mark 10.

Thesis title: "Characterization of mitochondrial F₀F₁-ATPase isolated from female rat brain synaptosomes".

Doctoral Studies:

10.2000 -12.2003 Advisor: Prof. Dr. Angelika A. Noegel,
Institute of Biochemistry I, Medical Faculty,
University of Cologne, Cologne, Germany

Köln,

Marija Marko

Lebenslauf

Persönliche Daten:

Name, Vorname: Marko, Marija

Anschrift: Eythstr.4
51103 Köln

Geburtsdatum: 07.06.1974

Geburtsort: Jugoslawien/Serbien

Staatsangehörigkeit: Serbin

Familienstand: verheiratet

Eltern: Aleksandar Marko und Dragica Tasic-Marko

Schulbildung:

1981-1989 Grundschule, Belgrad
1989-1993 Naturwissenschaftliches Gymnasium, Belgrad

Studium

1993-1999 Biologische Fakultät, Universität Belgrad,
Institut für Molekularbiologie und Physiologie

Hauptstudiengang: Experimentelle Biomedizin
Abschluss mit der Durchschnittsnote 9,09 (auf einer Skala von 6 bis 10)
Diplomprüfung mit der Note 10
Diplomarbeit:
"Characterization of mitochondrial F₀F₁-ATPase isolated from female rat brain synaptosomes" / „Charakterisierung von mitochondrialer F₀F₁-ATPase aus weiblichen Rattenhirnen isolierten Synaptosomen"

Okt 2000 -Dez 2003 Dissertation bei Prof. Dr. A.A. Noegel am Institut für Biochemie der Medizinischen Fakultät der Universität zu Köln mit dem Ziel der Promotion an der Math. Nat. Fakultät der Universität zu Köln

Köln den, Marija Marko

